

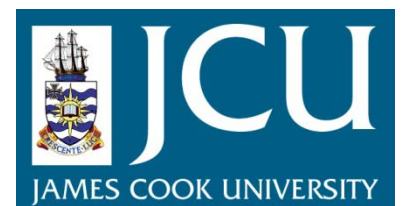
JCU ePrints

This file is part of the following reference:

Cappo, Mike (2010) *Development of a baited video technique and spatial models to explain patterns of fish biodiversity in inter-reef waters*. PhD thesis, James Cook University.

Access to this file is available from:

<http://eprints.jcu.edu.au/15420>



1. GENERAL INTRODUCTION

Between coral reefs and on tropical shelves there are vast unmapped mosaics of soft-bottom communities interspersed with shoals, patches and isolates of ‘hard ground’ supporting larger epibenthos. These poorly-known habitats can be dominated by phototrophic corals, seagrasses and algae in clearer waters, and by filter-feeding alcyonarians, gorgonians, sponges, ascidians, and bryozoans in more turbid or deeper waters (Putt *et al.* 1986; Spalding & Grenfell 1997; Pitcher *et al.* 2008). The smooth plains and patchy epibenthos support diverse and abundant demersal fish and elasmobranch communities, including large, economically important species, and others comprising ‘bycatch faunas’ (Ramm *et al.* 1990; McManus 1997; Sainsbury *et al.* 1997; Hill & Wassenberg 2000; Stobutzki *et al.* 2001b; Pauly & Chuenpagdee 2003; Ellis *et al.* 2008; Heupel *et al.* 2009).

Knowledge of fish-habitat associations in these mosaics is generally very poor, principally because of their inaccessibility to SCUBA divers, the taxonomic challenges in identifying the vast diversity of demersal and semi-pelagic fishes found there, and the selectivity of fishing gears used to sample them. Early studies were based solely on trawl surveys associated with commercial fisheries in the tropical Atlantic and Indo-Pacific (Bianchi 1992; Koranteng 2002; Garces *et al.* 2006a) and were constrained to families of economic interest within the goals of fisheries development or single-species stock assessments.

Unlike the demersal fisheries of the temperate zones (Hall & Greenstreet 1998), the diversity and taxonomic uncertainty amongst the vast remainder of the catch has discouraged the maintenance of long-term datasets comparable over large temporal and spatial scales (Pauly *et al.* 2005). More recently, the need for ‘ecosystem-based fisheries management’ (Sherman *et al.* 2003; Pikitch *et al.* 2004) has advanced the identification of difficult families, such as leiognathids, monacanthids and carangids, and has allowed a focus on the range of bycatch species in broad-scale surveys of trawl grounds (Garces *et al.* 2006b; Stobutzki *et al.* 2006).

The relatively recent concern about overfishing of spawning aggregations of long-lived serranids and lutjanids has also sparked awareness that there exist relatively small, discrete banks and shoals in the ‘off-reef’ habitat mosaics that are critical spawning sites for large piscivores normally associated with fringing and barrier reefs (Coleman *et al.* 1996; Koenig *et al.* 1996; Koenig *et al.* 2000; Scanlon *et al.* 2003; Mikulas Jr. & Rooker 2008). The depletion by line, trap and spear fishing of these shallower habitats has produced a shift in commercial and recreational effort down-slope or into the ‘inter-reef’ in the ‘Coral Triangle’, the Caribbean, Hawaii and Gulf of Mexico, facilitated by ‘technology leaps’ in marine navigation devices and

fishing gear that enable small vessels to find and fish these features (Cooke & Cowx 2004; DeMartini *et al.* 2008). Fisheries managers are not well equipped to deal with this shift in fishing effort in the deep, inter-reef domain because there is almost no information about the distribution and nature of these submerged seabed habitats and their biology (Craik 1989; Pitcher *et al.* 2002; Salas *et al.* 2007; Mapstone *et al.* 2008).

The few reviews available suggest that the fish communities on tropical shelves are structured by biogeography, regional sources of upwelling and runoff, thermoclines, mud content of sediments, topographic complexity, depth, latitude, ontogenetic migrations and species replacements through the effects of fishing (Longhurst & Pauly 1987; Lowe-McConnell 1987; Blaber *et al.* 1994; Sainsbury *et al.* 1997; Letourneur *et al.* 1998; Bianchi *et al.* 2000; Blaber *et al.* 2000; Bax & Williams 2001; Joanny & Menard 2002; Koranteng 2002; Le Loeuff & Zabi 2002; DeMartini & Friedlander 2004; Parrish & Boland 2004; Auster 2007; Beaman & Harris 2007; Friedlander *et al.* 2007; Kracker *et al.* 2008; Anderson *et al.* 2009). In turn, some species such as serranids and dasyatids may also act as ‘ecosystem engineers’ in modifying the seafloor topography at relatively large scales (Scanlon *et al.* 2005).

Faced with global depletion of fisheries and damage to the ecosystems they inhabit (Myers & Worm 2003; Pauly *et al.* 2005), the Congress of the United States of America defined the concept of ‘Essential Fish Habitat’ as “*those waters and substrate necessary to fish for spawning, breeding, feeding, or growth to maturity*” (16 U.S.C. 1802(10)). The term ‘waters’ in the definition refers to the “*aquatic areas and their associated physical, chemical, and biological properties that are used by fish.*” ‘Substrate’ refers to “*sediment, hard bottom, structures underlying the waters, and associated biological communities,*” and “*spawning, breeding, feeding, or growth to maturity*” encompasses the full life cycle of the fish (Kelley *et al.* 2006). To develop an EFH definition for fish species managed under such legislation requires not only an understanding of the influences of substrata and hydrological drivers, but also the other living organisms interacting with that species.

As a consequence of this legislation and the desire for ecosystem-based fisheries management there have been some remarkable advances in the application of fishery-independent techniques based on remote sensing of the seafloor topography with laser airborne depth soundings and multi-beam side-scan sonar (Able *et al.* 1987; Ojeda *et al.* 2004; Beaman & Harris 2007; Bowell *et al.* 2008; Wedding *et al.* 2008), video sensing of seafloor habitats with towed or autonomous underwater vehicles (Pitcher *et al.* 1999; Holmes *et al.* 2008; Williams *et al.* 2009), and direct observations from submersibles (Parker & Ross 1986; Ralston *et al.* 1986; Yoklavich *et al.* 2000; Reed *et al.* 2007). Perhaps nowhere has this been applied more comprehensively

than to the cold-temperate *Sebastes* rockfish complex (Yoklavich *et al.* 2000; Anderson *et al.* 2005; Yoklavich *et al.* 2007; Love & Yoklavich 2008; Rooper 2008; Anderson *et al.* 2009; Love *et al.* 2009), and the Hawaiian banks (Merritt 2005; Kelley *et al.* 2006). As Stoner *et al.* (2008) stated, “*There is no good substitute for direct observation of fish distribution, behaviour and abundance*”, and the development of new ways to make these observations is an imperative of modern marine science.

In the case of the Great Barrier Reef Marine Park (GBRMP), only six percent of the total area is comprised of emergent coral reefs and there is a compelling need to provide knowledge of inter-reef patterns and processes for both their intrinsic value and their relationship with adjacent coral reefs (Pitcher *et al.* 2000; Pitcher *et al.* 2007; Pitcher *et al.* 2008; Coles *et al.* 2009; Pitcher *et al.* 2009). Tagging studies are documenting widespread movements between inshore, or off-reef, nursery areas and coral reefs for members of a number of economically important fish families (Russell & McDougall 2005; Sheaves 2009), leading to a call for better understanding of this exchange (Sale 2002). There is a rapid diminution in net primary production with depth down the reef slopes, and Polunin (1996) predicted that this is generally accompanied by a down-slope shift toward dominance of larger planktivorous and piscivorous fish. This generalisation remains untested in the deeper (>15m) areas of phototrophic *Halimeda* bioherms, *Halophila* seagrass beds and ‘live coral’ habitats in the GBRMP, and on the deep *Microdictyon* algal meadows of Hawaii (Parrish & Boland 2004). The trophic subsidies provided by filter-feeding megabenthos, such as gorgonians and sponges, are considered to be small (Alongi 1990; 1998), and Hall (2002) proposed that while some juvenile fish do aggregate near seabed structures, our current understanding of the functional role of the larger benthos as habitat features is limited and should be addressed to predict or explain the outcome of chronic disturbances by fishing.

The depth limits of scientific SCUBA diving have rendered these fish-habitat interactions very difficult to observe directly. The coarse selectivity and ‘priority effects’ (Whitelaw *et al.* 1991; Williams & Bax 2001) of the trawls, traps and hook-and-line methods normally used in these depths adds further difficulty in describing patterns of biodiversity (Cappo & Brown 1996), and are prohibited activities for scientists in many areas of the GBRMP. As a result, the patterns and processes in size and species compositions of communities of fishes, so well documented for the shallow reefs of the GBRMP (Williams 1991; Syms & Kingsford 2009), have been poorly studied at depths beyond thirty metres (Watson *et al.* 1990; Newman *et al.* 1997; Wassenberg *et al.* 1997; Burrridge *et al.* 2006).

In the inter-reef waters of the GBRMP, the managers of fisheries and the marine park require information at the scale of the entire shelf on the vulnerability of metapopulations of inter-reef species to capture by trawling, on the impact of closures to fishing upon biodiversity, and on the 'comprehensiveness' and 'representativeness' of existing park zoning (Fernandes *et al.* 2005). This requires fishery-independent survey methods, stratified by knowledge of the key drivers of marine biodiversity as well as spatial position within the shelf.

The existence of a long cross-shelf gradient in the central section of the GBRMP has been very well documented for epibenthos, fish and corals along the 'Townsville transect' (Williams & Hatcher 1983; Russ 1984; Wilkinson & Cheshire 1988; Gust *et al.* 2001; Wismer *et al.* 2009), largely because of the proximity of this section to research institutions and the safety in navigation afforded by the well-mapped, open nature of the outer shelf reef matrix. However, simple application of the cross-shelf models to manage the southern and northern regions are of questionable value because those sections are semi-enclosed by barrier reefs and have much different flushing regimes. It is therefore critical to attempt to provide biologically-informed spatial models of species occurrence to help predict the patterns existing in the GBRMP. These models may have direct application to predicting the fish assemblages on other tropical shelves, or should offer a guide to the selection of key explanatory variables to measure in future studies there.

The challenge in providing useful information on inter-reef vertebrates is two-fold. Firstly, non-extractive, non-destructive approaches to surveys of all topographies and zones of the marine park must be developed. Such techniques should have the least selectivity possible, given the fact that a narrow focus in monitoring programs, on economically important predators for example, has great risk of failing to detect fundamental changes in biodiversity (Jones *et al.* 1993). Secondly, robust models must be developed that explain and predict the distribution of species and assemblages along critical environmental gradients. Relationships between the covariates should be examined for interactions to derive more proximal predictors and surrogates that are easily measured (Williams & Bax 2001; Austin 2007).

To overcome the limitations and selectivity of extractive methods, I develop in this thesis a harmless baited video technique that offers the benefits of aggregating fishes of any size by use of bait for visual census on seabed topographies of any form, which is permitted in any zone of the GBRMP. I base this approach on the earlier use of baited video-photography in studies of abyssal scavengers (Priede & Merrett 1996), juvenile lutjanids (Ellis & DeMartini 1995), the fate of bycatch discards (Hill & Wassenberg 2000) and the densities of carnivorous fish inside and outside marine protected areas (Willis & Babcock 2000). Unlike these earlier approaches, I

apply a fleet of up to six replicate units within a ‘biologically-informed’ stratification of the GBRMP study area to describe the spatial patterns of species richness, relative abundance and assemblage structure of demersal and semi-pelagic vertebrates. This was made possible by participating in the largest exploration of seafloor biodiversity ever undertaken on a tropical shelf (Pitcher *et al.* 2007).

Measurements of fish diversity and abundance on even the smooth seafloors of least complexity are notoriously over-dispersed in the tropics. Studies of bycatch faunas show that Indo-Pacific surveys regularly list over three hundred species – yet relatively few species were ubiquitous and these species were not always the ones dominating catches in terms of numbers or biomass (Blaber *et al.* 1994; Wassenberg *et al.* 1997; Stobutzki *et al.* 2001). To further complicate the understanding of spatial patterns, species-environment relationships tend to be inherently asymmetric and non-linear (Austin 2007). They also tend to show heterogeneous scatter of abundances at points along a gradient – often as a consequence of the fact that other unmeasured biotic or abiotic factors are limiting abundances and are interacting with the measured covariates in complex ways (Anderson 2008).

To cope with these challenges I chose to use models based on regression trees (De’ath & Fabricius 2000; De’ath 2002; 2007). Boosted regression trees (BRT) and multivariate classification and regression trees (MRT) represent complex information in a visual way that is easily interpretable. They are robust and flexible, because explanatory (predictor) variables can be numeric, categorical, binary, or of any other type, and model outcomes are unaffected by transformations and different scales of measurement of the predictors. They are not sensitive to outliers, and handle missing data in predictors by applying best surrogates with little loss of information. Trees are hierarchical structures, and input variables at the tree ‘leaves’ are dependent on input variables at higher nodes. This allows simple modelling of complex, non-linear interactions that simply cannot be handled by other approaches (Leathwick *et al.* 2006; Elith *et al.* 2008).

In this thesis I follow key reviews (Longhurst & Pauly 1987; Lowe-McConnell 1987; Longhurst 2007) to derive predictors from the dataset of Pitcher *et al.* (2007) based on sediment composition, salinity, temperature, depth, seafloor rugosity and epibenthic cover of marine plants and ‘megabenthos’ and infer their relative influence on single species and species assemblages. I also focus on comparing the predictive performance of these environmental covariates with simple measures of spatial position across and along the GBRMP, which undoubtedly act as surrogates for many known and unknown environmental gradients (Fabricius & De’ath 2001; 2008).

My objectives are framed in three main questions, covered in five data chapters:

1. What are the biases and selectivity in samples caused by time of day, fish behaviour and the use of bait in the application of baited video techniques to describe vertebrate assemblages?
2. What are the shelf-scale spatial patterns of species richness and relative abundance in GBRMP inter-reef vertebrate assemblages from 8-80m depths?
3. How are these patterns correlated with position on the continental shelf, physical and biological characteristics of the sediments and water column, and epibenthic cover?

These patterns and processes are discussed in reference to the paradigms regarding biodiversity on tropical marine shelves.

2. GENERAL METHODS

2.1 A REVIEW OF BAITED VIDEO TECHNIQUES TO ESTIMATE RELATIVE ABUNDANCE OF FISH

There has been a recent expansion in the application of baited video techniques (see Table 2.1). In general terms, a bait plume is used to attract vertebrates and invertebrates into the field of view of a video camera where they are identified, counted and often measured. In this brief review I introduce the application of baited video studies using single cameras.

The history of the technique may be traced back to searches by Parrish (1989) for the location and nature of key nursery grounds for deepwater *Pristipomoides* snappers on the Hawaiian shelf with simple camera systems. Meanwhile, the University of Aberdeen's OceanLab was developing autonomous underwater 'landers' with advanced camera systems (e.g. AUDOS and ROBIO) to assess the abundance, behaviour and metabolic rates of demersal scavengers at abyssal depths (Priede *et al.* 1990; Priede *et al.* 1994; Priede & Merrett 1996). These systems have video or stills-flash camera units, onboard computer storage of data, and depth, temperature and current sensors. They are retrieved by means of acoustic release of sacrificial weights under buoy packs.

Later use of closed-circuit television recording at the surface by Willis & Babcock (2000) sparked further applications to shallow reef sparids and paraperoids in studies making comparisons inside and outside marine reserves (Denny *et al.* 2004; Kleczkowski *et al.* 2008). Coarse methods of length estimation were used by all of these teams, until the development and testing of stereo-video techniques and software proved that very high accuracy and precision could be obtained efficiently with cheap camera systems (Shortis *et al.* 2009).

The general benefits of the technique lie in three main areas. Firstly, baited video approaches are non-extractive and non-intrusive. This means they can be used in marine reserves, and to gather information on numbers, size and behaviour of animals of special conservation significance. Secondly, large, mobile animals that avoid SCUBA divers and extractive fishing gears are included in samples. This lack of size selection, and the powerful sampling replication afforded by multiple camera units, avoids 'false negatives' (Tyre *et al.* 2003) and allows standardised sampling at any depth, time of day and seabed topography. Thirdly, the acquisition of a permanent tape record removes the need for specialist observers to conduct all fieldwork, allows impartial, repeatable measurements, enables standardised data collection and training in

association with remote taxonomists (via emailed imagery), and provides a remarkably popular format to communicate science to the public.

2.1.1 General approaches and applications

There are two main orientations of bait and camera. Vertical, look-down systems utilise a camera that films a bait canister fixed to a scale bar within a frame on the seabed (Willis & Babcock 2000). This gives a fixed depth of field and a good reference for measurements, but the subjects must be identified by the view of their dorsum from above and the full length of larger animals cannot be seen. Indeed, large sharks and rays cannot physically fit between the camera and the bait. A field comparison by Langlois *et al.* (2006) showed that major tropical reef fish families, such as serranids, lethrinids and carcharhinids, were shy of entering the field of view underneath a look-down camera.

Horizontal, look-outward systems film bait canisters lying on the seabed (Gledhill *et al.* 2005; Stobart *et al.* 2007; Wells & Cowan 2007), suspended above the seabed (Merritt 2005), or suspended just below the sea surface to sample pelagic species (Heagney *et al.* 2007). The depth of field is generally not fixed or measured with such systems, although this parameter can be fixed accurately using stereo-video systems. To identify and count fish all around the bait station, the ‘SEAMAP’ system used by NOAA-NMFS has four cameras filming simultaneously at all points of the compass (Gledhill *et al.* 2005).

The bait plume aggregates fish for counting and measurement through olfactory, auditory and behavioural cues (Armstrong *et al.* 1992). The action of bait is reviewed in detail in Chapter 3, but in general terms bony fishes, sharks and rays come not just to feed, but are also influenced by the general activity in the field of view. Some species, such as labrids, are highly territorial and, if a video system lands in their home range, they are likely to move about in the field of view in agonistic encounters. Others, like some herbivorous scarids and corallivorous chaetodontids, seem indifferent to the bait, but may be interested in the general activity around it. Fish feeding behaviour at the bait canister stimulates others to approach (Watson *et al.* 2005) and it is probable that some large predatory carangids and sphyraenids are attracted by the presence of small prey species. Such behaviour has been documented by Whitelaw *et al.* (1991) for the depredations on captives in fish traps by large serranids.

Table 2.1. Examples of baited video studies. Abbreviations are HBRUVS/VBRUVS (Horizontal/Vertical baited remote underwater video stations), VBUV /HBUV (Vertical (V) or Horizontal (H) baited underwater closed circuit television), SBRUVS (Stereo horizontal baited remote underwater video stations) and MPA (Marine Protected Areas).

Source	Region	Camera system	Depth Range	Diversity (n taxa)	Study type
Wells <i>et al.</i> 2008	Northern Gulf of Mexico	HBRUVS CCD HandiCams (four camera array)	Not reported	<i>Lutjanus campechanus</i>	Compare the catch per unit area, length-specific bias, and relative 'catchability' (q-ratio) of traps, trawls and cameras for different size classes on low-relief reef habitats.
Kleczkowski <i>et al.</i> 2008	Rottneest Island, WA, limestone/algal reefs	VBUV pencil TV camera; VBRUVS CCD HandiCams	Not reported	59 spp, 28 fam.	Tests for differences in density, size, biomass and assemblage structure of reef fishes between MPA and adjacent areas using <i>MaxN</i> and length measurements from scale bars.
Stoner <i>et al.</i> 2008a	Kodiak Island, Alaska, seagrass and algal beds	HBUV low-light monochrome TV camera	2.5-5m	0+ gadids ; <i>Gadus macrocephalus</i> , <i>Eleginus gracilis</i> , <i>Theragra chalcogramma</i>	Tank tests for reaction to bait; Field tests of <i>Tarr</i> , <i>MaxN</i> and other metrics in comparison with beach seine catches to assess potential for baited video surveys of young-of-the year gadids.
Malcolm <i>et al.</i> 2007	Entire NSW coast sub-tropical rocky reefs	HBRUVS CCD HandiCams	15-30m	101 spp, 44 fam.	Tests for effects of along-shelf region (hundreds of kilometres), and within-MPA location (km) scale variation on assemblage structure, and species <i>MaxN</i> . Temporal variation over five years examined in one MPA.
Heagney <i>et al.</i> 2007	Lord Howe Island pelagic on shelf to 100m depth	HBRUVS CCD HandiCams	Surface waters (10m)	Carangidae (2), Carcharhinidae (2), Scombridae (2), Lutjanidae (1)	Tests for effects of shelf region, MPA zoning, depth, water temperature and current speed on pelagic assemblage structure and abundance (<i>MaxN</i>); Development of simple models to weight results by current speed and plume spread.
Stobart <i>et al.</i> 2007	Rocky reefs of Spain and France	HBRUVS CCD HandiCams	10-20m	51 spp, 31 fam.	Comparisons of BRUVS with UVC; examination of species accumulation curves, species arrival times.

Source	Region	Camera system	Depth Range	Diversity (n taxa)	Study type
Watson <i>et al.</i> 2007	Abrolhos Islands; sub-tropical coral/algal reefs	SBRUVS CCD HandiCams	8-12m, 22-26m	137 spp, 42 fam.	Comparison inside and outside MPAs of 'target' and 'unfished' reef fish species (species richness, family richness, <i>MaxN</i>).
Cappo <i>et al.</i> 2007a	GBRMP; inter-reef and shoals	HBRUVS CCD HandiCams	8-110m	347 spp; 58 families of teleosts, chondrichthyans and hydrophid seasnakes	Regional-scale community discrimination along spatial and depth gradients.
Langlois <i>et al.</i> 2006	SW lagoon, New Caledonia; coral reef	VBUV CCD HandiCam X 1; HBRUVS CCD HandiCam	<10m ?	HBRUVS – 14spp; Serranidae, Lethrinidae, Carcharhinidae, Acanthuridae VBUV – 3 spp; Serranidae	Comparison of remote baited systems (presence/absence and <i>MaxN</i>).
King <i>et al.</i> 2006	Mid-Atlantic ridge abyssal plain	ROBust BIOdiversity lander (ROBIO) downward facing digital stills camera/flash on 1.5 min time lapse	924-3,420m	22 taxa; chondrichthyans, holocephalan, teleosts, eels. Including <i>C.(Nematonorus) coryphaenoides</i> , <i>Synaphobranchus kaupii</i> , <i>Antimora rostrata</i>	Community structure analysis along depth and latitudinal gradients. *Density and length estimates for three species using Priede <i>et al.</i> (1990) models.
Watson <i>et al.</i> 2005	Hamelin Bay; limestone/algal reefs	SBRUVS CCD HandiCams	<10m ?	33 spp; 22 families of teleosts and chondrichthyans	Comparison of diver-swum video and remote baited and unbaited video; species richness and <i>MaxN</i> .
Gledhill <i>et al.</i> 2005	Gulf of Mexico banks	HBRUVS CCD HandiCams (changing to SBRUVS with low-light, monochrome cameras)	80-120m ?	<i>Lutjanus</i> , <i>Mycteroperca</i> , <i>Balistes</i>	Development of fishery-independent indices of abundance (<i>MaxN</i> , presence/absence), measurement of length, analysis of fish-habitat associations.
Merritt 2005	Hawaiian shelf edge/slope	SBRUVS ultra low-light, monochrome board camera	200-400m	<i>Pristipomoides</i> , <i>Seriola</i> , <i>Epinephelus</i>	Gear development, fishery-independent indices.

Source	Region	Camera system	Depth Range	Diversity (n taxa)	Study type
Denny & Babcock 2004	NE New Zealand; sub-tropical rocky/algal reefs	Tethered VBUV high resolution colour camera	6-30m	7 spp, Sparidae, Labridae, Monacanthidae, Pomacentridae, Carangidae, Muraenidae, Scorpidae	Comparisons of <i>MaxN</i> , length measurement inside/outside MPA.
Denny <i>et al.</i> 2004	As above	Tethered VBUV high resolution colour camera	≤50m	<i>Pagrus auratus</i>	temporal comparisons [four years] of <i>MaxN</i> , length measurement.
Westera <i>et al.</i> 2003	Ningaloo Reef; coral reef	HBRUVS CCD HandiCams	1.5-2m	23 spp; Lethrinidae, Lutjanidae, Haemulidae, Serranidae, <i>Choerodon</i> (Labridae)	Comparisons of <i>MaxN</i> inside/outside MPA.
Yau <i>et al.</i> 2001	South Georgia/ Falkland Islands	AUDOS downward facing colour film still camera/flash on 1 min time lapse	900-1,735m	<i>Dissostichus eleginoides</i> , lithodid crabs	Estimates of relative abundance using time of first arrival in Priede and Merrett (1996) model; length estimates.
Hill & Wassenberg 2000	GBRMP; prawn trawl grounds	HBRUVS CCD HandiCam	10-29m	9 fish taxa, unidentified sharks, crabs, squid and gastropod	Monitoring fate of discarded fish bycatch at night on the seabed.
Willis <i>et al.</i> 2000	NE New Zealand; sub-tropical rocky/algal reefs	Tethered VBUV high resolution TV camera	<20m	<i>Pagrus auratus</i> , <i>Parapercis colias</i>	Comparisons of time-based indices, lengths, and <i>MaxN</i> inside/outside MPA with angling and underwater visual census (UVC).
Ellis & DeMartini 1995	Hawaii, slopes near embayments	HBRUVS CCD HandiCams	52-87m	<i>Pristipomoides filamentosus</i> , <i>Torquigener florealis</i>	Comparisons of precision, accuracy and efficiency of time-based indices and <i>MaxN</i> from video with longlines; power analysis.

2.1.2 Estimation of abundance from fish sightings

There are a number of measures of the timing and magnitude of sightings of vertebrates that have been derived from tapes to produce counts and indices of abundance. The first type concern the time elapsed before arrival and departure of species in the field of view. The difference between the two times is the duration on tape. The second type comprises the counts of maximum number of individuals ($MaxN$ or n_{peak}) within particular short segments (usually thirty seconds or one minute) or frames of video. Given the nature and expense of field conditions and logistics, it is somewhat surprising that the greatest advances in the theory to estimate densities from these parameters have been made in the studies of abyssal scavengers (Sainte-Marie & Hargrave 1987; Priede *et al.* 1990; Priede & Merrett 1996). These models do not translate directly to shallow water species, so there has been a marked divergence in indices of abundance between abyssal and shallow studies. These divergent approaches are reviewed here.

Very long camera deployments (tens of hours to days) were made to study abyssal scavengers. The foundation of these studies was the theory developed by Priede and Merrett (1996) that the number of fish visible at the bait is the result of an equilibrium between arrivals and departures, and the ‘staying time’ or ‘giving up time’ is governed by Charnov’s marginal value theorem of optimal foraging. This states that the staying time of an animal at an exhaustible food source is inversely related to the probability of finding an alternative food source. Thus Priede *et al.* (1994) found the n_{peak} of abyssal grenadiers was higher at an oligotrophic location with low fish population and low food abundance because individuals stayed longer at the bait, whereas in a food-rich area with high population density the arrival rate was high because of the higher population, but n_{peak} was low because individuals gave up trying to gain access to the bait and left within an hour.

Using strict assumptions that all fish were distributed randomly and evenly, and that they responded immediately, positively and independently from one another to interception of a bait plume, Priede *et al.* (1990) developed a model of fish density using the ‘shark’s fin curve’. In a plot of number of fish at time t (N_t) against the soak time (t minutes), an initial fish arrival rate is relatively rapid, rising to a peak (n_{peak}) and declining as fish depart. A curve fitted to the data cloud can be broken up into a steeper arrival curve and a shallower departure curve, which are identical in shape, but are separated by a time that corresponds to the mean ‘staying time’ of fish. The difference between the two curves gave the actual number present in the OceanLab studies (Farnsworth *et al.* 2007).

Theoretical population densities were calculated by Priede *et al.* (1990) from the time of arrival of the first scavengers to the bait using an inverse square law:

$$N = C/t_{arr}^2$$

where N is the density of fish per square kilometre, t_{arr} is the time delay between the bait landing on the seafloor and the arrival of the first fish in seconds;

$$C = 0.3848(1/V_f + 1/V_w)^2$$

The constant C depends on the water velocity in ($V_w \text{ ms}^{-1}$) dispersing the bait plume down-current, and swimming velocity of the fish toward the bait ($V_f \text{ ms}^{-1}$).

Such estimates are strongly affected by the assumed foraging behaviour of the fish species concerned (Bailey & Priede 2002). Three of the possible foraging strategies (cross-current foraging, sit-and-wait, and passive drifting) of abyssal scavengers produced a distinctive pattern of animal arrivals that may be diagnostic of each foraging strategy.

The abyssal scavenger model was tested for Patagonian toothfish by Yau *et al.* (2001), who noted that for shallow-water applications, the inverse relationship between abundance and the square of the average arrival time will cause problems. Since abundance is proportional to the reciprocal of the square of the arrival time, a doubling of the arrival time produces a four-fold decline in Priede and Merrett's (1996) abundance estimate. Mean arrival times in shallow deployments occur at the level of seconds to minutes, rather than the tens of minutes to hours recorded in abyssal studies. Shallower deployments also can produce far larger numbers of fish in the field of view. Shallow water studies have therefore neglected a theoretical approach and density estimation in favour of informative comparisons of indices of relative abundance amongst treatments, times and places.

Ellis and De Martini (1995) recorded the maximum number seen in a one-second interval (*MAXNO*), the time of arrival (*TFAP*), and a total duration of visit during a sequence (*TOTTM*). Their best video indices of relative abundance were calculated as means to standardise for multiple deployments per station and were derived as:

$$\text{Log of Means (LM)} = \ln[(\sum_{i=1}^n x_i / n) + 1]$$

where x_i = the individual datum for a variable (*MAXNO*, *TFAP*, or *TOTTM*) for each deployment at a station, and n = the number of deployments per station.

They found that *MAXNO* for the sharp-tooth snapper *Pristipomoides filamentosus* and puffers *Torquigener florealis* was highly correlated with the total duration on video and time to first appearance of the respective species. They also found a positive correlation between *MAXNO* and long-line catch rates. *MAXNO* and *TFAP* were highly correlated, suggesting the greater the snapper and puffer density, the faster the fish arrived at the bait.

Willis and Babcock (2000) and Willis *et al.* (2000) compared the MAX_n from baited underwater video (BUV) with underwater visual census (UVC) and angling, and also found that MAX_n was positively correlated with fish abundance. Their studies inside and outside a marine reserve included snapper *Pagrus auratus* and blue cod *Parapercis colias*. During a thirty-minute BUV deployment, the number of each species recorded at the bait in thirty-second intervals was recorded to derive the MAX_{sna} and MAX_{cod} present in a sequence, together with the time at which these maxima were recorded (t_{MAXsna}), the time of first arrival of each species (t_{1stsna}), and the persistence of the external bait (t_{BG}). MAX_n was the best index, but blue cod responded to bait so well that speed of arrival t_{1stcod} also reflected abundance. Statistically significant effects were detected after only five minutes, and only became more significant with increasing time of deployment of the BUV.

The SEAMAP system uses a single 'pod', baited with squid, with four cameras mounted orthogonally at a height of 30cm above the seabed (Gledhill *et al.* 2005). Analysts interrogate twenty minutes of one video tape from each station to identify and enumerate all species. The time when each individual fish enters and leaves the field of view is recorded. This is referred to as a time in/time out procedure (TITO). Tapes are sub-sampled if a large number of fish of a given species makes following individual fish difficult, if large numbers of fish occur in pulses periodically during the tape, and if single or multiple schools of fish pass in the field of view. Three estimators of relative abundance are derived from the video data – presence and absence, the maximum count (each individual of each species is counted repeatedly each time it appears in the field of view), and the greatest number of each species that appear at once, termed 'minimum count' (*mincount*). A delta-lognormal model is employed to make a combined annual *mincount* index from two distinct generalised linear models – a binomial (logistic) model which describes the proportion of positive *mincount* (presence/absence), and a log-normal model which describes variability in the non-zero *mincount* data.

The *mincount* of Gledhill *et al.* (2005), the *Max_{sna}* of Willis *et al.* (2000), the *MAXNO* of Ellis and DeMartini (1995), the *n_{peak}* of Priede *et al.* (1996) and the *MaxN* employed in this thesis are all homologous. They have the advantage of avoiding multiple counts of the separate visits of the same individual fish to the field of view, and they offer conservative comparisons. The laboratory time consumed by tape interrogation and data recording, coupled with observer fatigue, are a major bottleneck in the ‘tape segment’ and ‘TITO’ approaches described above. Tape processing ratios of about 1:1 tape reading time to tape duration were reported for single-species interrogation of BUUV tapes by T. Willis (pers. comm.) and 13:1 for SEAMAP stations by Gledhill *et al.* (2005).

With the exception of Heagney *et al.* (2007), shallow water studies are yet to directly estimate the area of attraction caused by bait plumes, but there have been some attempts to ensure that replicates are independent of one another. Ellis and DeMartini (1995) proposed that at distances of greater than one hundred metres separation their replicate ten-minute sets of baited videos were independent, because the greatest distance of fish attraction was only 48-90m for a 200mm fish in a current velocity of 0.1-0.2 ms⁻¹. This assumed a maximum swimming speed of approximately three body lengths per second for a 200mm fish ($V_f = 0.6 \text{ ms}^{-1}$).

2.2 BAITED REMOTE UNDERWATER VIDEO STATIONS (BRUVS)

The development of the BRUVS hardware progressed from a ‘roll-bar’ frame used in Chapters 3 and 4, to a 700mm high ‘trestle-shaped’ frame that raised the camera housing 480mm above the substratum in the subsequent chapters (Figure 2.1). The higher vantage point was designed to allow a full field of view when vertical cover of gorgonians, plants and octocorals was high, or vertical relief of the seabed was particularly rugose. Frames were fabricated from 10mm steel reinforcing rod and 3mm steel plate and were galvanized. Steel camera arms were bolted onto the trestle frames to provide a camera aspect at an angle of ten degrees to the horizontal (Figure 2.2). To cope with the snagging of BRUVS on hard ground, a system of weak links was designed to enable the legs on the trestle frames to break open and allow the unit to be retrieved (Figure 2.3).

Simple camera housings were made from PVC pipe with acrylic front and rear ports (Figure 2.4). Sony™ Hi-8 (model TR516E) or Sony™ Mini-DV HandiCams (models TRV18E, TRV19E) with wide-angle lens adapters (Hama™ 0.5X or Sony™ 0.6X) were used in the housings. The cameras were fixed to a plastic plate and then fitted into the housings through a removable rear port by way of a dove-tail slide (Figure 2.5).

The cameras were turned on, camera exposure was set to ‘Auto’, focus was set to ‘Infinity/manual’ for the best depth of field and ‘Standard Play’ mode was selected to provide standardised periods of 45, 60 or 90 minutes of filming at the seabed. The cameras were then sealed in the housings before deployment. Flexible bait arms, made from 1500mm lengths of 20mm plastic electrical conduit were attached and detached during and after deployment. The bait arm supported a 350mm plastic mesh bait canister containing one kilogram of crushed oily sardines (*Sardinops* or *Sardinella* spp). BRUVS were deployed with 8mm polyethylene or polypropylene ropes and 200-300mm polystyrene surface floats bearing a marker flag, and were retrieved with a hydraulic pot-hauler wheel (Figures 2.1 and 2.7). Ballast weights of 5kg and extra floats were added in conditions where wave action and currents were not mild to prevent the BRUVS toppling and to prevent the head gear being dragged underwater by water pressure on the ropes. The total weight was normally 23kg, but in extreme conditions of swell and current, a fully loaded BRUVS weighed ~43kg at the surface.

Once the camera was loaded, the floats and rope were streamed astern of the vessel first, before the BRUVS was lowered into the water (Figure 2.6). A scope of 1½ (shallower than 50m) to 2 (deeper than 50m) times the water depth was used in the length of float ropes. Details of location, time and depth were immediately captured from ships’ instruments using event-logging software. The vessel approached upwind along the float line to retrieve the BRUVS, and a grapple was cast from the stern quarter to bring the rope aboard and through a snatch block. An hydraulic pot-hauler wheel with variable speed was used to haul the rope, which was manually flaked into a rope bin before being turned over for the next set (Figure 2.7).

Replicate BRUVS were set about 300-450 metres apart along transects bracketing sampling stations in this study. This spacing was designed to minimise the possibility of large-scale interference of the replicates with each other. Given a seasonal prevalence of current of $\sim 0.2\text{ms}^{-1}$ in GBRMP study locations (V_c), the sixty-minute (S_t) soaks of the BRUVS may have had an effective range of attraction (AR) of $\sim 480\text{m}$ for fish of $\sim 200\text{-}300\text{mm}$ length. This comprised forty minutes of advection of the bait plume down-current and twenty minutes of fish swimming time up-current to reach the field of view in time to be recorded on the BRUVS. I formalised this relationship as $AR = 60 \times (S_t) \times ((V_f \times V_c) - V_c^2)/V_f$.

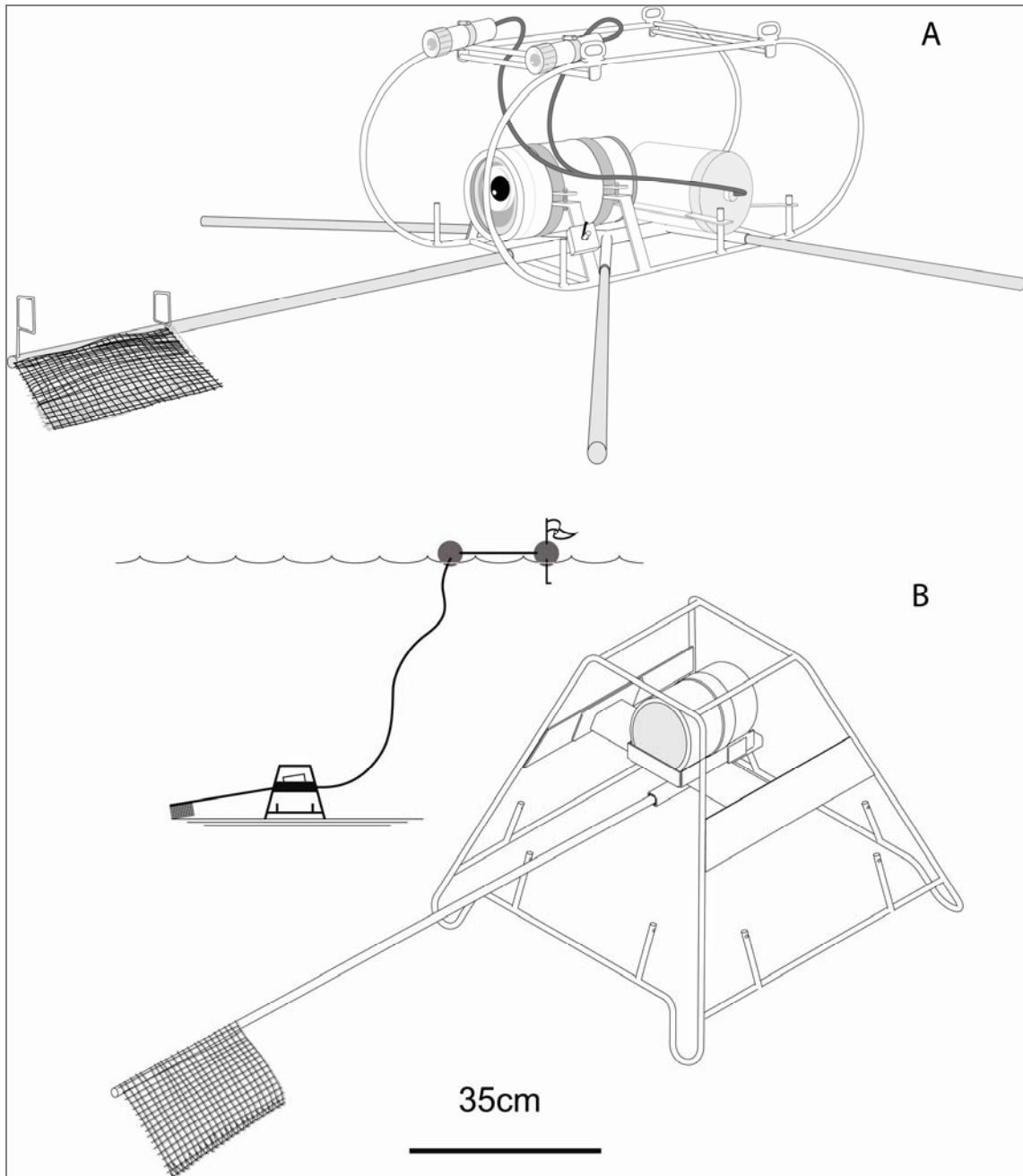


Figure 2.1. BRUVS prototypes used in Chapters 3 and 4 (A) and subsequent chapters (B). For night use, prototype (A) had lights powered by a 12 Volt gel-cell battery enclosed in a housing.

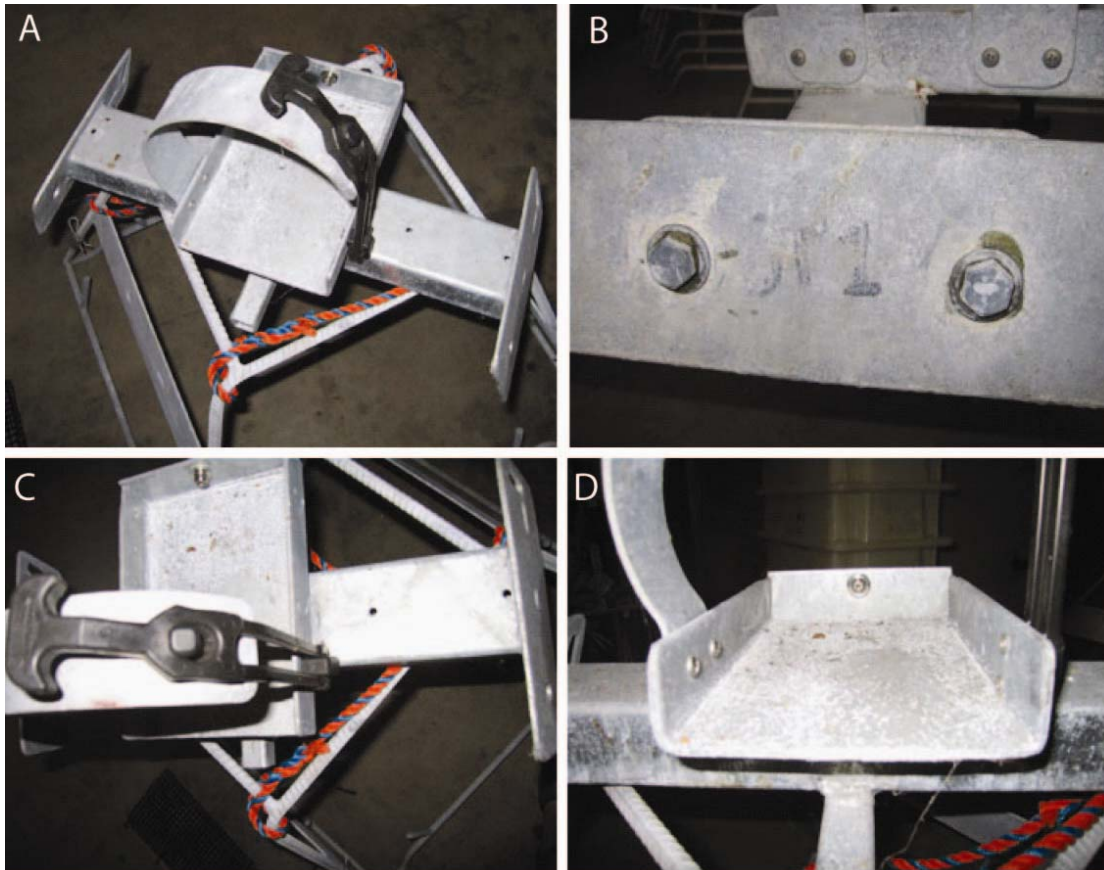


Figure 2.2. Rubber bonnet tie-downs held housings on camera arm clamps (A, C). Bolting camera arms through slots allowed 10 degrees of tilt (B). A locator lug mated with a socket in the camera housing faceplate (D).



Figure 2.3. The lug and socket in each leg of the frame (A) used #18 gauge (1.25mm) galvanized wire and a B10 'R' Clip to enable (B,C) or bypass the weak-link (D) .

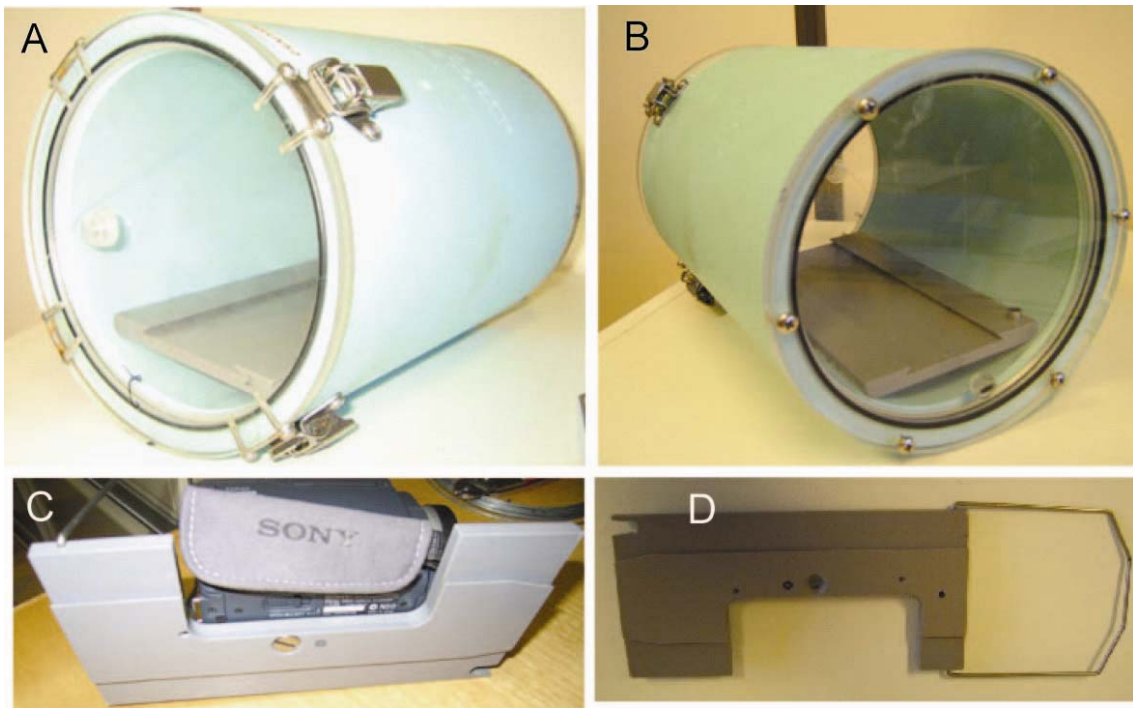


Figure 2.4. Rear (A) and front view (B) of a housing showing the fixed, female dove-tail plate for camera, and the lug in the faceplate (B) that fitted a locking pin on the camera arm (Figure 2.2). The locator pin on the dovetail plate (B) locked onto a female lug on the camera baseplate (C). The camera was screwed onto the male plate (C) and slid into and out of the female dove-tail joint with the aid of a wire handle (D).

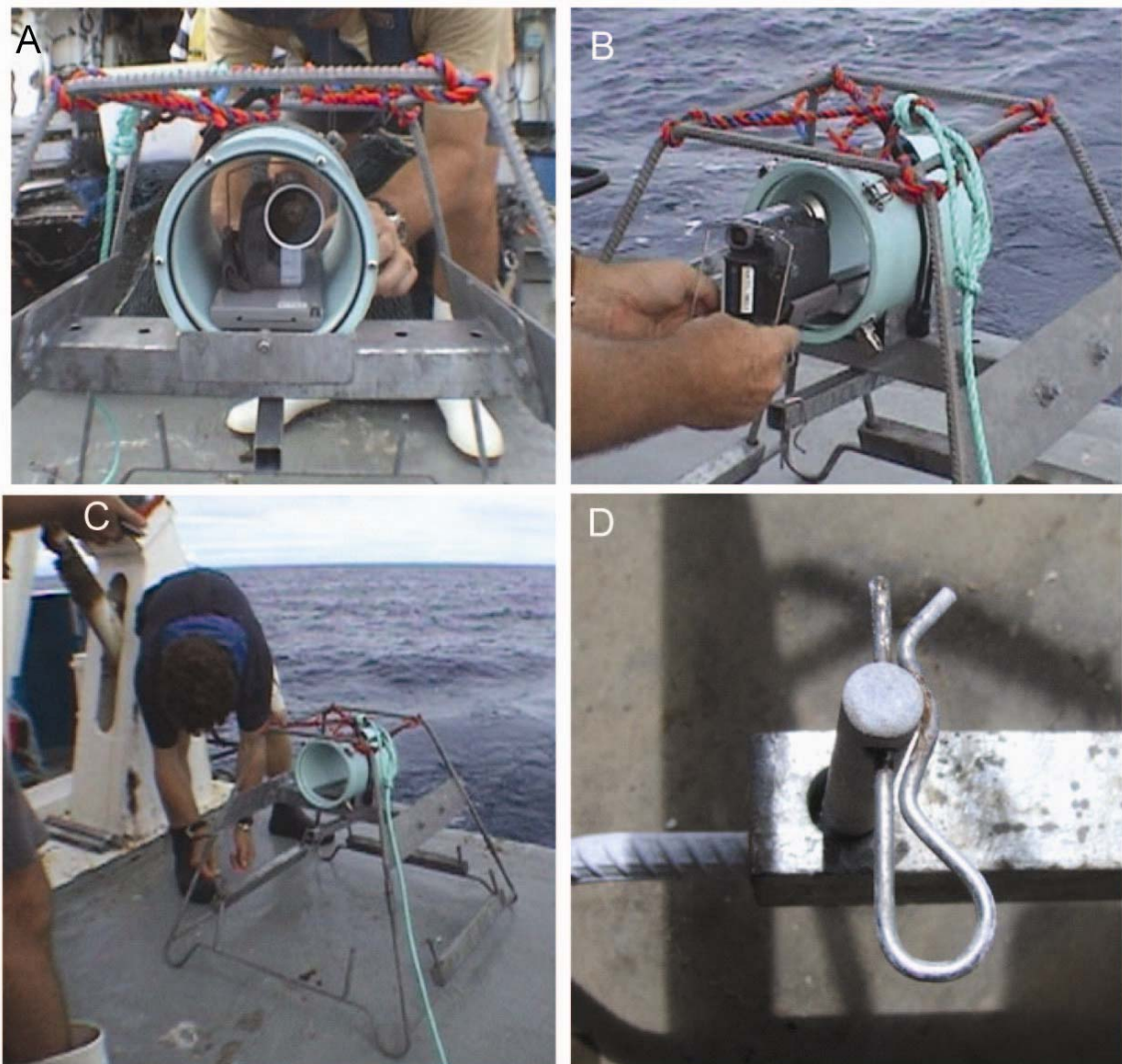


Figure 2.5. Loading of camera (A,B) and ballast weights (C,D) to a BRUVS.

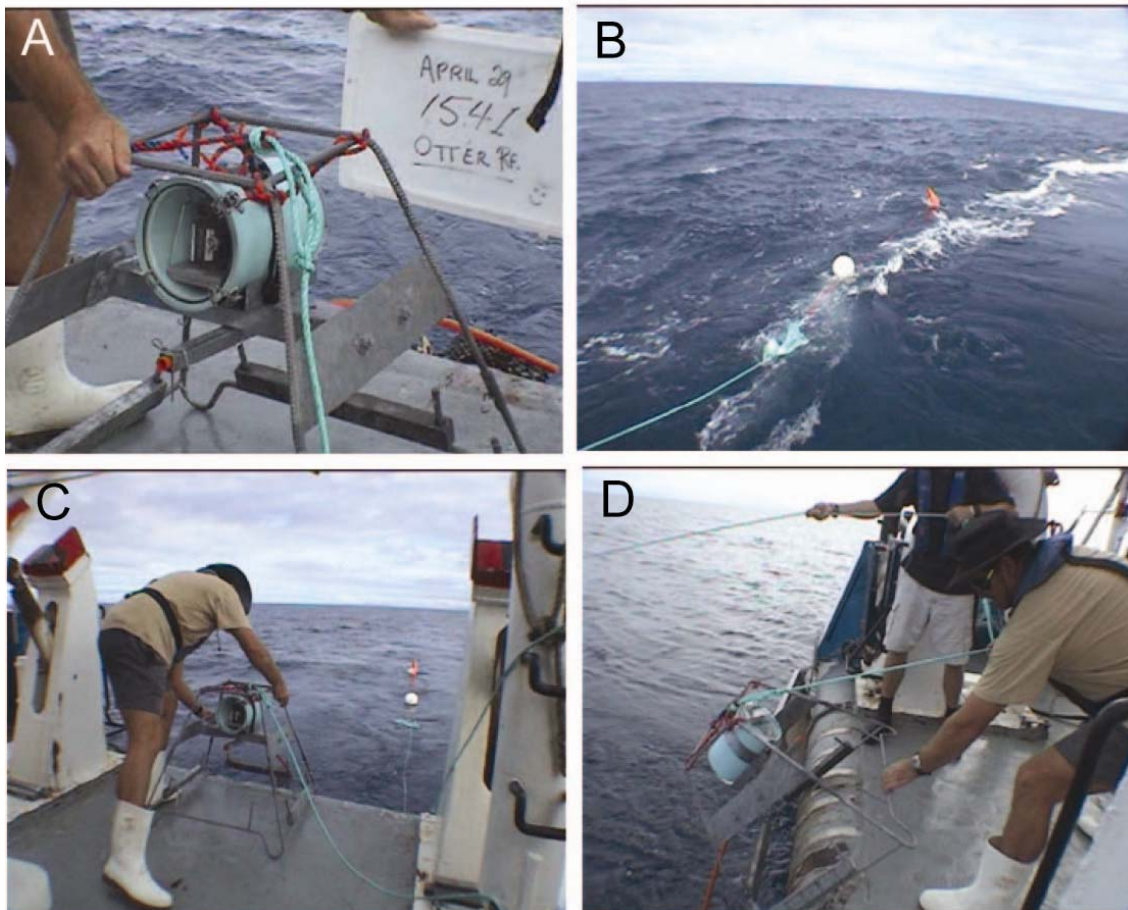


Figure 2.6. Once the camera was loaded (A), the floats and rope were streamed astern of the vessel first (B) , and tied off (C) to await the final position of the drop (D).

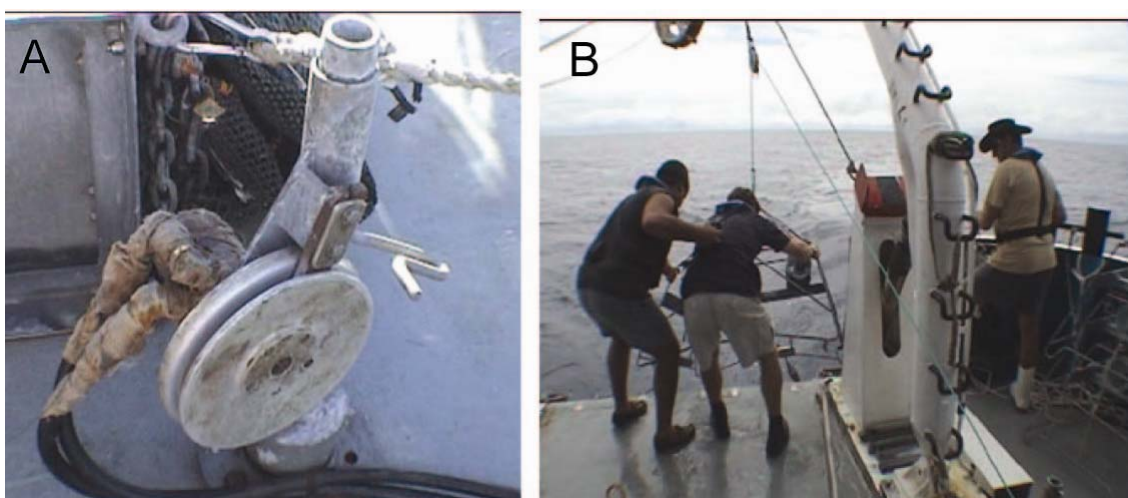


Figure 2.7. A grapple was cast to snag the buoy line and bring it through a snatch block for hauling with an hydraulic pot-hauler wheel (A).

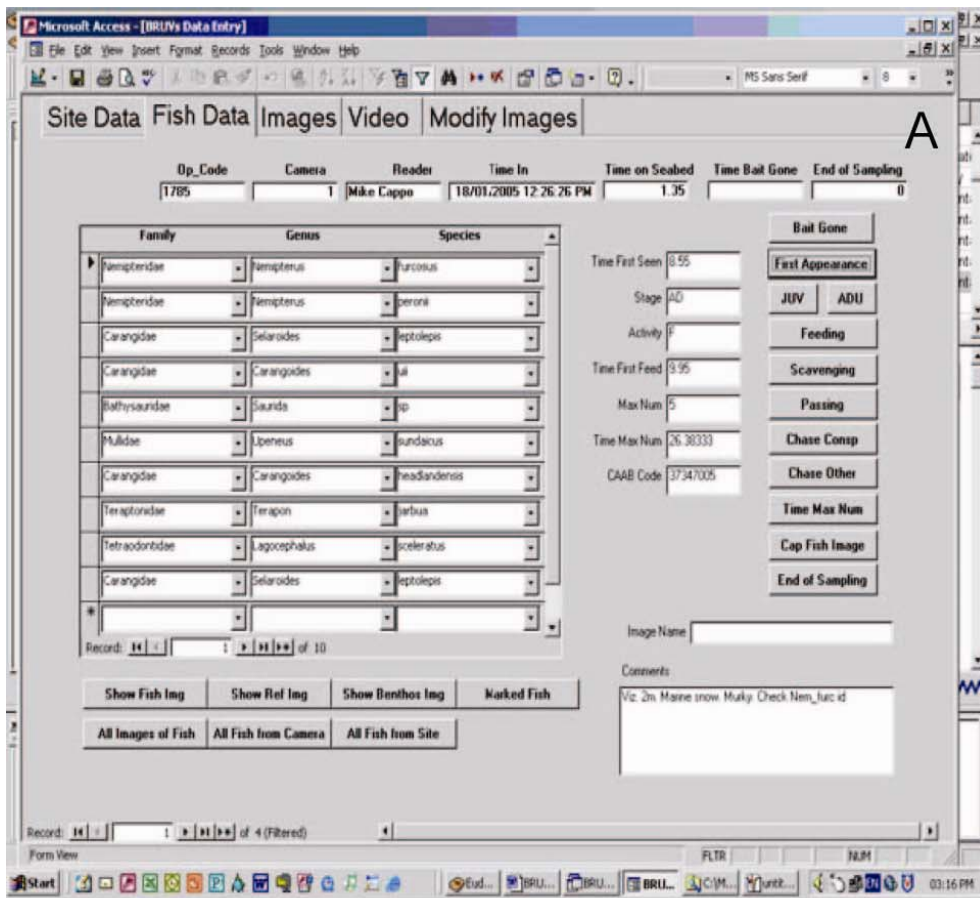
2.3 PROCEDURES FOR TAPE INTERROGATION

Interrogation of each tape was conducted using a custom interface (BRUVS2.1.mdb[©], Ericson and Cappo, unpublished, Australian Institute of Marine Science 2006) to *store* data from field operations and tape reading, to capture the timing of events and to capture reference images of the seafloor and fish in the field of view. Records were made, for each species, of the time of first sighting, stage (adult or juvenile), time of first feeding at the bait, the maximum number seen together in any one time on the whole tape (*MaxN*), time at which *MaxN* occurred, and the intraspecific and interspecific behaviour in eight categories.

Species identifications were made according to the Australian CAABCodes national standard (Yearsley *et al.* 1997) confirmed by checking the collection of reference images with museum taxonomists (Drs B. Hutchins, B. Russell, J. Johnson, and Mr D. Gledhill). It was decided some taxa were indistinguishable on video footage, so these were pooled at the level of taxa, genus, family or order. These taxa, hitherto referred to as species, were signified by the use of 'sp' or 'grp'. The *MaxN* data were then summed for each species over all single BRUVS replicates at a site. The term 'fish' hitherto refers to any marine vertebrate seen in the field of view, including sharks, rays and seasnakes.

The tapes were played in a Sony™ DSR20 tape deck with a jog shuttle control to a 50cm screen. The tape deck was connected via 'firewire' to the BRUVS2.1.mdb, where the video playback was also visible in small windows. The tape was played to and fro and the timecodes (converted to decimal minutes) of important events were captured via firewire from the tape deck. When a new fish was seen, drop-down menus in BRUVS2.1.mdb offered selections for family, genus and species. Once species was selected a CAABCODE was generated with the record. When certain 'events' buttons were selected, the timecode was downloaded from the tape deck and stored with the record. The tape deck was paused to allow capture of 'benthos' and 'fish' images, which were named by the software and distributed to folders. If the species was unknown, various buttons allowed the reference imagery to be searched for a match. If the species was new, a dialogue box enabled generation of custom CAABCodes and a description.

The BRUVS2.1.mdb added this data to, and called up, 'operations' data collected at sea when each BRUVS was deployed. The unique combination of a 'site' and a 'camera number' linked all records in all tables of the relational database. The database contained information on over 39,900 individual vertebrates seen during the course of fieldwork for this thesis, and over 17,000 images for reference by site, with 2,200 of the best reference images in the 'reference library' (Figure 2.8). These protocols, and the design, operation, and troubleshooting for BRUVS2.1.mdb were fully described in a manual. The software and manual can be obtained with the reference image library, under certain terms and conditions of use, by contacting BRUVS@aims.gov.au.



A



B

Figure 2.8. Tape interrogation interface from BRUVS2.1.mdb[©] (A). Reference image for *Pristipomoides multidens*, with *Lutjanus sebae*, *L. adetii* and *Epinephelus undulatostratus* and *E. areolatus* in the background (B).

2.4 STATISTICAL ANALYSES OF INDICES OF RICHNESS AND ABUNDANCE

The $MaxN$ for each species was summed over adults and juveniles within camera replicates, and transformed by 4th root to represent abundance of species i as $(\sum MaxN_i^{0.25})$. This transformation down-weighted highly abundant species and reduced skewness in the distributions of values for each species. Species columns were ranked in descending order of prevalence (rather than abundance) in the multivariate data sets, to enable quick filtering of analyses by species occurrence. The number of species was summed to represent species richness (S). A range of other indices were calculated and used in preliminary tests, including indices of taxonomic diversity and distinctness, Pielou's evenness, Simpson's index, and the Shannon-Weiner index (Warwick & Clarke 1998; Hall *et al.* 2006). None of these indices matched simple richness and abundance for ease of interpretation in describing fish assemblages, and they are not presented here.

I wished to develop models of univariate and multivariate responses, such as S , $\sum MaxN_i^{0.25}$ and occurrences of multiple species, to detect and describe patterns. To do this I used techniques based on boosted regression trees (BRT) and multivariate regression trees (MRT). These were introduced to the ecological literature only recently by De'ath (2002; 2007). This approach derives from both classification and regression trees (CART) starting with a data model (De'ath & Fabricius 2000) and from 'machine learning' where no data model is specified and algorithms are used to learn the relationship between a predictor and its response (Breiman 2001). Boosted regression trees are therefore an 'ensemble' method, whereby models are improved by first fitting many simple models and then combining them for prediction. BRT uses an algorithm from classification CART and a 'boosting' algorithm, which combines a collection of models (Elith *et al.* 2008).

Boosted regression trees are complex, but can be summarised in ways that give powerful ecological insight. Detailed descriptions for ecologists with worked examples are available in the papers cited above, and an excellent example of BRT applied to deep water trawl catches is given by Leathwick *et al.* (2006). Here I provide only a brief summary of those reviews, and the methods are best described in close reference to the presentation and interpretation of results in the following Chapters 5 and 6.

2.4.1 Classification and regression trees (CART)

Univariate tree-based models use simple rules to partition the 'predictor space' into rectangles to identify 'regions' having the most homogeneous responses to predictors. Classification trees fit the most probable 'class' as a constant for the region and regression trees fit the mean response

for observations in that region, assuming normally distributed errors. Growing a tree involves recursive binary splits, where a binary split is repeatedly applied to its own output until some criterion for stopping is reached. Predictors and splits are chosen to minimise prediction errors (Elith *et al.* 2008).

Splits are generally chosen to maximise the homogeneity of the resulting two nodes. This is also referred to as ‘minimisation of impurity’ where impurity is defined as the total sum of squared errors of the response variable about the node mean. Impurity takes the value zero when nodes are completely homogeneous. Each binary split minimises the total sum of squares of the response variable within the two nodes, which is equivalent to maximising the between nodes sums of squares (De’ath 2002). Large trees are grown, and then pruned by collapsing the weakest links identified by cross-validation. The terminal nodes, or ‘leaves’ represent the groups of data formed by the tree. Trees can be summarised by their size (number of leaves, or terminal nodes), and by overall fit, or relative error, which is the summed impurity of the leaves divided by the impurity of the undivided, root node (De’ath & Fabricius 2000). The ‘best’ tree has the property of giving the most accurate predictions, on average. The prediction error (PE), or accuracy, of a statistical model is a measure of how close model predictions are to their true values on average. It is dependent on the sum of the bias squared plus the variance and pure error. There is a trade-off between model complexity, bias and variance. Increasing model complexity by adding more parameters decreases bias, but increases variance, and vice-versa.

For smaller datasets ($n < 1,000$ cases), like those presented in this thesis, 5-10 fold cross-validation is used to compare PE in this trade-off. Firstly, the dataset is divided into 5-10 mutually exclusive subsets of approximately equal size (the ‘training’ data). Secondly, each subset in turn is dropped from the analysis, and a tree is grown using data from the remaining subsets. This tree is used to predict the responses for the omitted subset (the ‘test’ data). Thirdly, the estimated error for each subset is calculated. For a sums-of-squares regression tree, the error is the sum of squared differences of the observations and predictions. These errors are summed over all subsets. Fourthly, steps (2) and (3) are repeated for trees of each size. Finally, the tree with the smallest estimated error rate is selected (De’ath 2007).

Trees represent complex information in a visual way that is easily interpretable. They are robust and flexible, because explanatory (predictor) variables can be numeric, categorical, binary, or of any other type, and model outcomes are unaffected by transformations and different scales of measurement of the predictors. They are not sensitive to outliers, and handle missing data in predictors by applying best surrogates with little loss of information. Trees are hierarchical structures, and input variables at the tree leaves are dependent on input variables at higher

nodes. This allows simple modelling of complex, non-linear interactions that simply cannot be handled by other approaches (see examples in De'ath 2007). Fitting multiple trees in BRT overcomes the relatively poor predictive power of single trees.

The degree to which predictors interact in determining the response can be determined by examining the change in the PE with increasing tree size. For trees comprising a single split, the estimated response depends only on main effects, but trees with two splits include first-order interactions, trees with three splits include up to second-order interactions, and so on. Thus a large increase in the PE from trees of size 2 to size 3, but relatively stable PE for larger trees in the sequence, would indicate strong first-order interactions but no higher-order interactions of importance. The partial dependencies between the response and subsets of different predictors can be quantified to identify precisely which predictors are involved in these interactions (De'ath 2007).

2.4.2 Boosting

For regression tree problems, Elith *et al.* (2008) conceptualised boosting as a form of 'functional gradient descent'. A 'loss function' represents the loss in predictive performance (measured by deviance, for example) due to a suboptimal model. Boosting can then be seen as a numerical optimisation technique that minimises the loss function by adding, at each step, a new tree that 'steps down the gradient' of (reduces) the loss function. For BRT, the first regression tree is selected to reduce the loss function to the maximum extent possible for the given tree size. For the second step, the focus is on the residuals of the original tree and the new tree may split on different predictors. After this step the model is updated to contain the two trees as two terms, and the residuals from this two-term model are calculated. A third tree is grown from these residuals, and so on. The process is stage-wise, because existing trees are left unchanged as the model is enlarged. Only the fitted value for each observation is changed at each step to represent the contribution of the newly added tree. This contribution is 'shrunk' by a learning rate substantially less than one, because the model-building process performs best if it progresses slowly down the gradient in the loss function. The sequential fitting of trees increasingly focusses on the hardest observations to predict. Thus the final BRT model is a linear combination of thousands of trees that can be thought of as a regression model where each term is a tree.

The performance of gradient boosting is also improved by injecting randomness into the sequential fitting (see Friedman 2001; 2002). This involves taking sub-samples of the training data (typically 40-60%) for each iteration (De'ath 2007). This is termed the 'bag fraction'. It can

be conceived that if the perfect fit was indeed a single tree, the stochastic gradient boosting process would fit a sum of identical, shrunken versions of this single tree. ‘Regularisation’ of the process is applied to avoid overfitting (Elith *et al.* 2008). This is done in the relevant ‘R’ libraries by specifying the learning rate as a ‘shrinkage parameter’ determining the contribution that each new tree makes to the growing model, and the tree complexity, or ‘interaction depth’, which controls the interactions amongst the predictors to be fitted. A ‘tree complexity’ of 1 implies a single decision ‘stump’ with two terminal nodes (leaves). This will fit an additive model of only the main effects. An interaction depth of 3 will have two decision nodes and three terminal nodes, and will fit a model with up to three-way interactions, and so on. These two specifications determine the number of trees to be fitted for optimal prediction.

A vector specifying the slope of the function relating the response to each predictor can also be used. A parameter of 0 implies the functions can take any shape; 1 implies a monotonic increase; and -1 implies a monotonic decrease. For the value 1 the sign of the slope of the function is always positive (the curve of partial dependence plots tending upwards) or zero (non-decreasing or asymptotic, or depicted as a horizontal, flat line). Likewise, the value -1 constrains the sign of the slope to tend always downwards on partial dependence plots, or be zero.

The specification of a distribution for the loss function is foremost in using the boosting technique. For the species richness and transformed abundance data analysed here, the ‘Gaussian’ loss function was used. This function can be used to minimise squared error for continuous outcomes (responses) (Ridgeway 2000; 2007). The ‘Bernoulli’ distribution was used when the responses were classification outcomes, such as presence (1) or absence (0) of a species at a site. For tree-based methods the approximate ‘relative influence’ of a variable is the empirical improvement by splitting on that variable at a particular point (node). Friedman’s (2001) extension to boosted models was to average the relative influence of each variable across all the trees generated by the boosting algorithm.

2.4.2.1 Reporting prediction errors

This thesis relied heavily on the reporting of prediction errors. An example is described here to explain the basic implications of these statistics. In the case of analyses of presence or absence of a species at n sites, the data can be envisioned as an $n \times n$ matrix of zeroes (absences) and ones (presences). Once the model was fitted, an $n \times n$ matrix of predictions was constructed. The two matrices were compared by cross-tabulating the observations with the predictions. Three basic statistics were drawn from the cross-tabulation. The ‘*sdt*’ was the sum of the diagonals of the table, and it represented the total number of sites for which the predictions were correct. The ‘prediction error’ was the number of sites for which the predictions were incorrect,

which was simply the number of sites, n , minus the sdt ($\text{pred.err} = n - sdt$). The ‘variation in the response explained’ by the model was sdt / n , or $(1 - \text{rel.pred.err})$. The ‘relative prediction error’ was the proportion of the overall number of sites for which the predictions were wrong ($\text{rel.pred.err} = 1 - sdt / n$).

2.4.3 Multivariate regression trees (MRT)

The BRT approach can be extended by replacing the univariate response by a multivariate response, such as the abundances or occurrence of a large number of species at each site (see De’ath 2002). The impurity measures are redefined as sums of squares about the multivariate mean, which is simply the sum of squared Euclidean distances (SSD) of sites about the node centroid in geometrical terms. Each split minimises the SSD of sites from the centroids of nodes to which they belong. This is equivalent to maximising the SSD between node centroids. Each terminal node (leaf) can be defined by the multivariate mean of its sites, the predictors that define it, the number of sites that grouped there, and by species indicators (see Chapter 2.4.4). A comparison of the MRT with unconstrained, k -means clustering can be used to determine if the tree constrained by predictor variables is accounting for all the groups in the species data. If not, there is some unconstrained variation that is being caused by other variables not included in the analysis.

The species that influence the splits most in the tree can be determined in tabular form by partitioning the total species variance by each split of the tree, by the whole tree and by the total for each species (see De’ath 2002). The structure of the multivariate responses can be examined by plotting them in a low-dimensional space using principal components analysis. The ‘distance biplot’ is most appropriate, and species scores projected onto the biplot are located closest to node centroids where they are most abundant.

For data characterised by moderate to high alpha diversity, relationships between species dissimilarity and ecological distance can be enhanced by the choice of an appropriate similarity measure and use of extended dissimilarity (De’ath 1999). Dissimilarity matrices were used to grow MRT for some analyses in Chapters 3 and 4. If the dissimilarities are Euclidean distances, a distance-based (db) MRT will be exactly equivalent to the MRT based on SSD (SS-MRT). I used the extended, site standardised Manhattan distance for dbMRT (De’ath 1999). This distance is ‘Euclidean embeddable’, implying that a principal coordinates analysis (PCoA) generates site coordinates where the Euclidean distances between sites are directly proportional to the dissimilarities of sites. Using these coordinates as the responses in an SS-MRT will provide a tree identical to the dbMRT, and in a more efficient manner (De’ath 2002).

In cases where beta-diversity (species turnover) is high many sites will have no species in common, and ordinations will under-estimate true ecological distance, thereby ‘bending’ such sites toward each other when environmental gradients are portrayed in low-dimensional space. De’ath (1999) developed the extended, site standardised Manhattan distance to overcome this ‘horseshoe effect’, and I used this metric, hitherto referred to as ‘*xdiss*’, in all distance-based ordinations and MRT in the thesis.

2.4.4 Species indicators for site groups

Indicator values (DLI; Dufrêne & Legendre 1997) can be calculated for each species for each node of the trees. For a given species and a given group of sites, the DLI is defined as the product of the mean species abundance occurring in the group divided by the sum of the mean abundances in all other groups (specificity), times the proportion of sites within the group where the species occurs (fidelity), multiplied by 100. The DLI has a maximum value of 100 if the species occurs at all sites in the group and nowhere else. Each species can be associated with the tree node (assemblage) where its maximum DLI value occurred. The index distinguishes between ubiquitous species that dominate many groups in absolute abundance, and species that occur consistently within single groups but have low abundance (Dufrêne & Legendre 1997). This enables use of the numbers of indicator species and their values to characterise each node of the trees. The DLI for species at the root node are simply the prevalence of those species in the entire dataset. Species with high DLI can be used as characteristic representatives of each assemblage, and the spatial extent of the group indicates the region where the species was predominantly found.

2.4.5 Smoothing splines

Selected responses and explanatory variables were mapped in two-dimensional space using generalized additive models ($\text{gam}()$). Rather than just treating them as residuals, this approach incorporates non-linearities in the relationship between a response (such as species richness, or measurements of environmental covariates) and the position of the sampling sites ‘across’ and ‘along’ the GBRMP shelf. In simple terms, the $\text{gam}()$ used here in Chapters 5 and 6 employed a scatterplot smoother to let the data itself suggest terms representing the non-linearities (Venables & Ripley 2002). These terms are called ‘smoothing splines’. The flexible $\text{gam}()$ does not require the non-linear terms to be parametric or polynomial. The smoothing spline minimises least squares in a ‘penalized’ fashion that controls the trade-off between fidelity to the data cloud and smoothness. I overlaid the colour-contoured plots of the model fits with symbols scaled by the measurements of the response at each BRUVS site. This gave a direct

visualisation of the smoothed fit in relation to both the original data and the boundaries of the entire GBRMP.

2.4.6 Statistical software

All analyses used the open-source 'R' statistical package ('R' Development Core Team 2006). 'R' is a free software environment for statistical computing and data visualisation, maintained on the Comprehensive 'R' Archive Network (CRAN). I used the public libraries 'mvpart', 'vegan', 'gbm', 'car', 'MASS', 'pixmap' and 'maptools', and another in the Ecology Archives ('gbmplus'; De'ath 2007)¹.

Functions 'taxondive' and 'taxdist' to calculate (and improve) the Warwick and Clarke (1998) indices of taxonomic diversity and distinctness were developed for my use by Prof. J. Oksanen (University of Oulu) in the package 'vegan'. Private libraries 'gdTools', 'gbmMV', 'veganFuns', 'gisTools', 'surfer.gam.aa', 'pintol' and 'omniRDA' were provided to me by Dr G. De'ath. These contained powerful functions designed for manipulation, analysis and illustration of data to explore complex interactions of species and communities with their environment, including measures of location and spread for categorical explanatory variables. I used the 'surfer.gam.aa' and 'geoPlot' functions to carry out the `gam()` smoothing. These were developed by Dr G. De'ath to analyse ecological data in the low-dimensional space of the position of sampling sites across and along the GBRMP. I overlaid the colour-contoured plots of `gam()` model fits (prepared with library `geoTools`) with symbols at each BRUVS site scaled by the measurements of the response. The freely available ImageMagick[®] software was used for manipulating image formats, and Adobe[®] Illustrator[®] was used to polish final illustrations. The bibliography was maintained in EndNote[®].

¹ <http://www.esapubs.org/Archive/ecol/E088/015/suppl-1.htm>

3. HOW DOES THE USE OF BAIT AFFECT ABILITY TO DISTINGUISH DEMERSAL FISH ASSEMBLAGES?

3.1 INTRODUCTION

Critics of the baited video technique persistently argued that there is selection for carnivores and scavengers at the expense of herbivores when bait is used to attract fish into the field of view, yet there were no empirical tests of this presumption in the literature until recently (Watson *et al.* 2005; Harvey *et al.* 2007), and it was apparently based on knowledge of the performance of fish traps (see Cappo & Brown (1996) for review). There were indeed striking differences recorded in catches of baited and unbaited fish traps on coral reefs, with a few families of predators (lutjanids, lethrinids and serranids) dominating catches of baited traps, and only herbivorous siganids and scarids predominating in unbaited sets of the same 'Z' traps (Newman 1990). However, video footage of the fauna around and outside 'Z' traps set in coral reef habitats showed that trap catches were an extremely biased representation of fish diversity regardless of the presence or absence of bait (Cappo & Speare 2004).

Baited video recorded higher species richness and abundance than unbaited video in shallow algal reefs (<10m), with significant interactions occurring between sampling location and topographic relief, and sampling technique and topographic relief (Watson *et al.* 2005). This interaction was caused by higher diversity in the more complex matrix and algal habitat of the high-relief limestone reef. There were numerous species recorded only by the baited video, including larger planktivores and carnivores (*Scorpiis*, *Heterodontus*, *Dasyatis* and *Seriola*). Rarity within the study area did not explain the absence of these genera from unbaited video, because they were sighted on 20-40% of the sites sampled.

The same type of comparison was made by Harvey *et al.* (2007) for both temperate and tropical habitats, but the analyses were aggregated by assigning species to one of ten 'trophic groups'. Of particular interest was the finding that the use of bait produced slightly more individuals and a higher species diversity of the 'herbivorous', 'invertebrate/algae' and 'algae/invertebrate' feeders. This result contradicted the common inferences about bait attractants made from fish trapping studies. In seagrass, algal reefs and deep sand habitats of the Great Australian Bight, there were significantly higher richness and abundance recorded by baited video for five of the eight trophic groups present. In the lagoon of the GBRMP, and adjacent to emergent and fringing coral reefs, higher mean abundance and richness were recorded when using bait for all tropical functional groups, with the exception of 'algae/invertebrate' and 'sponge/invertebrate' feeders. Greater numbers of individuals and species were recorded by baited than unbaited

video in both temperate and tropical marine habitats, and Harvey *et al.* (2007) considered this to be a major factor in improving the discrimination of these habitat types based on their fish assemblages. The ratio (baited:unbaited) of ‘allocation success’ of a Canonical Analysis of Principal Coordinates (CAP) was 1.15 for temperate habitats and 1.3 for tropical habitats.

In this chapter I examine these differences in detail with a more comprehensive dataset, with particular scrutiny of the indicator species and sources of mis-classification of site groups. I compare the performance of video sampling with (BRUVS) and without bait (RUVS) in the deep (>30m) channels between the Palm Islands, and the deep (>40m) lagoon, inter-reef shoals and reef bases of the central GBRMP. My objectives were three-fold. Firstly, I aimed to use linear, univariate models to quantify differences in species richness and abundance. The tests in these models used the presence or absence of bait as a fixed factor, and the location of the sampling as a random factor. Secondly, I used multivariate regression tree (MRT) analyses to distinguish groups in the abundance data at the level of both species and families, and find “indicators” of baited and unbaited video sets. Prevailing criticism of the use of BRUVS concerns bias away from herbivorous groups, so such a bias should be detectable by an examination of the indicators and groupings in the MRT. However, arbitrarily assigning species to trophic groups has proven problematic in the past (see Bellwood 1998), so I used family-level MRT analyses to test if scarids, chaetodontids, siganids and other “non-predatory” families were indicators for unbaited sampling. Finally, an examination of “performance” when comparing techniques (such as baited and unbaited video) should not be limited to comparing metrics such as richness and abundance, or indicator species. Rather, it should test for errors in discriminating and predicting known groups. In this case, I test the success of each technique in discriminating and predicting known groups based on the fish assemblages detected by the MRT.

3.2 METHODS

Six remote underwater video stations of the design shown in Figure 2.1(A) were deployed about 300-450m apart along transects within coarse habitat types in an alternating sequence of baited and unbaited units. The bait canisters on baited units contained one kilogram of crushed pilchards *Sardinops neopilchardus*. A total of 126 one-hour deployments (sets) of baited (BRUVS) and unbaited (RUVS) units were made in the central section of the GBRMP near Calliope and Curacoa Channels in the Palm Islands, at Robbery Shoals offshore from the Palm Islands, Kelso Shoals, and around Rib and Davies Reefs (Figure 3.1). One hour samples were chosen on the basis of species-sampling time curves derived by Cappo *et al.* (2001) in the lagoon of a diverse oceanic atoll reef, where most species were sighted within the first 45 minutes of deployment (mean $\sim 12.3 \pm 6.9$), with an addition of less than one species, on

average, with an increase to 60 minutes soak time (13.5 ± 7.5). Doubling the time on the seabed to 90 minutes accumulated only an extra 3 species (15.3 ± 8.2).

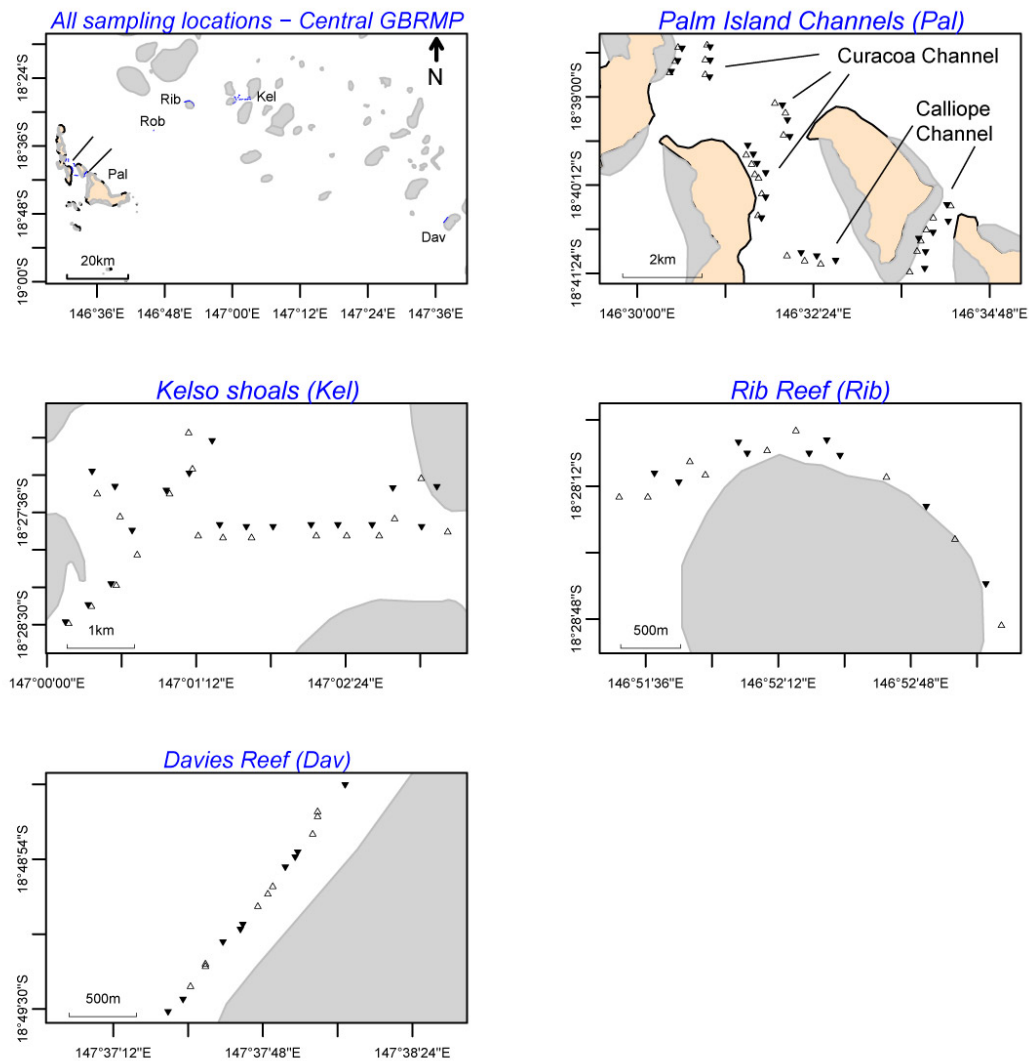


Figure 3.1. Location of video sampling sites in the central GBRMP. Triangle symbols represent baited BRUVS (filled symbols point upwards) and unbaited RUVS (open symbols point downwards).

3.2.1 Univariate analyses

Fish abundances and species richness were univariate responses to the effects of bait and location, and were analysed using univariate statistical approaches (`lmer`) with the R statistical package (R Development Core Team 2005). The *MaxN* data were overdispersed and highly skewed by counts made when shoals of pelagic fish passed the field of view, so raw data were analysed with a “quasipoisson” (or “log-link”) function (Ver Hoef & Boveng 2007). The univariate analyses assessed differences in species richness and abundances between the use of

bait (bait) and sampling location (location) using linear, mixed-effects models (`lmer`) with a quasipoisson link function. This approach can account for unbalanced sampling designs, and does not need prior transformation of raw data. The factor “bait” was fixed and “location” was random. The few samples (3 pairs of baited and unbaited video sets) from Robbery shoals were excluded from the analysis, leaving pairs of samples from Davies and Rib Reefs (each with 9 pairs), Kelso Shoals (18 pairs) and Palm Island Channels (24 pairs).

The null model for this design was:

$response \sim 1+(1|location)$

where the random effect of location was recognized, but all other main effects and interactions equated to an intercept of 1

The following models were compared with each other and the null model:

$response \sim bait*location+(1|location)$

where the interaction of bait and location was recognized, as well as allowing a different intercept for a possible effect of each location

$response \sim bait+(1|location)$

where no interaction of bait and location was recognized, but allowance was made for a different intercept for each location.

The most parsimonious model was chosen as the one with the lowest Akaike Information Criteria (AIC) in an analysis of variance of the two models.

3.2.2 Multivariate analyses

Multivariate regression tree (MRT) analyses were carried out on the entire dataset of transformed species abundances (4th root), including singletons (species seen only once). The data were then amalgamated at the level of family and analysed with MRT. In both cases the DLI (Dufrêne-Legendre Index) were calculated for each node of the trees. Extended, site-standardised Manhattan dissimilarities (*xdiss*) of transformed species abundances were used in Constrained Analysis of Principal Coordinates (CAP). This is an ordination method similar to Redundancy Analysis (*rda*), but it allowed non-Euclidean dissimilarity indices, such as *xdiss* or Bray-Curtis distance. Function `capscale` in library `vegan` was used as a constrained version of Principal Coordinates Analysis (PCoA). This function ordines the dissimilarity matrix using `cmdscale` and analyses these results using `rda` (Oksanen *et al.* 2009). Permutation tests were made for significant differences in ‘distance variation’ of constrained eigenvalues.

An extended assessment of the relative performance of baited and unbaited video sets was provided by testing their success in discriminating and predicting the fish assemblages represented by the six 'location' groups. This was done by using linear discriminant analysis (LDA) of the principal coordinates from the PCoA and by repeatedly and randomly excluding one video set and predicting its group membership from the other video sets.

3.3 RESULTS

There was an obvious trend for decreasing diversity and abundance from the mid-shelf reefs to the inshore channels and lagoonal shoals (Figure 3.2). The lack of overlap of notches representing (1.5 X interquartile range of $MaxN/SQRT(n \text{ samples})$) for all locations in the boxplots of Figure 3.2 was a robust test that the medians differed significantly between baited and unbaited samples. This test was independent of any assumptions about normality of data distributions or equivalence of variances (see Chambers et al. 1983, p. 62).

On average across locations, there were about 2.3 times as many species and 3.1 times as many individual fish recorded on baited BRUVS when compared to unbaited units (Table 3.1). However, Davies Reef sets had the highest diversity and abundance, and a lower ratio of baited: unbaited samples for species richness. This suggested that the habitats there had rich and abundant fish assemblages, and that video units could record relatively high diversity irrespective of the presence of bait.

Analysis of variance showed the most parsimonious model for both species richness and abundance to be $response \sim bait*location+(1/location)$ with a significant interaction of bait and location for Davies Reef, and different intercepts for the different locations (Table 3.1). This model had a deviance reduced by about 34% compared with the null model.

Simple comparison of the data showed a large number (85) of species from a wide range of families were seen only on baited BRUVS, but less than half this number (30) was sighted only on unbaited RUVS (Table 3.3). With the exception of a dasyatid stingray and an ostraciid boxfish, the families from which these thirty species came were also seen on baited BRUVS. There was no trend for large or small herbivores to be sighted only on unbaited RUVS. In fact, some herbivorous scarid parrotfish and siganid rabbitfish were sighted only when using bait.

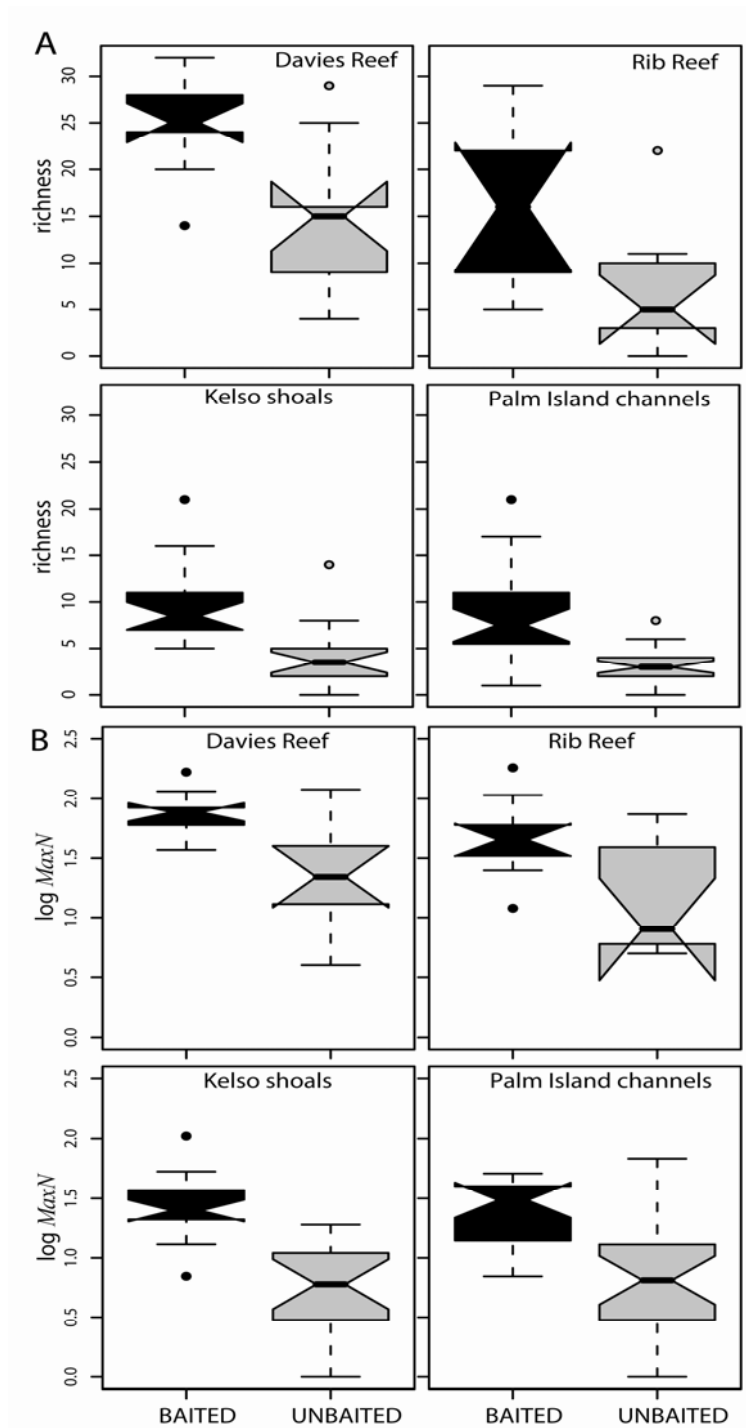













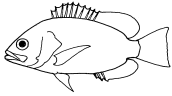









Figure 3.2. Box and whisker plots of the raw species richness (S) and transformed abundance ($\log_{10} MaxN$). The boxplots show the median and 95% Confidence Intervals. The notches represent $1.5 \times$ (interquartile range of $MaxN/SQRT(n)$). If the notches do not overlap this is ‘strong evidence’ that the two medians differ, independent of any assumptions about normality of data distributions or equivalence of variances (see Chambers *et al.* 1983, p. 62).



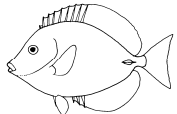
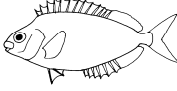

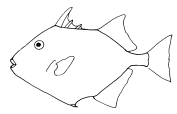
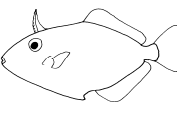
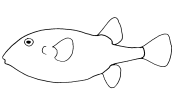

Table 3.1. Fitted, mean values of the effects of *bait X location + (1/location)* on species richness (*S*) and abundance (*MaxN*), using a quasipoisson link function to account for overdispersion in the raw data. The number of pairs of sets of baited (BRUVS) and unbaited (RUVS) video units are shown for each location (*n*). On average across locations, there were about 2.3 times as many species and 3.1 times as many individual fish recorded on baited BRUVS when compared to unbaited units.

Location	<i>n</i>	Richness <i>S</i> BRUVS	Richness <i>S</i> RUVS	Ratio <i>S</i> (Baited: Unbaited)	Abundance (<i>MaxN</i>) BRUVS	Abundance (<i>MaxN</i>) RUVS	Ratio (<i>MaxN</i>) (Baited: Unbaited)
Davies Reef	9	24.78	14.78	1.68	83.22	34.89	2.39
Rib Reef	9	16	7.11	2.25	61.36	26	2.36
Kelso Shoals	18	9.6	3.78	2.54	34.67	7.33	4.73
Palm Island Channels	24	8.5	3.17	2.68	28.89	9.63	3
Averages		14.72	7.21	2.29	52.04	19.46	3.12

Table 3.2. Species sighted only on baited BRUVS and only on unbaited RUVS.

Order: Family		Species seen only on baited BRUVS	Species seen only on unbaited RUVS
Orectolobiformes: Ginglymostomatidae		<i>Nebrius ferrugineus</i>	
Carcharhiniformes: Carcharhinidae		<i>Loxodon macrorhinus</i> , <i>Carcharhinus dussumieri</i> , <i>Negaprion acutidens</i> , <i>Rhizoprionodon taylori</i> , <i>C. melanopterus</i>	<i>Triaenodon obesus</i>
Carcharhiniformes: Sphyrnidae		<i>Sphyrna mokarran</i>	
Rajiformes: Rhinidae		<i>Rhynchobatus djiddensis</i>	
Myliobatiformes: Myliobatidae		<i>Aetobatus narinari</i>	
Myliobatiformes: Dasyatidae			<i>Dasyatis kuhlii</i>
Anguilliformes: Muraenidae		<i>Gymnothorax favagineus</i> , <i>G. flavimarginatus</i> , <i>G. chilospilus</i> , <i>G. undulatus</i>	
Gasterosteiformes: Fistulariidae		<i>Fistularia commersonii</i>	
Perciformes: Serranidae		<i>Cephalopholis miniata</i> , <i>C. sp</i> , <i>Epinephelus</i> <i>areolatus</i> , <i>E. rivulatus</i> , <i>E. quoyanus</i> , <i>E. malabaricus</i> , <i>Plectropomus laevis</i>	<i>E. fasciatus</i> , <i>C. argus</i>
Perciformes: Rachycentridae		<i>Rachycentron canadum</i>	
Perciformes: Carangidae		<i>Elagatis bipinnulata</i> , <i>Carangoides plagiotaenia</i> , <i>C. sp</i>	

Order: Family		Species seen only on baited BRUVS	Species seen only on unbaited RUVS
Perciformes: Lutjanidae		<i>Lutjanus sebae</i> , <i>L. erythropterus</i> , <i>L. argentimaculatus</i> , <i>L. lemniscatus</i> , <i>L. bohar</i> , <i>L. adetii</i> , <i>L. fulviflamma</i> , <i>L. russelli</i> , <i>Pristipomoides sp.</i>	<i>Anthias sp.</i>
Perciformes: Nemipteridae		<i>Nemipterus nematopus</i> , <i>N. peronii</i> , <i>N. sp2 (stripe)</i>	
Perciformes: Lethrinidae		<i>Lethrinus lentjan</i> , <i>L. laticaudis</i> , <i>L. rubrioperculatus</i> , <i>L. ornatus</i> , <i>L. sp.</i> , <i>Gymnocranius sp</i>	<i>L. genivittatus</i> , <i>L. erythracanthus</i> , <i>Monotaxis grandoculis</i>
Perciformes: Sparidae		<i>Argyrops spinifer</i>	
Perciformes: Mullidae		<i>Parupeneus pleurostigma</i> , <i>Parupeneus barberinoides</i>	
Perciformes: Ehippidae		<i>Platax batavianus</i>	<i>Platax teira</i>
Perciformes: Pomacanthidae		<i>Chaetodontoplus duboulayi</i> , <i>Chaetodontoplus conspicillatus</i> , <i>Centropyge tibicen</i>	<i>Pomacanthus imperator</i> , <i>Centropyge bicolor</i>
Perciformes: Chaetodontidae		<i>Chaetodon auriga</i> , <i>C. aureofasciatus</i> , <i>C. kleinii</i>	<i>Parachaetodon ocellatus</i>
Perciformes: Pomacentridae		<i>Amblyglyphidodon aureus</i> , <i>A. curacao</i> , <i>Dascyllus trimaculatus</i> , <i>D. reticulatus</i> , <i>Pomacentrus wardi</i> , <i>Stegastes apicalis</i>	<i>Chromis margaritifer</i> , <i>Chromis nitida</i> , <i>Chromis xanathochira</i> , <i>Chrysiptera talboti</i> , <i>Lepidozygus tapeinosoma</i> , <i>Pomacentrus nigromarginatus</i>
Perciformes: Sphyraenidae		<i>Sphyraena jello</i>	<i>Sphyraena obtusata</i>

Order: Family		Species seen only on baited BRUVS	Species seen only on unbaited RUVS
Perciformes: Labridae		<i>Cheilinus trilobatus</i> , <i>Bodianus mesothorax</i> , <i>C. oxycephalus</i> , <i>Oxycheilinus unifasciatus</i> , <i>Hologymnosus doliatus</i>	<i>Bodianus loxozonus</i> , <i>Choerodon jordani</i> , <i>Hemigymnus fasciatus</i> , <i>Cirrhilabrus sp.</i>
Perciformes: Scaridae		<i>Cetoscarus bicolour</i> , <i>Scarus niger</i>	
Perciformes: Acanthuridae		<i>Acanthurus dussumieri</i> , <i>A. nigroris</i> , <i>Naso annulatus</i> , <i>N. vlamingii</i>	<i>Naso lituratus</i> , <i>Naso unicornis</i>
Perciformes: Siganidae		<i>Siganus argenteus</i> , <i>S. javus</i> , <i>S. puellus</i>	
Perciformes: Scombridae		<i>Scomberomorus queenslandicus</i> , <i>Euthynnus affinis</i>	
Tetraodontiformes: Balistidae		<i>Balistoides conspicillum</i> , <i>Balistapus undulates</i> , <i>Balistoides viridescens</i> , <i>Sufflamen bursa</i>	<i>Pseudobalistes flavimarginatus</i>
Tetraodontiformes: Monacanthidae		<i>Paramonacanthus otisensis</i>	<i>Aluterus scriptus</i> , <i>Cantherhines dumerilii</i> , <i>Pervagor janthinosoma</i>
Tetraodontiformes: Tetraodontidae		<i>Lagocephalus sceleratus</i> , <i>Arothron stellatus</i> , <i>Feroxodon multistriatus</i> , <i>A. nigropunctatus</i>	
Tetraodontiformes: Ostraciidae			<i>Lactoria sp.</i>

The MRT analysis of all species had a high prediction error of nearly ninety percent, but this was not surprising given the inclusion of singletons and the very high alpha diversity (210 species) in the response (Figure 3.3). The first split in the MRT separated the mid-shelf ‘reef’ locations from both the Palm Island channels and the mid-shelf ‘shoals’ locations. On the reef side of the tree, Davies and Rib Reefs were split from each other and then split symmetrically within each reef location by the presence or absence of bait. No baited BRUVS sets were included in the ‘unbaited’ location groups for reefs, and vice-versa (Figure 3.3). On the other side of the tree, ‘shoals’ and ‘channels’ were split from each other, and there was symmetry in the terminal nodes representing baited and unbaited treatments in the ‘shoals’ location group. On the ‘channels’ side of the terminal splits, Calliope and nearby Curacoa channels were distinguished on baited BRUVS, but not unbaited RUVS.

The plots of mean species abundance under the terminal nodes in the MRT (Figure 3.3) showed that ‘unbaited’ leaves of the tree were characterised by both lower abundances and lower species diversity. This was also strongly reflected in the analysis of DLI values (Table 3.3). Only nine species (4.2%) in the MRT had high DLI >50 and all of these, with the exception of *Pentapodus paradiseus*, were located on the ‘reefs’ branches. About 23% (48 species) had moderate values ($50 > \text{DLI} > 20$) and most of these were characteristic of the ‘baited’ leaves of the tree. Davies Reef had relatively large numbers of indicator species with moderate to high values on both baited (82%) and unbaited (18.7%) leaves. The leaves representing channel and shoal locations without bait had few indicator species, with very low $\text{DLI} < 12$.

Strong within-genera differences in distributions of lethrinids, labrids and mullids were identified by the MRT in the reef branches. Amongst the small lethrinids, *Lethrinus semicinctus* was characteristic of Davies Reef, but *L. ravus* was representative of the Rib Reef baited leaf. The larger *Lethrinus miniatus* was more common at Davies, and its bigger congener *L. nebulosus* had highest DLI at Rib Reef. The labrid *Choerodon fasciatus* was ubiquitous at Davies Reef and its congener *C. venustus* was characteristic of the Rib-Baited node. The goatfish *Parupeneus multifasciatus* had high DLI at “Davies-Baited”, whereas *P. heptacanthus* predominated at “Rib-Baited”.

Monacanthids and tetraodontids were notable on the off-reef branches of the tree, and the species with the highest DLI inshore were the piscivorous school mackerel *Scomberomorus queenslandicus* and the benthic omnivore *Pentapodus paradiseus*. In general terms the shoals nodes were characterised by a lack of species, and a lower abundance of the ubiquitous species identified at the root node, or stump (Figure 3.3). There was no evidence in Figure 3.3 and Table 3.3 that herbivores were more abundant or prevalent on unbaited branches of the tree.

Herbivorous scarids and siganids were not expected to be in high numbers in the depths sampled, but nonetheless *Scarus flavipectoralis* was ubiquitous at Davies Reef, and *Scarus ghobban* and *Siganus argenteus* were characteristic of baited BRUVS at Davies Reef, with moderate DLI values.

A MRT of the same data amalgamated at the level of family also showed no bias toward particular trophic groups (Figure 3.4). The primary splits occurred on reef and off-reef locations, followed by the presence or absence of bait. Channels and shoal sets without bait were remarkably depauperate, especially when compared with the diverse reef sets. The few families indicative of unbaited terminal nodes were not common, nor were they from functional groups normally associated with herbivory, corallivory or detritivory. In contrast, chaetodontids normally associated with corallivory were representative of baited, reef branches of the tree, and acanthurids and siganids had highest DLI on the terminal node at Davies Reef for baited BRUVS.

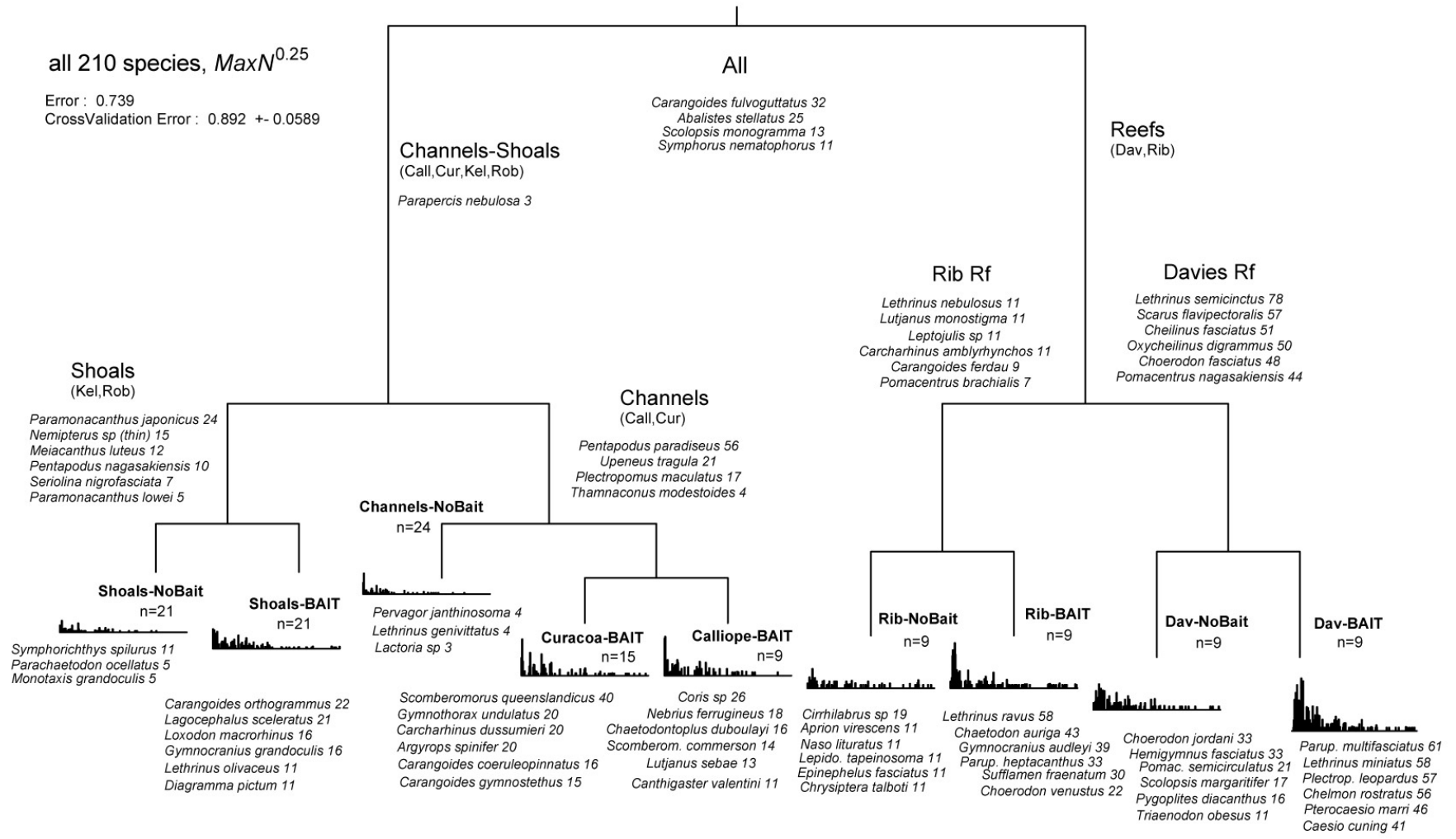


Figure 3.3. Multivariate regression tree analysis (MRT) of the transformed abundance of all 210 species at 126 sites. The top six species indicators are shown with DLI values at each node.

Table 3.3. Node names and species indicators (DLIs) for the terminal nodes (leaves) of the MRT examining the effects of bait (Figure 3.3). The number of sites in the groups are shown, and the percentage of moderate DLIs (>19) are outlined in brackets for each node. The ranges and means \pm standard deviation (in brackets) are given for raw abundance ($\text{abund} = \sum_i^p \text{Max}N_i$) and richness.

Node name (%moderate DLI)	Nsites	DLIs	abund	richness
Shoals-NOBAIT (-)	21	<i>Symphoricthys spilurus</i> (11), <i>Parachaetodon ocellatus</i> (5), <i>Monotaxis grandoculis</i> (5)	0-19 (65 \pm 57)	0-14 (34 \pm 31)
Shoals-BAIT (11.7%)	21	<i>Carangoides orthogrammus</i> (22), <i>Lagocephalus sceleratus</i> (21), <i>Loxodon macrorhinus</i> (16), <i>Gymnocranius grandoculis</i> (16), <i>Lethrinus olivaceus</i> (11), <i>Diagramma pictum</i> (11), <i>Nemipterus nematopus</i> (8), <i>Sufflamen bursa</i> (5), <i>Rhizoprionodon taylori</i> (5), <i>Rachycentron canadum</i> (5), <i>Nemipterus peronii</i> (5), <i>Negaprion acutidens</i> (5), <i>Lutjanus bohar</i> (5), <i>Lethrinus</i> sp (5), <i>Carangoides plagiotaenia</i> (5), <i>Balistoides viridescens</i> (5), <i>Arothron nigropunctatus</i> (5)	2-105 (303 \pm 277)	1-21 (85 \pm 46)
Channels-NOBAIT (-)	24	<i>Pervagor janthinosoma</i> (4), <i>Lethrinus genivittatus</i> (4), <i>Lactoria</i> sp (3)	0-68 (96 \pm 137)	0-8 (32 \pm 19)
Curacoa-BAIT (25%)	15	<i>Scomberomorus queenslandicus</i> (40), <i>Gymnothorax undulatus</i> (20), <i>Carcharhinus dussumieri</i> (20), <i>Argyrops spinifer</i> (20), <i>Carangoides coeruleopinnatus</i> (16), <i>Carangoides gymnostethus</i> (15), <i>Rhynchobatus djiddensis</i> (14), <i>Arothron stellatus</i> (13), <i>Paramonacanthus otisensis</i> (7), <i>Sphyrna mokarran</i> (7), <i>Pristipomoides</i> sp (7), <i>Platax batavianus</i> (7), <i>Nemipterus</i> sp2 (stripe) (7), <i>Gymnothorax favagineus</i> (7), <i>Gymnothorax chilospilus</i> (7), <i>Euthynnus affinis</i> (7)	8-50 (291 \pm 128)	1-21 (81 \pm 51)
Calliope-BAIT (7%)	9	<i>Coris</i> sp (26), <i>Nebrius ferrugineus</i> (18), <i>Chaetodontoplus duboulayi</i> (16), <i>Scomberomorus commerson</i> (14), <i>Lutjanus sebae</i> (13), <i>Canthigaster valentini</i> (11), <i>Stegastes apicalis</i> (11), <i>Pomacentrus wardi</i> (11), <i>Parupeneus barberinoides</i> (11), <i>Cheilinus oxycephalus</i> (11), <i>Lutjanus vitta</i> (9), <i>Lutjanus carponotatus</i> (8), <i>Pastinachus sephen</i> (8), <i>Meiacanthus lineatus</i> (8)	7-51 (284 \pm 171)	5-17 (92 \pm 36)

Node name (%moderate DLI)	Nsites	DLIs	abund	richness
Rib-NOBAIT (-)	9	<i>Cirrhilabrus sp</i> (19), <i>Aprion virescens</i> (11), <i>Naso lituratus</i> (11), <i>Lepidozygus tapeinosoma</i> (11), <i>Epinephelus fasciatus</i> (11), <i>Chrysiptera talboti</i> (11), <i>Chromis xanthochira</i> (11), <i>Chromis nitida</i> (11), <i>Chromis margaritifer</i> (11), <i>Cephalopholis argus</i> (11), <i>Bodianus loxozonus</i> (11), <i>Anthias sp</i> (11), <i>Sphyraena obtusata</i> (11), <i>Dasyatis kuhlii</i> (9), <i>Lutjanus malabaricus</i> (7)	0-74 (26 ± 282)	0-22 (71 ± 66)
Rib-BAIT (37.5%)	9	<i>Lethrinus ravus</i> (58), <i>Chaetodon auriga</i> (43), <i>Gymnocranius audleyi</i> (39), <i>Parupeneus heptacanthus</i> (33), <i>Sufflamen fraenatum</i> (30), <i>Choerodon venustus</i> (22), <i>Lutjanus adetii</i> (19), <i>Parupeneus indicus</i> (16), <i>Gnathanodon speciosus</i> (16), <i>Carangoides chrysophrys</i> (15), <i>Heniochus acuminatus</i> (11), <i>Lutjanus fulviflamma</i> (11), <i>Lutjanus erythropterus</i> (11), <i>Lutjanus argentimaculatus</i> (11), <i>Lethrinus ornatus</i> (11), <i>Hologymnosus doliatus</i> (11)	12-181 (613 ± 522)	5-29 (16 ± 88)
Dav-NOBAIT (18.7%)	9	<i>Choerodon jordani</i> (33), <i>Hemigymnus fasciatus</i> (33), <i>Pomacanthus semicirculatus</i> (21), <i>Scolopsis margaritifer</i> (17), <i>Pygoplites diacanthus</i> (16), <i>Triaenodon obesus</i> (11), <i>Pseudobalistes flavimarginatus</i> (11), <i>Platax teira</i> (11), <i>Pomacanthus imperator</i> (11), <i>Naso unicornis</i> (11), <i>Lethrinus erythracanthus</i> (11), <i>Centropyge bicolor</i> (11), <i>Cantherhines dumerilii</i> (11), <i>Aluterus scriptus</i> (11), <i>Pomacentrus nigromarginatus</i> (8), <i>Thalassoma lunare</i> (7)	4-119 (349 ± 359)	4-29 (148 ± 82)
Dav-BAIT (82%)	9	<i>Parupeneus multifasciatus</i> (61), <i>Lethrinus miniatus</i> (58), <i>Plectropomus leopardus</i> (57), <i>Chelmon rostratus</i> (56), <i>Pterocaesio marri</i> (46), <i>Caesio cuning</i> (41), <i>Cephalopholis miniata</i> (40), <i>Pomacanthus sexstriatus</i> (35), <i>Siganus argenteus</i> (31), <i>Sufflamen chrysopterum</i> (25), <i>Scarus ghobban</i> (23), <i>Plectropomus laevis</i> (22), <i>Naso annulatus</i> (22), <i>Chrysiptera rollandi</i> (21), <i>Choerodon vitta</i> (19), <i>Pentapodus sp2</i> (18), <i>Dascyllus trimaculatus</i> (15)	37-167 (832 ± 379)	14-32 (248 ± 53)

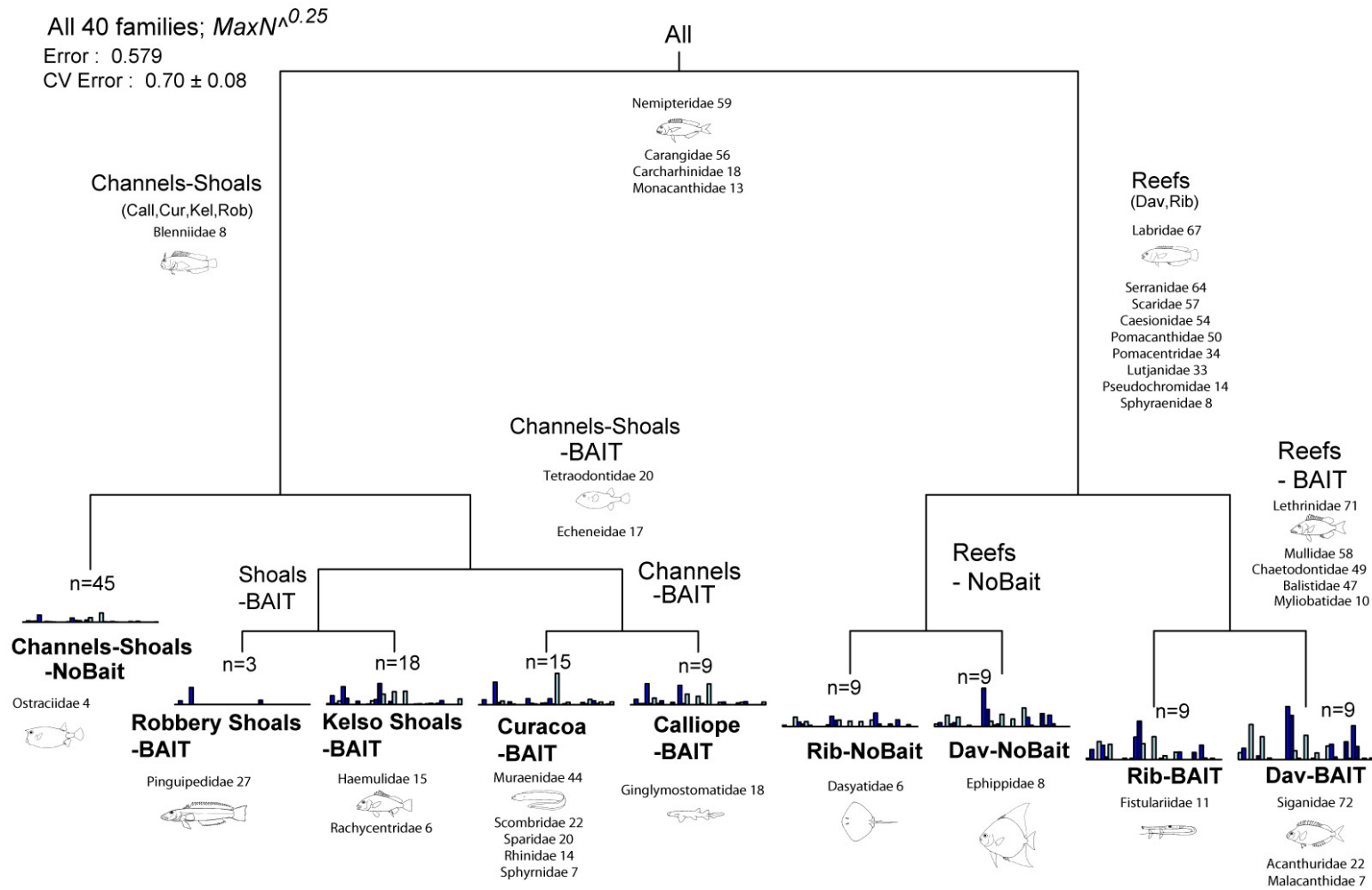


Figure 3.4. Multivariate regression tree analysis (MRT) of the transformed abundance of all 40 families at 126 sites. The top six indicator families are shown with DLI values at each node.

Species accumulation curves for the nine terminal nodes in Figure 3.4 indicated that the limited number of sets was still ascending in terms of representing the true species diversity of each assemblage (Figure 3.5). More importantly, it was clearly evident that unbaited RUVS would never match the baited BRUVS in terms of accumulating species richness, independent of any level of replication. The trends in the pairs of curves were either diverging or parallel, with unbaited RUVS sets consistently 10-30 species behind baited BRUVS. The difference was least in highly diverse coral reef assemblages, and greatest in depauperate shoal communities.

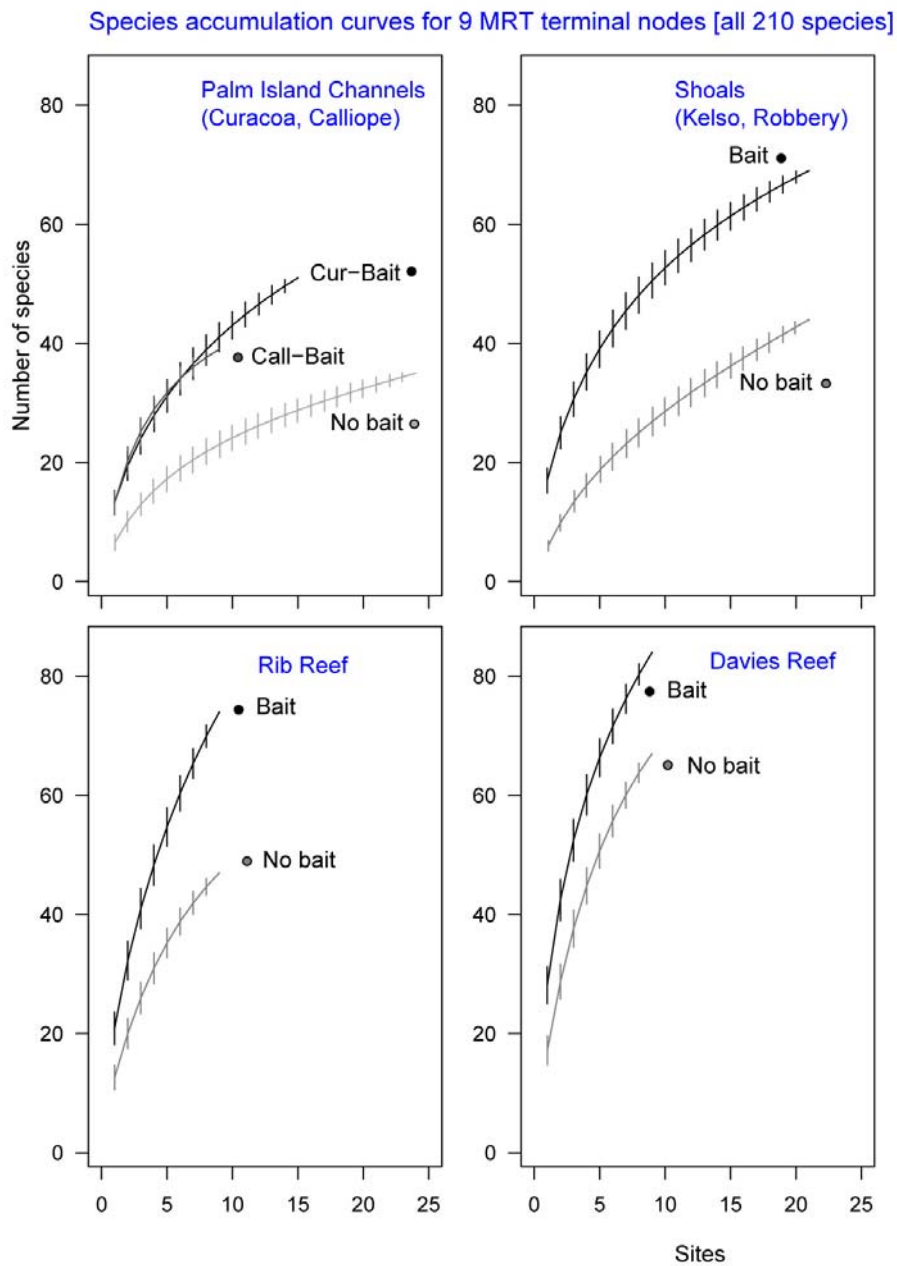


Figure 3.5. Species accumulation curves for the nine terminal nodes of the MRT in Figure 3.3.

The six location groups, or species assemblages, accounted for 56% of the ‘distance variation’ for the baited BRUVS, and only 14% for the unbaited RUVS (Table 3.4). Permutation tests for significance of all constrained eigenvalues were significant for baited BRUVS (Pseudo- $F = 64.47$, $p < 0.001$), but not for unbaited RUVS (Pseudo- $F = 4.89$, $p = 0.151$).

Table 3.4. Distance-based redundancy analysis of full dissimilarity matrices for transformed baited (BRUVS) and unbaited (RUVS) samples at 63 sites in six locations. MSEd = the Mean Square of Euclidean distance.

Effect	<i>df</i>	BRUVS			RUVS		
		MSEd	Pseudo- F	P	MSEd	Pseudo- F	P
Location (locn)	5	322.1	14.6	<0.001	0.65	1.81	0.041
Residual	57	251.2			3.93		
Total		573.3			4.57		
%explained		56.1			14.2		

Polygons shown in Figure 3.6 outlined the individual video sets and the centroids of group means in the PCoA. Eigenanalysis of the variance extracted by each axis showed the first two axes explained 83% of the total ‘distance variation’ (~56%) for baited BRUVS, and only 42% of the distance variation for the unbaited RUVS (~14%). The scale of distance variation for baited BRUVS was more than ten times that of unbaited RUVS, and clearly separated ‘reef’ locations from ‘shoal’ and ‘channel’ locations on the first dimension. Davies Reef and the two Palm Island channels were also displaced along the second axis (Figure 3.6A). In contrast, there was very poor separation of unbaited RUVS sets along both axes, with the centroids close to the origin (Figure 3.6B).

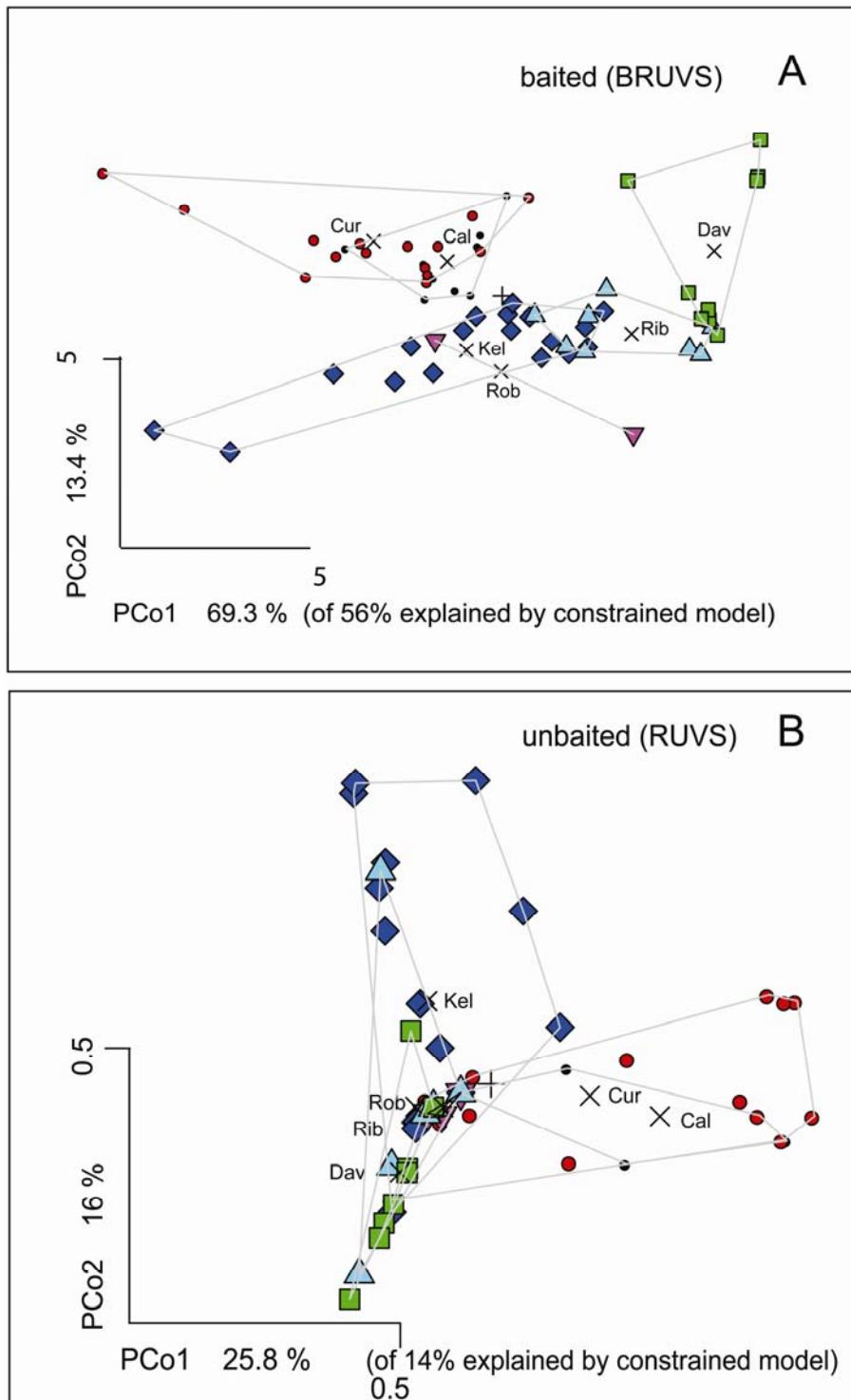


Figure 3.6. Principal Coordinates Analysis (PCoA) of baited (BRUVS, A) and unbaited (RUVS, B) video units. Group means of the six locations are shown.

The PCoA solution provided the coordinates, or “location” in multivariate space, of each of the 63 video sets in each treatment along each of 8 dimensions. The linear discriminant analysis (LDA) made a regression of the site grouping (the six levels of sampling location) of each video set on the sum of these principal coordinates ($location \sim a+b+c+d+e+f+g+h$). Given there were six levels of sampling location, the LDA provided coefficients for five linear discriminants, and the percentage of the overall variation between the six “location groups” explained by each discriminant. Linear discriminants were derived from principal coordinates, and should not be confused with them when comparing Figures 3.6 and 3.7.

The LDA showed that about eighty percent of the distance variation between the six location groups discriminated by baited BRUVS was accounted for by the first two discriminant axes, and there was clear separation of the six groups, with pairs of channel and reef locations adjacent to each other within the pairs, but widely separated between the pairs (Figure 3.7A). The two-fold smaller scale of the LDA plot for unbaited RUVS (Figure 3.7B) showed that discrimination was much poorer for the unbaited RUVS. There was weak separation of channel locations. About 81% of the variation between location groups was accounted for by the first two linear discriminants for unbaited RUVS (Figure 3.7B), but the squared sum of the singular value decomposition (*svd*) was only about 27.8 for unbaited RUVS compared to 70.1 for baited BRUVS. The *svd* diagnostic is used in LDA to partition the singular values, which give the ratio of the between- and within-group standard deviations on the linear discriminant variables. Their squares are the canonical F-statistics, so a two-fold higher value for baited BRUVS indicated both a better separation of location groups, and lower variation amongst samples within location groups.

The LDA models were then used to predict the coordinates of each video sample in the space of the five discriminant axes, based on the location from which the sample was taken. Measures of the mean and the standard error of these projections onto the first two linear discriminants were calculated for each of the six levels of sampling location, and overlain on plots in Figure 3.7. The lack of separation of Palm Island Channel locations using unbaited RUVS was evident in the overlapping standard errors (Figure 3.7B).

Finally, drop-out analyses were performed using “leave-one-sample-out” cross-validation, where posterior probabilities of group membership of a sample were based on proportions of the whole dataset comprised of samples from each of the six locations.

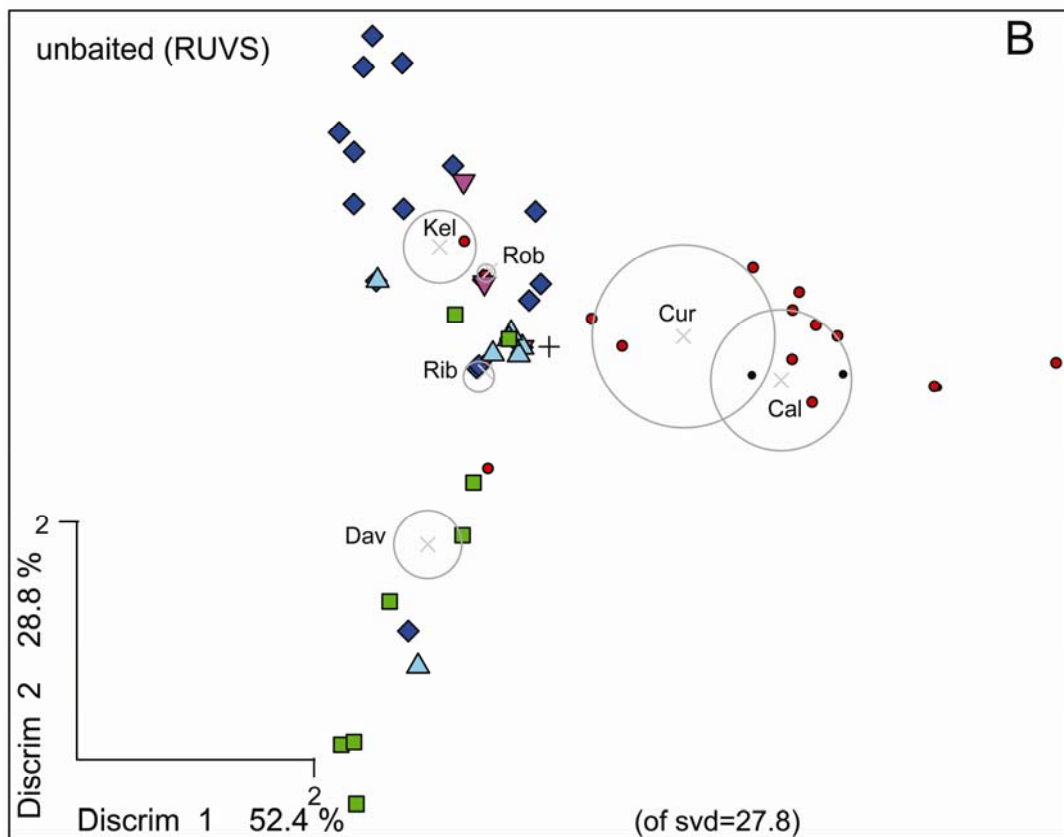
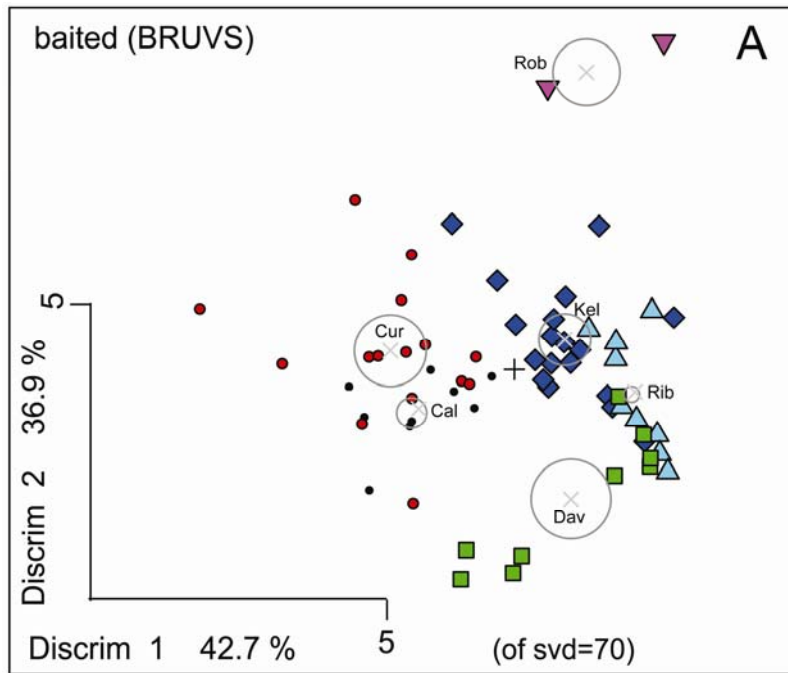


Figure 3.7. Linear Discriminant Analysis (LDA) of baited (BRUVS, A) and unbaited (RUVS, B) video units. Centroid means \pm 1 Standard Error of the six locations are shown.

Drop-out analyses using different numbers of principal coordinates showed that increasing the number of coordinates reduced the error rate of predictions for both baited and unbaited sets, but baited BRUVS had error rates consistently less (~60%) than those of unbaited RUVS sets (Table 3.5). Tabulation of the misclassifications showed that none of the baited sets at reef locations were misclassified as channel locations (Table 3.6). Channel sites were confused only with each other. All baited sets at Davies Reef were classified correctly, or erroneously as ‘Rib Reef’ (Table 3.6). In contrast, there were numerous misclassifications amongst all types of locations for unbaited RUVS (Table 3.7).

Table 3.5. Prediction of membership of video sets by location using single drop-out linear discriminant analysis for varying numbers of discriminants from principal coordinates analysis (PCoA).

PCoA variables	BRUVS error rate%	RUVS Error rate%
1,2	42.8	65.1
1,2,3	39.7	57.1
All 8	31.7	55.5

Table 3.6. Misclassification table for the use of baited (BRUVS) video and the first two discriminants (dimensions 1 and 2). Diagonal numbers in bold font show successful predictions by the model.

Baited (1,2,3)	Call	Cur	Dav	Kel	Rib	Rob
Call	1	4	0	0	0	0
Cur	5	11	0	0	0	0
Dav	0	0	4	0	0	0
Kel	3	0	0	15	4	2
Rib	0	0	5	3	5	1
Rob	0	0	0	0	0	0
Success %	11.1	73.3	44.4	83.3	55.5	0

Table 3.7. Misclassification table for the use of unbaited (RUVS) video and the first two discriminants (dimensions 1 and 2). Diagonal numbers in bold font show successful predictions by the model.

Unbaited (1,2)	Call	Cur	Dav	Kel	Rib	Rob
Call	0	5	0	0	0	0
Cur	5	5	0	1	0	0
Dav	0	1	6	1	2	0
Kel	1	5	3	11	7	2
Rib	0	2	0	5	0	1
Rob	0	0	0	0	0	0
Success %	0	27.7	66.6	61.1	0	0

3.4 DISCUSSION

Baited ‘video-fishing’ techniques have been used to count juvenile fishes, to identify the scavengers of prawn (shrimp) trawl discards, to measure the performance of marine protected areas and to measure abundance of abyssal scavengers and other deep-water species (see Table 2.1 for review). In these instances baited video has been used to sample single species, or small groups, of a restricted range of carnivores or scavengers. Such video techniques do have biases, but they also offer a ‘hybrid’ of the sampling advantages offered by underwater visual census and extractive “capture” techniques, whilst avoiding some of the selectivity associated with these techniques. Some species are known to flee from divers and cannot be counted underwater (Westera *et al.* 2003), and the mesh selectivity of traps and nets, herding by trawls, and hook-selectivity of line fishing are well known sources of bias (see Cappo & Brown 1996 for review).

When the goal of a survey is to sample the diversity of a large portion of the fish community living within a range of habitats, and determine the differences in assemblage structure between habitats, the advantages or disadvantages of using bait have not been examined adequately. Previous studies on the selectivity of fish traps on tropical reefs supported a long-standing presumption that the use of oily fish bait will affect the diversity and abundance of species that consume algae, seagrass and epiflora. Furthermore, it could be argued that the additional predators attracted to the baited video may interact with herbivorous species in a way that reduces the number of individuals and species recorded in these functional groups.

A compelling result of this chapter was my finding that baited video sampled more individuals and a higher species diversity of the families colloquially known as herbivores, corallivores and detritivores, as well as the piscivores and predators of large and small invertebrates. There was no evidence of bias against recording any trophic group of fishes in the field comparison I conducted. This was an important finding that contradicted common inferences about bait attractants made from fish trapping studies where herbivorous siganids and scarids dominated catches of unbaited traps on coral reefs, but seldom appeared in baited traps. In fact, the herbivores may have been seeking shelter sites in traps without predators rather than being somehow attracted to an unbaited trap (Munro 1974). If the presence of predators such as serranids, lutjanids and muraenids was controlled for, or observed underwater, in those earlier studies, the inferences about the action of bait may have been different. My observations of fish behaviour during the tape analysis showed that many species known as herbivores, corallivores, detritivores or planktivores did not directly approach the camera or the bait canister, but tended to be visible in the far field of view grazing, swimming by or investigating the commotion around the bait canister.

Baited video recorded species of fish which were attracted to the bait plume or the structure of the BRUVS, species attracted by the activity of other fish feeding and aggregating around the BRUVS, species occupying territories within the field of view, and species indifferent to the BRUVS but passing through the field of view. The results presented here showed that these dynamics act to facilitate far greater discrimination of fish assemblages and also to increase the similarity of samples within such groups. 'Allocation success' in the linear discriminant analysis was much higher for the use of bait, and misclassification errors were restricted to nearby reefs, channels or shoals of the similar habitat type. In contrast, the unbaited RUVS sets produced misclassification of samples amongst very different habitat types and their assemblages.

The greater dissimilarity between site groups, and the lower dissimilarity between replicate samples within site groups, documented here when using bait would improve the statistical ability of detecting changes in fish populations at the assemblage level. These changes might be expected in monitoring programs aimed at detecting the effects of natural events or human activities such as fishing. When used to investigate the effects of deeper marine protected areas, it is now certain that baited BRUVS would detect changes in the relative abundances of individual species, or assemblages, of fish with greater statistical 'power' and fewer samples than unbaited RUVS. Indeed, the species accumulation curves presented here showed that no amount of replication of unbaited RUVS would approach the diversity recorded by baited BRUVS.

If the goal of sampling is to detect spatial and temporal changes in the species diversity or relative abundance of demersal fishes the most pertinent issue concerns which sampling technique will provide the greatest consistency across a broad range of species and habitat types. Sampling more individuals of a single species had several advantages. Firstly, the coefficient of variation was reduced for species within habitats when BRUVS were used. This was particularly important for the large ‘generalist carnivores’ (e.g. lutjanids), ‘macroinvertebrate carnivores’ (e.g. lethrinids) and piscivores (e.g. carangids) which are mobile, but have relatively low densities and patchy distributions. Fewer ‘false negatives’ and a lower coefficient of variation implied better statistical power to detect differences amongst samples.

By attracting more individuals of these species with bait close to the cameras there were also more and much better opportunities to obtain precise and accurate measurements of length using stereo-video systems (Watson *et al.* 2009). The measurement of each individual visiting the field of view would allow more accurate counts of fish appearing on the tape. Without these measurements, *MaxN* will remain a conservative estimate of relative abundance (Shortis *et al.* 2009). Like all fish sampling techniques, questions remain about the biases of baited underwater cameras in measuring fish species richness, diversity and relative abundances. Whilst BRUVS eliminate much of the selectivity associated with extractive fishing gears they were also likely to introduce other biases because of the multiplicity of behaviours adopted by demersal fishes. The only ways to discern the biases associated with BRUVS are to compare them with underwater visual census by divers in shallow waters (Willis *et al.* 2000; Watson *et al.* 2005) and with common extractive techniques in deeper waters, such as trawling (Priede & Merrett 1996), long-lining (Ellis & DeMartini 1995) and trapping.

It is highly likely that the human eye underwater is much better at detecting the subtle differences in hue and pattern in colouration of coral reef fish than the grainy imagery of the video. It is therefore probable that some species groups of the shallows, like the scarids, siganids, acanthurids and pomacentrids will be misidentified on video records in deeper waters. This does not detract from the utility of this sampling method for my thesis, for two main reasons. Firstly, I was focussing on deeper waters to 80 metres, beyond the shallow limits of scientific SCUBA diving. Secondly, the rapid decline in primary productivity with depth (Polunin 1996) implies that diversity of demersal families not attracted to bait plumes, such as scarids, kyphosids and siganids, should be low. This was evident in the multivariate analyses presented here, with only a few herbivores common in deeper waters (e.g. *Scarus flavipectoralis*, *S. ghobban*, *Siganus argenteus*). Larger carnivores and planktivores were predicted by Polunin (1996) to dominate on lower reef slopes and I expected these species to be more responsive to bait.

Underwater visual census on SCUBA will remain the technique of first choice for comprehensive biodiversity surveys of shallow reefs. The deficiencies of the BRUVS technique reported in other studies must be taken in the context of the shallow environments in which their tests were made. For example, Watson *et al.* (2005) compared baited and unbaited underwater stereo-video systems with a stereo-video system operated by a diver along transects in less than eight metres' depth. They found that baited cameras recorded more species with lower variances than either of the other two techniques, but that the baited and unbaited cameras did not record some of the nocturnal cave-dwelling pempherid species which were not attracted to the bait and ventured out into the open only at dusk. On Mediterranean rocky reefs, Stobart *et al.* (2007) observed that the behaviour of most of the species recorded on baited video was explained by an attraction to the bait, with most fish feeding actively at the bait canister or on food particles above it. They concluded that the baited system represented species richness well, but the mean abundance per species in the field of view was very low, and in most cases equal or lower than 1 due to a high frequency of 'zero' values.

It can be concluded that bait is important, and the type of bait has borne much scrutiny in studies of traps and hooks. Oily, soft-fleshed baits such as clupeid baitfish were clearly superior (four to five times more effective) to white-fleshed baits (Whitelaw *et al.* 1991) and octopus (High 1980) in terms of attractiveness, but not longevity. Whitelaw *et al.* (1991) reported that a white-flesh bait (of *Lethrinus* sp) resulted in 75% fewer fish being caught in traps when compared to pilchard bait. The probability of arrival of a fish at the baited trap or hook has been reported to be governed by the size, type and freshness of the bait, and the search pattern, appetite and response time of the fish (Miller 1983).

Seasonal, reproductive and lunar patterns of activity in the swimming speed, schooling behaviour and appetite of the fish presumably all affected this probability function. Various other factors such as conspecific attraction, curiosity, inadvertent entry, the presence or absence of predators in traps, thigmotropic associations, random movements, and home range sizes can also determine whether fish actually enter traps (Munro *et al.* 1971; Hartsuijker & Nicholson 1981; Ward 1988), and these may apply in similar ways to visits to baited video stations.

Three major challenges remain in applying baited video surveys to estimating relative abundances of fish and converting them to density estimates. Repeated visits of the same fish must be separated in tape interrogation from new arrivals to get better estimators of abundance. The sampling area of each station must be estimated to raise these counts to density estimates. Finally, the notion that *MaxN* is related more to the prevailing feeding opportunities in a habitat rather than fish abundance must be tested (see Farnsworth *et al.* (2007) for review). These topics

will require calibrations with other sampling techniques, ground-truthed models of bait plume dynamics, and closer attention to the dynamics of fish visits and interactions within single tapes.

4. HOW DOES TIME OF DAY AND FUNCTIONAL MORPHOLOGY OF FISHES AFFECT THE ABILITY OF BRUVS TO DISTINGUISH INTER-REEF FISH ASSEMBLAGES?

4.1 INTRODUCTION

Commercial trawling gear has been the sole technique used to derive generalisations about the environmental and anthropogenic influences on tropical shelf fish faunas (see Fager & Longhurst 1968; Lowe-McConnell 1987; Bianchi *et al.* 2000; Garces *et al.* 2006a). Locally, trawls have been used to describe patterns of distribution and abundance of fish species in the inter-reef waters of the GBRMP (Watson *et al.* 1990; Wassenberg *et al.* 1997). Demersal research trawling is an extractive activity, restricted to certain zones of the GBRMP, and cannot be used on very rough seabeds, palaeo-reef edges or other outcrops of ‘hard ground’. Such seabed topographies are known to provide the substrata for attachment of sponges, gorgonians, alcyonarians and macroalgae, but much softer sediments also provide the basis for enucleation of patches of such ‘megabenthos’ at much larger spatial scales (Birtles & Arnold 1988; Pitcher *et al.* 2008). The mosaics of soft and hard, biotic and biotic habitats on low-latitude shelves provide food resources, shelter and spawning aggregation sites for a significant and varied fish fauna – most notably a ‘bycatch fauna’ in prawn trawl fisheries on soft sediments (Ramm *et al.* 1990; Stobutzki *et al.* 2001b; Tonks *et al.* 2008), and the snapper-grouper complex on more complex topographies (Coleman *et al.* 2000). These shelf habitats are very extensive but largely unexplored because they occur in depths below the limits of scientific SCUBA diving.

Underwater visual surveys (UVS) using submersibles have been used to estimate fish densities in these deeper habitats (e.g. Parrish & Boland 2004; Stoner *et al.* 2008b; Anderson *et al.* 2009), but are expensive and not readily available in most Indo-Pacific countries – including Australia. Towed still cameras mounted on trawl head-ropes, or towed video cameras, have also been used to determine fish-habitat associations (Sainsbury *et al.* 1992). Hydro-acoustic measurements validated by video or submersible offer the potential to enumerate low-diversity fish communities (Barans & Holliday 1983; Stanley & Wilson 2000; Barans *et al.* 2005). Most commonly, however, selective trapping, hook and line fishing or trawling has been undertaken to survey fish communities (Bianchi 1992b; Newman *et al.* 1997; Newman & Williams 2001; Garces *et al.* 2006b; Heupel *et al.* 2009).

My goal was to develop a fleet of baited remote underwater video stations (BRUVS) for use in comprehensive biodiversity surveys of all management zones of the GBRMP, including those inaccessible to diver-based surveys and extractive techniques. Here I report on a direct field comparison of BRUVS with prawn trawls to evaluate the relative performance, inherent biases and selectivity of this video technique in the seafloor habitats between the reefs. The main factors I set up in the field comparison were contrasts in three locations during the day and night, based on knowledge that the largest catches of fish might be expected in night trawls; that distinct cross-shelf changes occur in habitats and fish communities of the GBRMP lagoon; and that distinct regional and biophysical patterns exist long-shore.

Specifically, I aimed to compare the two techniques in terms of species richness, the ability to discern spatial patterns, the ability to discriminate amongst groups in those patterns, the estimates of relative abundance of species common to both, and general logistics of data acquisition.

4.2 METHODS

The basic design was to set five BRUVS of the type shown in Figure 2.1(A) about 450 metres apart along an 1,800 metres (1 nautical mile) track in prawn trawl grounds, then trawl alongside (about 150-200 metres away) and parallel to that same 1,800 metre track with a prawn trawl. Each trawl and each set of five BRUVS is hereafter referred to as a 'transect'. The transect dimensions and trawl configuration were designed to standardise with previous studies in the region (Wassenberg *et al.* 1997). The number and separation of the BRUVS was chosen on the basis of prevailing currents and the formula:

$$AR = 60 \times (S_t) \times ((V_f \times V_c) - V_c^2)/V_f \quad (\text{see Chapter 2.1.2})$$

This was an informed attempt to achieve independence of each unit and to sample approximately the same area of seabed as that swept by the trawl.

Distinct biophysical regions exist north and south of Cape Grafton in the Cairns region of the GBRMP (R. Pitcher pers. comm., CSIRO Division of Marine Research, Cleveland). To maximise the contrast in habitat types for the comparison I selected two locations north of Cape Grafton ('Double Island' (DI): inshore, 18-23m depth; and 'Double Island Wide' (DIW): offshore, 31-33m depth) and one location south of the cape ('Scott Reef' (SR): offshore, 29-38m depth). The inshore DI location had terrigenous sediments, and the other two offshore locations had mixed terrigenous and carbonate sediments. Each comparison was made along a

new path on the trawl grounds, parallel to the prevailing wind (along current) prior to and during the full moon, 23-28 January 2002 (Figure 4.1). Three (DI, DIW) or four (SR) replicate pairs of trawls and BRUVS transects were made at each location during both the day and night, giving a total of 19 BRUVS and trawls transects.

The design and deployment of the BRUVS followed the descriptions in Chapter 2.2 and 3.2 with the exceptions that the bait arms had a 50mm square metal grid either end of the bait canister and that the night sets were made with lights. This lighting was provided by two 35-Watt, 12-Volt dichroic lamps in separate housings covered by Lee™ ‘Bright Red 026’ filters and ‘Night-Shot’ function was selected on the cameras.. These filters were selected to transmit red light in the wavelengths known to be above the sensitivity of many marine fish at night (J. Shand pers. comm., University of Western Australia). Power-packs for lights were made of 12-Volt rechargeable gel-cell batteries in waterproof housings. The BRUVS were deployed to provide 60 minutes of film recorded at the seabed.

Interrogation of each tape followed the protocols described in Chapter 2.3. Coarse measurements of the total length of the largest individuals of some species were made by comparing them with the scale grids on the bait arm. These measurements could be made only when the fish were perpendicular to the camera and immediately next to, or between, the scale grids. At such opportunities the tape play-back was paused to provide a still image, and the outlines of the fish and scale grids were compared using a plastic graduated ruler to provide a visual estimate of length. Harvey *et al.* (2002) showed that accuracy of such a procedure is degraded by the rotation of the subject beyond 20° relative to the camera; reduced when the subject is more than one metre to the left or right of the calibration bar; and severely compromised when the fish silhouette was behind or in front of the calibration bar.

The trawl gear deployed by FRV *Gwendoline May* was identical to that described by Wassenberg *et al.* (1997), with the exception that each net in the current study was fitted with the bycatch reduction devices (BRD) and turtle exclusion device (TED) required under the current legislation covering the East Coast Trawl fishery. The trawl gear consisted of an identical pair of 8m (footrope length) ‘Florida Flyer’ nets (50mm mesh) deployed over the stern of the vessel. The BRD in each was a ‘square mesh panel’ (100mm mesh), and the TED was an aluminium grid of deflector bars, angled backwards and spaced about 120mm apart (see Eayrs *et al.* (1997) for full description).

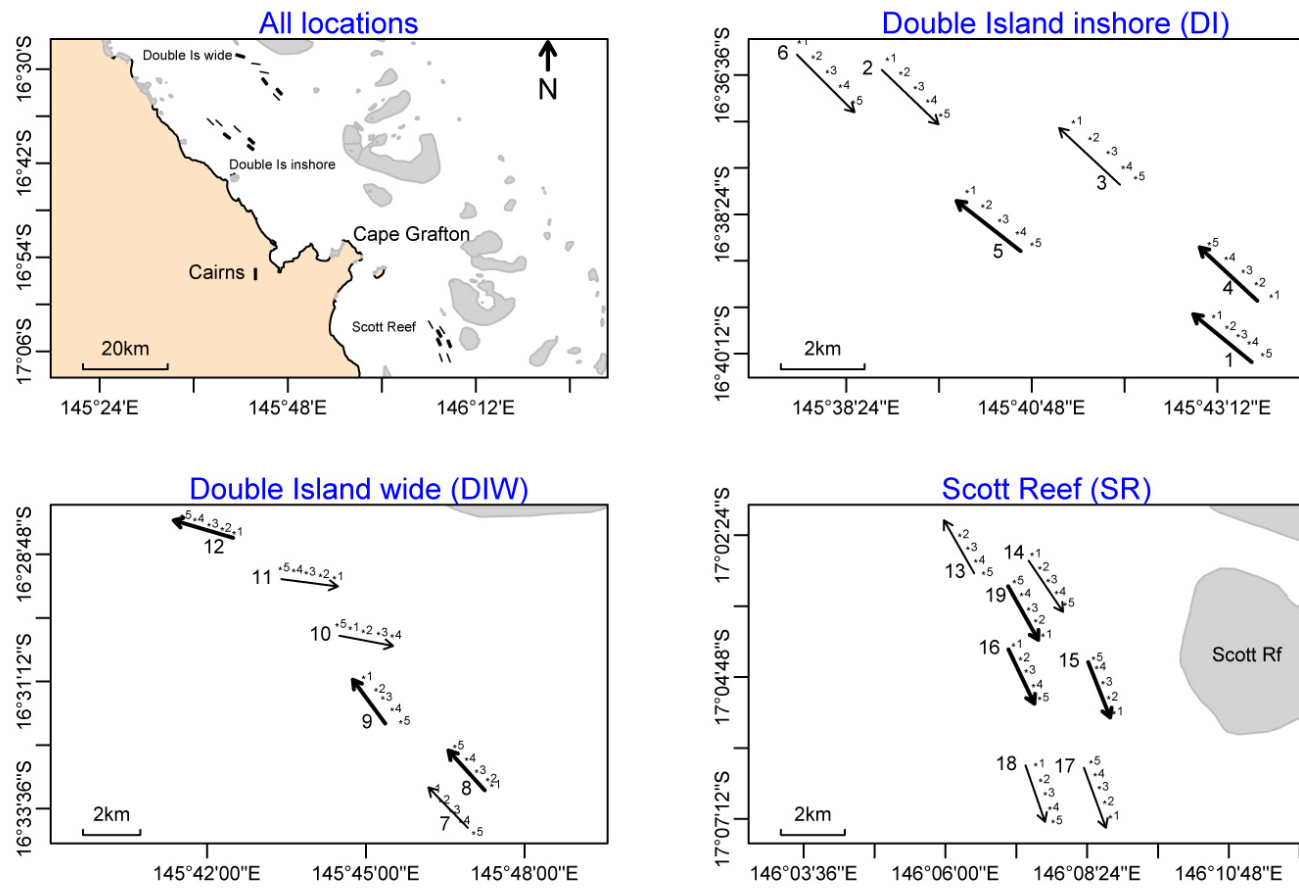


Figure 4.1. Location of 19 trawl and BRUVS transects either side of Cape Grafton. The arrows are scaled precisely to the trawl path and point in the trawl direction. Adjacent coordinates of each numbered BRUVS replicate are shown. Bolded arrows represent night samples.

The time, depth, position, duration and track was recorded for each set of BRUVS and trawls using MaxSea navigation software linked to a Garmin® GPS receiver. The trawls were about twenty minutes in duration (on bottom), during which a path approximately one nautical mile long (1.8km) and no more than sixteen metres wide was trawled. The catches from both nets was weighed to the nearest 0.1kg on a Salter spring balance. The ‘fish’ component of the catch was boxed and frozen for further analysis to record the number of each species in each catch (N), and the range in total length measurements ($MinLength$ and $MaxLength$) of each species.

Five main working approximations were made to allow definition of abundance measures. It was assumed that, (a) fish were not counted on more than one BRUVS in a transect; (b) the BRUVS and trawl transects were independent and did not influence each other; (c) the total area sampled by each BRUVS was the same; and (d) the total area sampled by five BRUVS was similar to the area swept by the trawl. These untested approximations provided the statistic used to compare the BRUVS transect with the associated trawl transect N as the sum of $MaxN$ pooled across the five BRUVS for each fish species.

4.2.1 Statistical analysis

The patterns of presence and absence of the fish species were highly variable, with only one species (on BRUVS) present on all transects. The data for all species were therefore transformed by 4th root before multivariate analysis. This down-weighted highly abundant species and reduced skewness in the distributions of values for each species. Multivariate analyses of two types were conducted. Firstly, the transformed abundance data was explored using multivariate regression trees (MRT). Species indicators that characterised each of the treatment groups for BRUVS and trawls were identified using the Dufrêne-Legendre Index (DLI) (see Chapter 2.4.4). The index distinguished between ubiquitous species that dominated many groups in absolute abundance, and species that occurred consistently within single groups but had low abundance.

Secondly, species dissimilarity was used in the remaining analyses to illustrate basic structure and groupings in the data. The extended version of site-standardised Manhattan dissimilarity ($xdiss$) was selected for the basis of all multivariate analyses (De’ath 1999). This measure is equivalent to extended, site-standardised Bray-Curtis and allows eigen-analysis to be used in diagnosing ordinations. Principal coordinates analysis (PCoA) and distance-based redundancy analysis (db-RDA) (Legendre & Anderson 1999; McArdle & Anderson 2001) were used to assess species variation between the six treatments (defined by the three locations, day and night) and the interactions between them. Permutation tests were used to assess the significance

of the variation (McArdle & Anderson 2001). Linear discriminant analysis (LDA) was used to assess how accurately information from BRUVS and trawls could predict the species assemblages. Analyses were carried out in R using the libraries `vegan`, `mvpart` and `treeDLI`. The functional morphology and habits of the numerous genera and families mentioned below in the text and tables are summarised in Table 4.8 to provide ecological context for the differences reported between sampling methods.

4.3 RESULTS

4.3.1 Species richness

Overall, there were 6,247 individuals of 128 teleost and elasmobranch species recorded in the study, from 53 families (Table 4.1). The trawl catch rates were low, between 2.25-33.63kg hr⁻¹ with an average of 16.55kg hr⁻¹. Trawls recorded higher species richness overall, at all sites, and at night (Table 4.2), but the average number of species and individuals recorded per transect were only about 26% and 19% lower for the BRUVS (Table 4.1). Catch rates in night trawls (22.62kg hr⁻¹) were higher than those in the day (11.09kg hr⁻¹). BRUVS recorded consistently higher diversity in the day (Table 4.2). Of the total species list, 52 (17 families) were caught only by trawls and 38 (15 families) were recorded only by BRUVS. There were 38 species (21 families) recorded by both sampling techniques.

Species accumulation curves (SAC) record the rate at which new species (y) are added with continued sampling effort (x) (Thompson *et al.* 2003). The classic method is ‘random’, which finds the mean SAC and its standard deviation from random permutations of the data, or by sub-sampling without replacement (Gotelli & Colwell 2001). Accumulation of new species by both techniques showed BRUVS consistently about eleven species below trawls for any extra transect in ‘random’ simulations (Figure 4.2, Table 4.2). These curves were fitted best by logarithmic functions:

$$\text{BRUVS} \quad y = 21.05 (\text{Ln}(x)) + 12.68, \text{adj } r^2 = 0.994;$$

$$\text{Trawls} \quad y = 22.68 (\text{Ln}(x)) + 22.89, \text{adj } r^2 = 0.999.$$

Table 4.1. Total number of families, species, and individuals (*n* fish) recorded by 19 trawls and 95 BRUVS sets along 19 transects. Average number of species and *n* fish for these transects are shown with standard errors and ranges.

	<i>n</i> families (species)	Avg <i>n</i> species ± SE (range)	<i>n</i> fish	Avg <i>n</i> fish ± SE (range)
BRUVS	36 (76)	16.7 ± 1.4 (6-27)	2,790	146.8 ± 15.9 (43-288)
Trawls	38 (90)	22.6 ± 2.2 (9-38)	3,457	181.9 ± 34.5 (48-588)

Table 4.2. Number of species and families (brackets) recorded by day and night and in total by 19 trawls and 95 BRUVS sets along 19 transects.

	BRUVS			Trawls		
	Day	Night	Total	Day	Night	Total
Double Island (DI)	29 (16)	20 (15)	39 (24)	23 (16)	41 (24)	48 (26)
Double Island Wide (DIW)	34 (16)	20 (15)	40 (20)	27 (20)	45 (25)	50 (28)
Scott Reef (SR)	43 (23)	18 (14)	51 (29)	36 (19)	54 (27)	62 (29)
Total	67 (30)	34 (21)	76 (36)	58 (30)	77 (35)	90 (38)

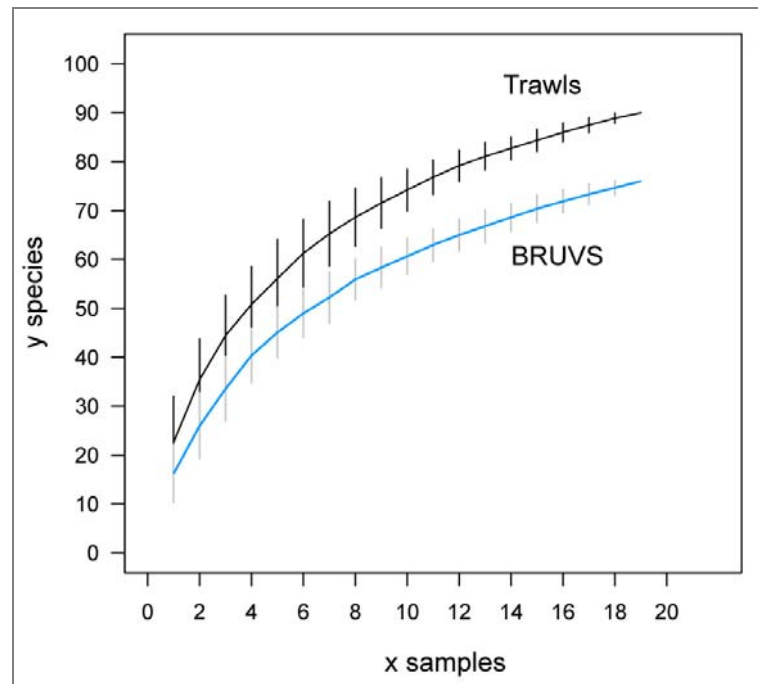


Figure 4.2. Species accumulation curves (method = 'random') for the data pooled by sampling technique.

The most notable features of these curves are their similarity, with low points of curvature on the ordinate axis, a long upward slope toward an asymptote, and evidence that there was insufficient sampling to estimate the asymptote and total species richness.

The BRUVS recorded fish families from a greater range of body sizes and functional groups than trawls. Large sharks and shovelnose rays (Carcharhinidae, Sphyrnidae, Rhynchobatidae) and pelagic scombrids and echeneids most likely evaded, or escaped from, the trawls and were recorded only by BRUVS. Eels were recorded on all transects by BRUVS, but were absent from trawls (Table 4.3). In terms of both prevalence and abundance along transects, the BRUVS recorded more demersal scavengers and predators in the Teraponidae, Tetraodontidae and Carangidae families, fewer herbivorous siganids and fewer labrids. The mobile black-banded kingfish (*Seriolina nigrofasciata*) and school mackerel (*Scomberomorus queenslandicus*) were almost ubiquitous on BRUVS sets in the two deeper locations, but only two specimens of *S. nigrofasciata* were caught by trawl (Table 4.4).

In contrast, trawls caught mainly small, sedentary or cryptic, demersal species found lower in the water column or on the seabed. Many of these species had small dorso-ventrally compressed bodies, heavy head and fin spination, venoms or toxins, armoured scales and specialised mouth parts adapted to a sedentary, demersal life history over soft sediments (see Table 4.8). The BRUVS did not record a single flatfish or flathead (bothids, psettodids, platycephalids), and apogonids were sighted only once, yet these families were major components of the trawl catch in terms of diversity, prevalence and abundance along transects. The flatfishes and flatheads, gurnard-like species (callionymids, dactylopterids, triglids, scorpaenids), catfishes (plotosids) and nocturnal planktivores (priacanthids) were exclusively caught by trawls, as were a variety of other sedentary or slow-moving species (Table 4.3).

Small schooling pomacentrids (*Pristotis jerdoni*)², gregarious labrids and mullids were more prevalent and abundant in trawls, but BRUVS recorded more schooling pelagic *Selaroides leptolepis* and other carangids. The lutjanids, sparids, serranids and some nemipterid and monacanthid species were recorded in similar numbers by both techniques, but there were notable differences in prevalence and abundance of *Scolopsis taeniopterus*, *Nemipterus furcosus*, *Pentapodus paradiseus*, *Paramonacanthus lowei* and *P. japonicus* (Table 4.4). These may relate to the nature of their small-scale distribution, aggregative behaviour, and vulnerability to the trawls and differential attraction to the BRUVS.

² Referred to as *Pristotis obtusirostris* in following chapters after taxonomic revisions.

The average of the difference between *MinLength* and *MaxLength* measured for all species caught by trawls was used as an estimate of total length for the same species recorded by BRUVS. The lengths of other species recorded only by BRUVS were estimated coarsely by comparison with the scale grids on bait arms where possible. Most of the trawl catch had an average length less than 300mm total length, yet nearly half the BRUVS species were at or beyond this length – up to direct estimates of 1.6-2.0 metres for sightings of large hammerhead sharks and shovelnose rays (Figure 4.3).

The identity of ten of the 38 taxa recorded uniquely by BRUVS was uncertain. These taxa were sometimes seen at such a distance, or aspect, that important diagnostic features were not visible. This may have caused under-estimation of the true commonality of records of some *Saurida* and *Carangoides* species for the two techniques in Table 4.4. The records for *C. talamparoides*, *C. uii*³, *Saurida undosquamis* and *S. micropectoralis* were grouped to the common level of their genus for BRUVS in the MRT analysis presented in Figure 4.4. A large proportion (42%) of the 76 species sighted by BRUVS were classified as passing through the field of view without ever feeding on the bait canister. Forty-four species (57.9%) fed on, or touched, the bait canister at least once during their appearance on BRUVS tapes.

³ Referred to as *Carangoides coeruleopinnatus* in following chapters after taxonomic revisions.

Table 4.3. Families recorded by only BRUVS or by only trawls in descending order of abundance. The number of species (*n* spp) is shown for each family in brackets, with total number of fish (*n* fish), the number of transects along which the family was recorded (*n* transects) and the average number of that family recorded on those transects, with standard errors.

BRUVS			Trawls		
Family (<i>n</i> _spp)	<i>n</i> fish (<i>n</i> _transects)	Avg <i>n</i> _fish ± SE	Family (<i>n</i> spp)	<i>n</i> fish (<i>n</i> _transects)	Avg <i>n</i> _fish ± SE
Muraenidae (2)	131 (19)	6.9 ± 0.70	Platycephalidae (4)	189 (14)	13.5 ± 3.81
Scombridae (2)	71 (10)	7.1 ± 2.00	Bothidae (9)	135 (17)	13.2 ± 9.48
Echeneidae (1)	24 (10)	2.4 ± 0.50	Callionymidae (3)	132 (10)	7.9 ± 1.67
Ophichthidae (1)	8 (6)	1.3 ± 0.21	Priacanthidae (1)	43(10)	4.3 ± 1.29
Carcharhinidae (2)	6 (4)	1.5 ± 0.50	Triglidae (1)	20(4)	5.0 ± 1.00
Rhynchobatidae (2)	3 (2)		Scorpaenidae (3)	17(7)	2.4 ± 0.37
Sciaenidae (1)	3 (2)	1.5 ± 0.50	Caesionidae (1)	12(1)	
Rachycentridae (1)	2 (1)		Plotosidae (1)	8(4)	2.0 ± 0.58
Blenniidae (1)	2 (1)		Gobiidae (1)	8(3)	2.7 ± 0.33
Sphyrnidae (2)	5 (4)	1.2 ± 0.25	Triacanthidae (1)	7(3)	2.3 ± 0.33
Congridae (1)	2 (2)		Ostracidae (2)	6(3)	2.0 ± 1.00
Dasyatidae (1)	1 (1)		Antennaridae (3)	4(4)	
Balistidae (1)	1 (1)		Psettodidae (1)	4(2)	2.0 ± 1.00
Stegastomatidae (1)	1 (1)		Gerreidae (1)	3(1)	
Muraenesocidae (1)	1 (1)		Dactylopteridae (1)	1(1)	
			Pseudochromidae (1)	1(1)	
			Centriscidae (1)	1(1)	

Table 4.4. Abundance (*n* fish) and occurrence (*n* transects) of species common to both techniques, ranked in descending order of abundance in the BRUVS records for the 19 transects. Average abundance and standard errors are shown for each species for those transects on which they were recorded.

Family	Species	BRUVS		Trawl	
		<i>n</i> fish (<i>n</i> transects)	AVG (<i>n</i> fish) ± SE	<i>n</i> fish (<i>n</i> transects)	AVG (<i>n</i> fish) ± SE
Teraponidae	<i>Terapon theraps</i>	537 (9)	59.7 ± 11.58	27 (7)	3.9 ± 1.28
Carangidae	<i>Selaroides leptolepis</i>	529 (10)	52.9 ± 17.56	124 (6)	20.7 ± 16.93
Tetraodontidae	<i>Lagocephalus sceleratus</i>	237 (19)	12.5 ± 3.15	99 (10)	9.9 ± 5.76
Nemipteridae	<i>Nemipterus furcosus</i>	149 (11)	13.5 ± 3.57	17 (5)	3.4 ± 1.91
Nemipteridae	<i>N. nematopus</i>	128 (7)	18.3 ± 4.56	99 (6)	16.5 ± 1.93
Nemipteridae	<i>N. peronii</i>	75 (10)	7.5 ± 2.18	47 (11)	4.3 ± 0.84
Lethrinidae	<i>Lethrinus genivittatus</i>	76 (12)	6.3 ± 2.33	39 (9)	4.3 ± 1.79
Nemipteridae	<i>Pentapodus paradiseus</i>	71 (8)	8.9 ± 5.24	10 (4)	2.5 ± 0.65
Carangidae	<i>Seriolina nigrofasciata</i>	55 (10)	5.5 ± 0.82	2 (2)	
Nemipteridae	<i>N. theodorei</i>	51 (6)	8.5 ± 2.45	7 (3)	2.3 ± 1.33
Nemipteridae	<i>Scolopsis taeniopterus</i>	46 (5)	9.2 ± 4.80	189 (15)	12.6 ± 3.30
Nemipteridae	<i>N. hexodon</i>	39 (7)	5.6 ± 1.74	31 (3)	10.3 ± 4.06
Labridae	<i>Choerodon sp</i> ⁴	33 (4)	8.3 ± 1.75	268 (12)	22.3 ± 6.59
Pomacentridae	<i>Pristotis jerdoni</i>	27 (4)	6.8 ± 2.50	606 (14)	43.3 ± 19.61
Monacanthidae	<i>Paramonacanthus japonicus</i>	22 (6)	3.7 ± 0.67	86 (9)	9.6 ± 4.49
Haemulidae	<i>Pomadasys maculatus</i>	16 (2)	8.0 ± 6.00	2 (2)	
Carangidae	<i>C. fulvoguttatus</i>	17 (5)	3.4 ± 0.81	1 (1)	
Carangidae	<i>C. talamparoides</i>	13 (1)		8 (2)	4.0 ± 3.00
Monacanthidae	<i>P. otisensis</i>	14 (5)	2.8 ± 0.58	31 (2)	15.5 ± 13.50
Sphyraenidae	<i>Sphyraena putnamiae</i>	13 (4)	3.3 ± 1.31	4 (1)	
Mullidae	<i>U. tragula</i>	13 (5)	2.6 ± 1.36	100 (7)	14.3 ± 6.52
Sparidae	<i>Argyrops spinifer</i>	10 (3)	3.3 ± 1.20	3 (3)	

⁴ Referred to as *Choerodon gomoni* in later chapters after taxonomic revisions.

Family	Species	BRUVS		Trawl	
		<i>n</i> fish (<i>n</i> transects)	AVG (<i>n</i> fish) ± SE	<i>n</i> fish (<i>n</i> transects)	AVG (<i>n</i> fish) ± SE
Lutjanidae	<i>Lutjanus malabaricus</i>	9 (3)	3.0 ± 1.53	2 (2)	
Siganidae	<i>Siganus canaliculatus</i>	9 (2)	4.5 ± 0.50	12 (8)	1.5 ± 0.38
Apogonidae	<i>Apogon quadrifasciatus</i>	9 (1)		158 (16)	9.9 ± 3.31
Tetraodontidae	<i>Torquigener pallimaculatus</i>	8 (6)	1.3 ± 0.21	10 (5)	2.0 ± 1.00
Mullidae	<i>U. moluccensis</i>	8 (1)		3 (1)	
Carangidae	<i>Carangoides chrysophrys</i>	7 (4)	1.8 ± 0.25	1 (1)	
Mullidae	<i>Upeneus luzonius</i>	6 (3)	2.0 ± 0.58	3 (2)	1.5 ± 0.50
Monacanthidae	<i>P. lowei</i>	5 (3)	1.7 ± 0.33	38 (6)	6.3 ± 2.75
Serranidae	<i>Epinephelus sexfasciatus</i>	5 (2)	2.5 ± 1.50	3 (3)	
Mullidae	<i>U. sundaicus</i>	4 (2)	2.0 ± 1.00	34 (11)	3.1 ± 0.58
Fistularidae	<i>Fistularia petimba</i>	4 (1)		18 (10)	1.8 ± 0.39
Synodontidae	<i>Saurida undosquamis</i>	3 (2)	1.5 ± 0.50	114 (18)	6.3 ± 1.10
Lutjanidae	<i>L. vitta</i>	2 (2)		1 (1)	
Labridae	<i>Xiphocheilus typus</i>	2 (1)		65 (9)	7.2 ± 1.84
Pinguipedidae	<i>Parapercis nebulosa</i>	2 (1)		6 (3)	2.0 ± 0.58
Chaetodontidae	<i>Coradion chrysozonus</i>	1 (1)		1 (1)	

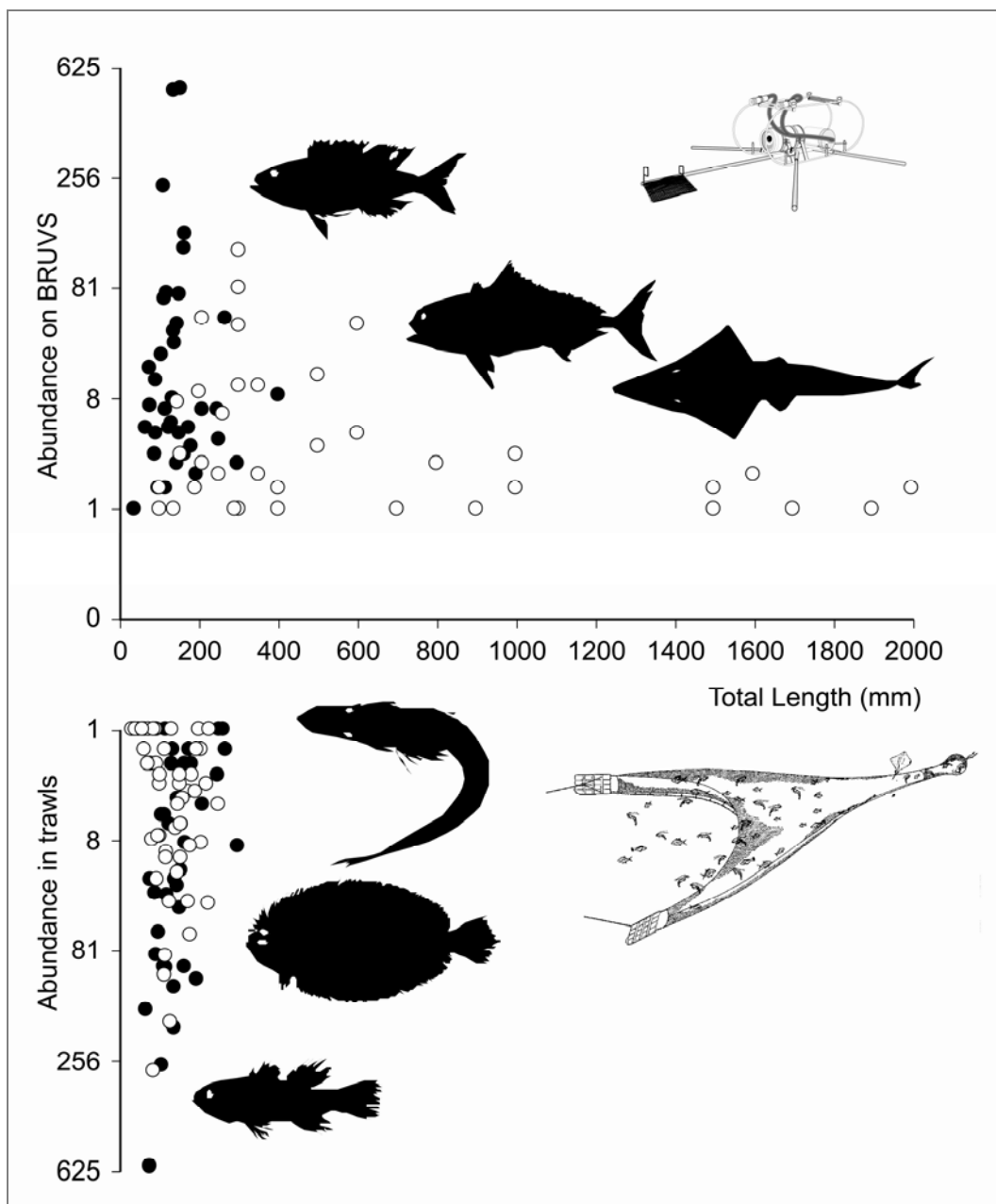


Figure 4.3. Scatter plots of the average total length of each species, measured or estimated, from trawl catches and BRUVS sightings. Abundance has been scaled using the fourth root transformation. Each point represents the number of individuals of a species. Filled symbols represent species recorded by both techniques and open symbols represent species unique to each technique.

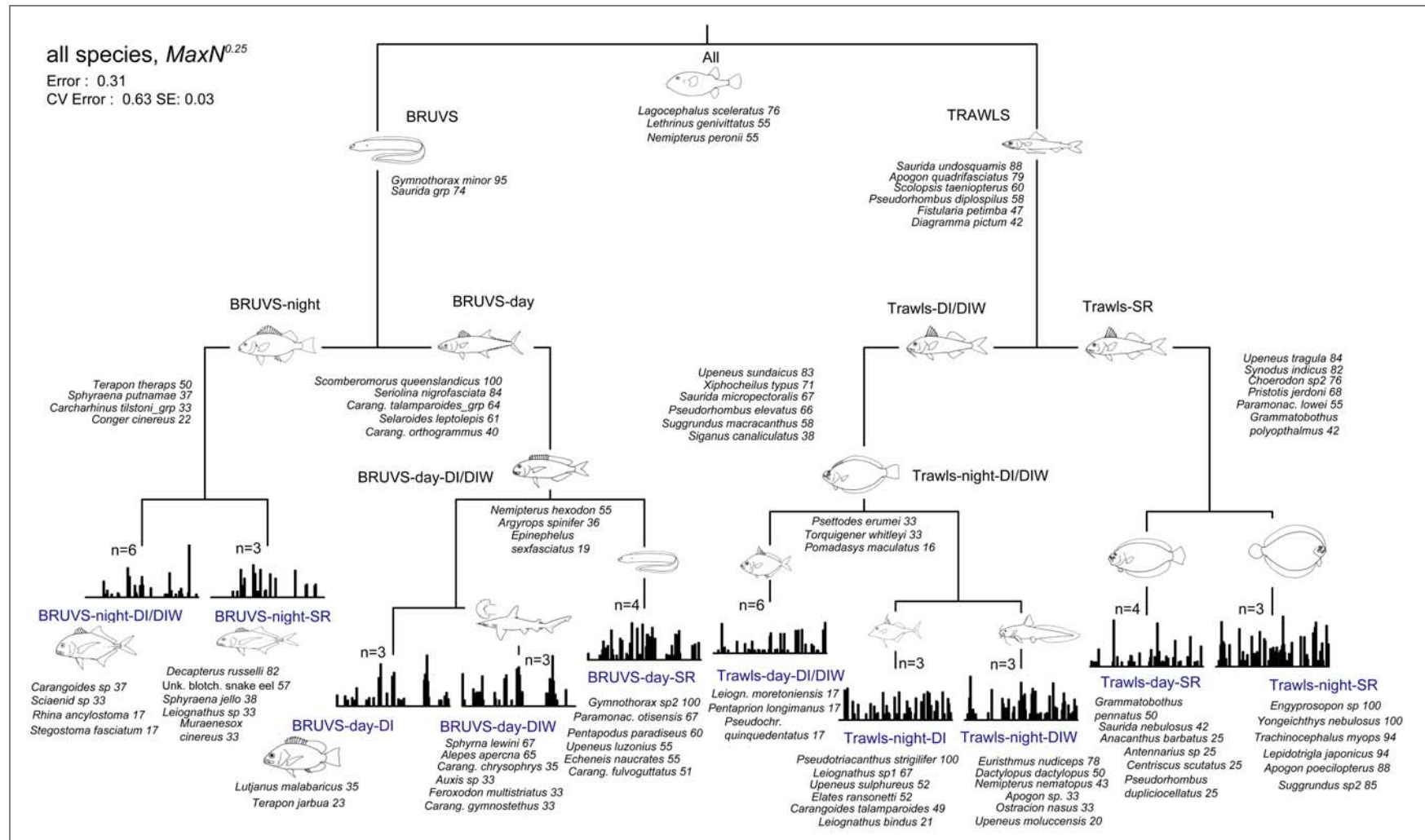


Figure 4.4. Multivariate regression tree (MRT) for BRUVS and trawl transects, showing top six DLI species scores for nodes. The bar plots show the distribution of species abundance at each of the terminal nodes, ranked from left to right in decreasing order of prevalence in the entire data set, with each vertical bar representing the mean abundance of a species in that group.

4.3.2 Description of patterns in fish assemblages

Both techniques recorded the same general trends in ranking of transects by diversity of fish species, with the difference amongst techniques greatest at night, when trawls performed best (Table 4.2). The MRT was used in exploratory clustering of the transformed data (Figure 4.4) to investigate the associations among the fish communities. The MRT explained about seventy percent of the dissimilarity amongst transects and had a relatively low prediction error (~63%), given the large number of species in the dataset. This analysis indicated the presence of ten strong groupings based on splits between trawl and BRUVS, day and night, and location. The primary split in the clustering was by technique. At the higher levels of dissimilarity the day transects were clustered in two groups for both techniques with Double Island and Double Island Wide separate from Scott Reef. There were clear diurnal differences amongst the two techniques. Whilst BRUVS could distinguish the inshore and offshore Double Island transects during the day, trawls could do so only at night. Scott Reef transects formed strong night and day groups for both techniques.

4.3.3 Indicator species for the ten fish assemblages

The extreme dissimilarity of the same five fish assemblages distinguished for each technique is represented by the very high DLI values. The school mackerel *Scomberomorus queenslandicus* had a DLI=100, representing its occurrence in high numbers on every one of the ten BRUVS 'day' transects (and none of the trawls) in the Double Island area. There were many DLI > 80, and the fish outlines in Figure 4.4 show the predominance of small, sedentary and cryptic species on trawls, and larger elasmobranchs, mobile teleosts and eels in BRUVS samples (Figure 4.4). For night-time BRUVS sets, the striped perch *Terapon theraps* was important as an abundant species characteristic of all areas, but few species were abundant. The higher DLI for the mobile Carangidae and Nemipteridae were distributed amongst both the terminal nodes and higher branches for the BRUVS, but different members of the genera *Carangoides*, *Decapterus* and *Alepes* characterised different terminal nodes. The nemipterids (*Nemipterus*, *Pentapodus* and *Scolopsis*) that were major indicator species for 'day' assemblages are small mobile predators of benthic organisms and scavengers (Table 4.8).

A wider variety of small, sedentary species, flatfish (e.g. bothids, psettodids), small demersal micro-carnivores (e.g. mullids, leiognathids and gerreids), cryptic demersal ambush predators (e.g. synodontids) and one small semi-pelagic carangid, were indicator species for the assemblages identified by trawls with very high DLI values. The sedentary, demersal, platycephalids (*Elates* and *Suggrundus* spp.) occurred at several levels in the tree. There were

only five species common to four of the terminal assemblages identified by both techniques: *Upeneus sundaicus* (Double Island-Day); *Terapon theraps* (Double Island-Night); *Argyrops spinifer* and *Saurida undosquamis* (Double Island Wide-Day); and *Choerodon* sp2 (Scott Reef-Day). These were relatively small (mainly 150-300mm TL), mobile, demersal predators of benthic invertebrates and fish, with the exception of the ambush predator *S. undosquamis* (see Table 4.8).

4.3.4 Predicting group membership

The MRT included both BRUVS and trawls in the same analysis. Separate, unconstrained ordinations of the site-standardised extended dissimilarity matrix (*xdiss*) showed clear separation of six fish assemblages based on location, night and day for each technique. These six treatment groups are outlined by polygons, with their group means, in the principal coordinates analysis (Figure 4.5). Both data sets showed strong group differences with the main effects of locations (DI, DIW and SR) and day-night forming the primary two dimensions in multivariate space. For the BRUVS, the first dimension showed strong day-night differences and Scott Reef separated strongly from the two Double Island locations on the second dimension. The patterns of separation for the trawls between the treatments were very similar to the BRUVS, but for trawls the variation within groups was somewhat larger.

The analysis then proceeded by constraining the dissimilarity matrix by the treatment groups, to enable a 'constrained analysis of principal coordinates' (CAPSCALE) which is identical to a distance-based redundancy analysis when using *xdiss*. Eigenanalysis showed that the six treatment groups, or species assemblages, accounted for 86.3% of the total (constrained + unconstrained) distance variation for the BRUVS data and 79.3% for the trawl data (Table 4.5). Only BRUVS detected a significant interaction between location and time of day with the full dataset. The distance variation explained by the model was reduced slightly to 82.8% for the BRUVS data and 81.8% for the trawl data when analyses were restricted to only those 38 species recorded by both techniques, and only trawls detected a significant interaction between location and time of day (Table 4.6).

Table 4.5. Distance-based redundancy analysis of full dissimilarity matrices for all transformed BRUVS and trawl data.

Effect	df	BRUVS			Trawls		
		SS	Psuedo-F	P	SS	Psuedo-F	P
Locations (L)	2	1.27	13.27	<0.001	1.95	14.42	<0.001
Day-Night (DN)	1	2.37	49.52	<0.001	1.21	17.84	<0.001
L * DN	2	0.27	2.81	0.028	0.21	1.56	0.157
(L*DN)/Transect	13	0.62			0.88		

Table 4.6. Distance-based redundancy analysis of full dissimilarity matrices for transformed BRUVS and trawl data restricted to 38 species recorded by both techniques.

Effect	Df	BRUVS			Trawls		
		SS	Psuedo-F	P	SS	Psuedo-F	P
Locations (L)	2	3.31	14.59	<0.001	1.44	20.85	<0.001
Day-Night (DN)	1	3.37	29.72	<0.001	0.33	9.52	<0.001
L * DN	2	0.41	1.81	0.126	0.25	3.58	0.015
(L*DN)/Transect	13	1.48			0.45		

A more useful assessment of the relative effectiveness of the two techniques was their capacity to discriminate and to predict the fish assemblages represented by the six treatment groups. This was assessed using linear discriminant analysis of the principal coordinates from the extended dissimilarities. A detailed description of the procedure was given in Chapter 3 where the same approach was followed. The linear discriminant analysis showed that 98.3% of the variation between the six assemblages discriminated by BRUVS was accounted for by the first two discriminant axes (Figure 4.6). In the case of trawls, these two axes accounted for 98.6% of the variation between assemblages (Figure 4.6).

Drop-out analyses were performed by repeatedly and randomly excluding one transect and predicting its group membership from the other transects. The best level predictions occurred when only the first two principal coordinates were analysed. The BRUVS data provided more

accurate predictions. The error rate using the BRUVS data was 10.5% (two transects in 19), and using the trawl data the error rate was 21% (four transects in 19). Misclassification rates also increased with the number of coordinates used (Table 4.7). Given the small sample size these misclassification rates were likely to be fairly imprecise. All BRUVS classification errors were between the night groupings of Double Island and Double Island Wide – that is, a ‘day’ fish assemblage was not predicted as a ‘night’ assemblage, and vice-versa. In contrast, the trawl misclassifications predicted the Double Island-night transect to be a day-time assemblage at the same location, and there were errors within both day and night assemblages.

Table 4.7. Prediction of treatment groups using single drop-out linear discriminant analysis (LDA) for varying numbers of variables from principal coordinates analysis (PCoA).

PCoA Variables	BRUVS Error Rate (%)	Trawls Error Rate (%)
1,2	10.5	21.05
1,2,3	10.5	15.8
All	36.8	31.6

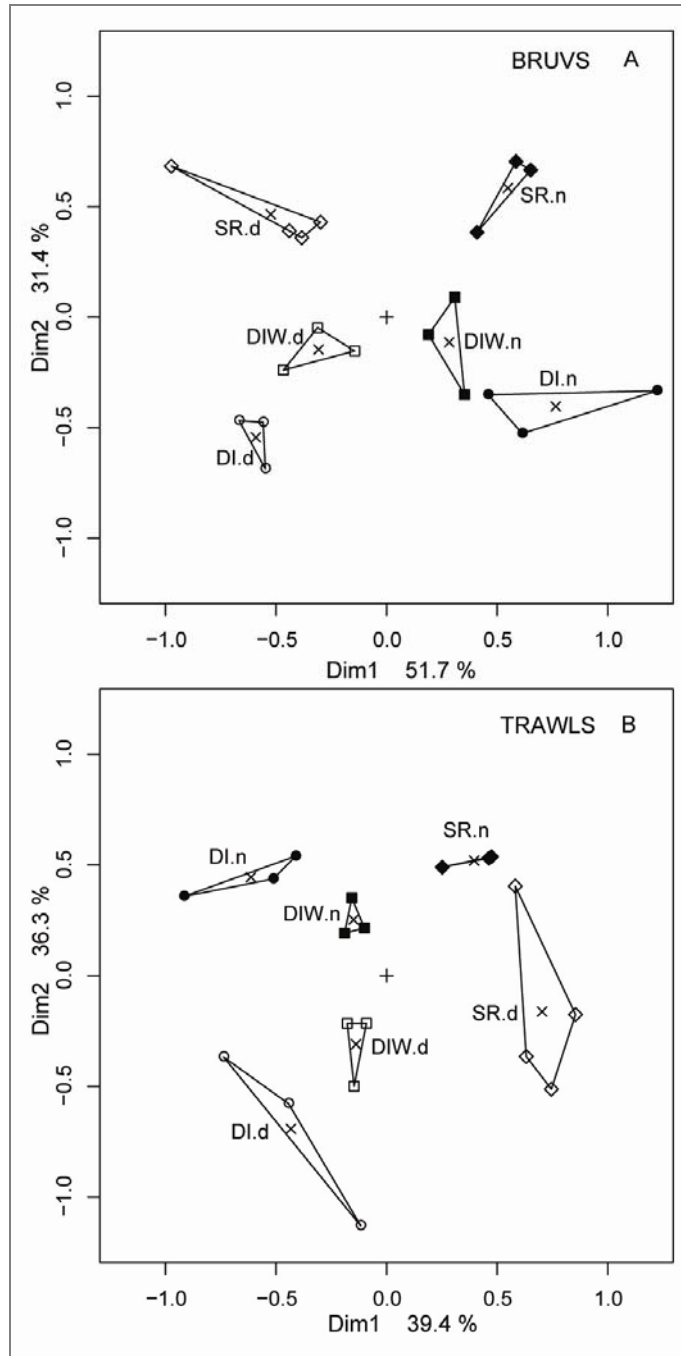


Figure 4.5. Principal Coordinates Analysis (PCoA) for species recorded by BRUVS (A) and trawls (B). The PCoA was based on extended dissimilarities calculated from species abundances which were transformed and row standardised. The 19 transects within each of the six treatment groups (three locations by day-night) are outlined by polygons. The locations are Double Island (DI), Double Island Wide (DIW) and Scott Reef (SR), the filled and open symbols are night and day sets.

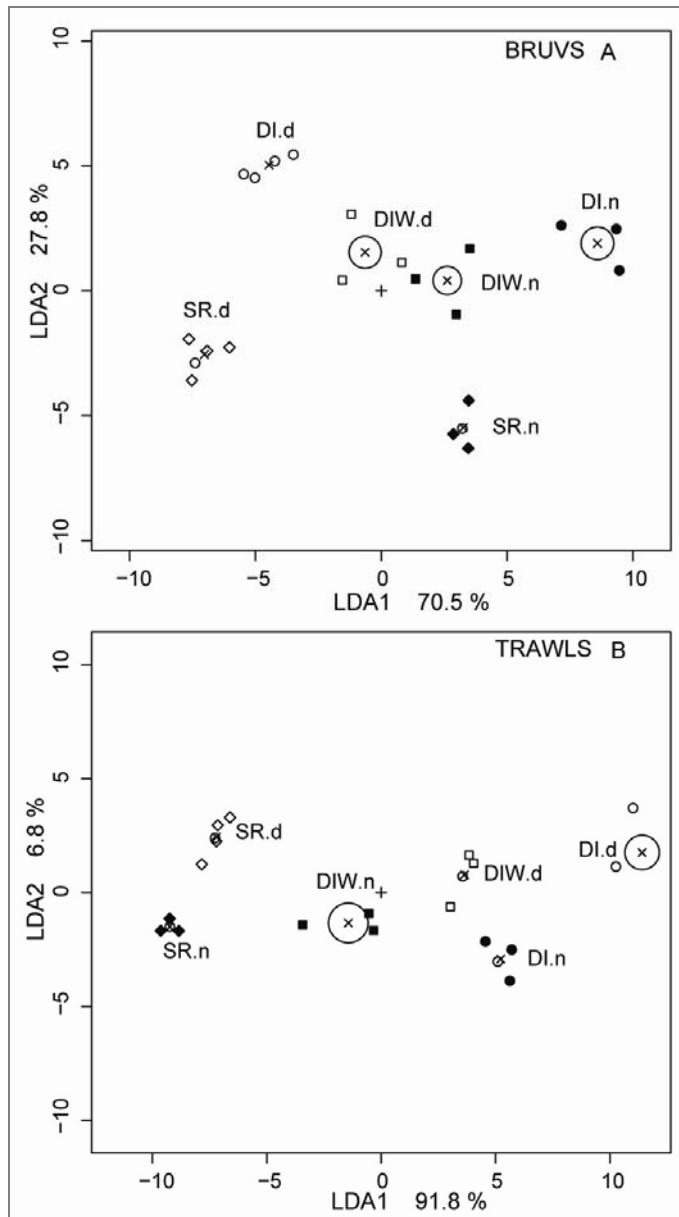


Figure 4.6. Linear discriminant analysis (LDA) plots based on the first two principal coordinates and six fish assemblages, defined by location and day-night, for the transformed BRUVS data (A) and trawls (B). The circles denote one Standard Error about the group means, and the symbols denote the transect means and assemblage membership. All conventions are the same as those for Figure 4.5.

4.3.5 Logistical consideration

The performance of BRUVS was governed by the prevailing levels of light and water clarity, and even moderate levels of turbidity can drastically alter the ability to identify and count fish in the field of view in deeper water. Trawls provided the highest possible level of taxonomic classification when specimens were retained, and can be used in any levels of turbidity or time of day. The need to freeze part or all of the trawl catch for later identification imposed strict limits on the type and size of vessel to be used in trawl surveys, but a fleet of BRUVS can be used from smaller, less specialised platforms.

Each BRUVS along a transect was set and retrieved rapidly (every three to five minutes), but the vessel had to retrace its path to retrieve them, consuming ninety minutes in the completion of a sixty minute BRUVS transect. The trawls consumed only twenty minutes fishing on the seabed for each transect, because the extra ten to fifteen minutes needed for setting and hauling the net was done whilst continually steaming toward new stations. The catch was partially processed during this time. The greatest time penalty in accumulating biodiversity data from the BRUVS was the need for a single skilled observer to scan five hours of videotape for each transect. This was shortened markedly, depending on the number and abundance of fish in the field of view, with the aid of fast-forward playback. Trawl samples were rapidly sorted and processed once a reference collection was assembled and identified, and this reference collection aided in the identification of the BRUVS reference images. The overall ratio of staff time in the field and laboratory to obtain the final BRUVS and trawl data was 3:2.

4.4 DISCUSSION

Studies of status and trends in multiple-use zones of marine protected areas require accurate estimates of species richness and abundance. A theoretical basis for the relationships between collecting effort and the number and abundance of species recorded provides both a planning tool for sampling expeditions and a predictive tool for conservation and biodiversity studies (Soberon & Llorente 1993). A first step in the planning process is to explore alternative or complementary sampling techniques, and I propose that the ability of different techniques to distinguish spatial and temporal patterns is of prime importance in most monitoring studies, and might be assessed with less field sampling than the intensive effort needed to establish definitive species accumulation curves in diverse faunas.

4.4.1 'Trawl ground' species show over-dispersion in relative abundance

The field comparison of BRUVS and industry-standard prawn trawls showed that both techniques detected the same spatial and temporal patterns in assemblages of fish biodiversity – despite sampling quite different portions of the fish fauna inhabiting commercial prawn trawl grounds. The relatively small sample size was insufficient to derive definitive species accumulation curves, and total species richness estimates, for the different assemblages, but important conclusions can be drawn from the shapes of the curves from the pooled data for each technique. Diversity, in terms of Simpson's and Shannon-Weaver indices, is positively correlated with the initial slope of species accumulation curves (Thompson & Withers 2003), so the curves for BRUVS and trawls were expected to cross if one sampling technique recorded a high proportion of both rare and abundant species compared with the other with a more even distribution of abundance amongst species. Instead, both curves were parallel and had very similar slopes and shapes, with BRUVS consistently about 6-11 species behind trawls for any extra transect, low points of curvature on the ordinate axis and a long upward slope to the asymptote. This curve shape is characteristic of faunas with a high proportion of rare species and a few abundant species (Magurran & Henderson 2003; Thompson *et al.* 2003).

Teleost and elasmobranch faunas of soft-sediment trawl grounds in the tropics are characterised by high diversity, and the limited sampling with BRUVS and prawn trawls recorded less than half (128 species) the number of species recorded in more extensive studies of similar habitats. In latitudes further north (11°-16° S), Wassenberg *et al.* (1997) caught over 340 species of teleosts and elasmobranchs (243 by prawn trawl), and Stobutzki *et al.* (2001b) recorded over 350 species of these two groups in prawn trawls. These inventories were dominated by species that occurred rarely and in low abundance and biomass. Stobutzki *et al.* (2001b) found that 75% of species occurred in less than ten percent of prawn trawls and were caught at low rates (< 10 individuals per hour and < 1kg hr⁻¹).

Like estuarine fish faunas, the teleosts and elasmobranchs on tropical trawl grounds probably comprise 'core species' which are persistent, abundant and biologically associated with particular habitats and 'occasional species' which occur infrequently in sampling records, are typically low in abundance and have different habitat requirements. The different distributions of these two groups can markedly increase the sampling effort needed to encounter the rarer species and those that have very small home ranges or avoid the sampling gear.

4.4.2 BRUVS discriminated better amongst site groups

As expected, the diverse assemblages on the Scott Reef grounds south of Cape Grafton were distinct from the northern grounds off Double Island, and day-night differences were significant. Significant cross-shelf differences in fish assemblages were also detected between the shallow, inshore Double Island (18-23m) and deeper, offshore Double Island Wide (31-33m) grounds. Even when analyses were restricted to the fish species common to both techniques, the same six fish assemblages were distinguished, but with marked differences in the relative abundance of many species. There were only five small, mobile species common to both techniques in the separate lists of top indicator species for these assemblages. The somewhat lower taxonomic resolution of the BRUVS might be expected to reduce the statistical power to discriminate between community types, yet the BRUVS technique more precisely and accurately described and predicted the fish assemblages in the field comparison. The BRUVS data produced greater separation of the fish assemblages than trawls, with the grouping into six fish assemblages accounting for 86.3% of the distance variation in the BRUVS data and 79.3% in the trawl data. The BRUVS also had only half the error rate of trawls in discriminating between the six fish species assemblages, and prediction errors occurred only between nearby locations at night.

4.4.3 Both techniques show selectivity

Both techniques showed selectivity in distinguishing the fish assemblages, but without a better knowledge of the true composition of the fish fauna in the study locations it was not possible to precisely identify these biases to adequately assess 'rarity' and other biodiversity indices. The trawl nets fitted with bycatch reduction devices exclusively sampled small (mainly <300mm), demersal, sedentary or cryptic species, such as bothids, platycephalids, apogonids, synodontids, triglids and callionymids. The BRUVS recorded more larger, mobile species from a much wider size range of families, including large sharks and shovelnose rays, many more pelagic species (such as carangids and scombrids) and numerous mobile eels. Herbivorous siganids were rarely recorded by BRUVS, but were more common in trawls. Mobile scavengers and benthic carnivores such as nemipterids and teraponids were abundantly recorded on BRUVS and caught in lesser numbers in trawls. The occurrence of 38 small mobile species was common to both techniques, but most showed marked differences in relative abundance. The BRUVS performed best in the day, and trawls caught more species at night.

Some aspects of these differences can be expected on the basis of how each technique operates. Trawls disturb the seabed sufficiently to scare flatfish and other sedentary or resting species upward and into their aperture (Stobutzki *et al.* 2001a). Small, diurnal schooling species, such as

the pomacentrid *Pristotis jerdoni*, and small, diurnal territorial species (possibly labrids like *Choerodon* sp2) might therefore be expected in larger numbers in trawls, especially at night. Large shovelnose rays and sharks may have been excluded from the nets by the bycatch reduction devices, but the total lack of eels in trawls is less readily explained. The small moray eel *Gymnothorax minor* was ubiquitous on BRUVS sets along many transects. Eels may have sheltered in holes in the seabed upon the approach of a trawl footrope, or may have escaped the trawl net by squeezing through the meshes. The cryptic and sedentary habits of the bothids and platycephalids explains their absence from BRUVS records, but the lack of relatively large priacanthids and small schooling apogonids that feed in the water column was unexpected. It may be that these fish shelter by day on the seabed, or in holes formed by bioturbators of the sediments.

The specific differences in species richness reported here are similar to a comparison of the catches made by Frank and Bryce fish trawls and prawn trawls in the far northern section of the GBRMP (Wassenberg *et al.* 1997). The fish trawl was expected to sample fish more effectively, because it had a higher headline opening (4-5m) and was linked to the otter boards by very long bridle wires known to herd fish toward the net (Ramm & Xiao 1995). Wassenberg *et al.* (1997) recorded 236 species of teleosts and elasmobranchs in the fish trawls and 243 species in prawn trawls, with 141 species common to both techniques. Like the BRUVS, the species caught only by the fish trawl were mainly pelagic species (scombrids, carangids) or large specimens of large species (lutjanids, sharks, rays), while the fish caught only by the prawn trawl were small benthic species, such as apogonids, platycephalids, scorpaenids and flatfish. For seven species, the prawn trawl caught significantly smaller specimens, and over eighty percent of the fish caught by both nets were small (<300mm standard length). There were also significant day-night differences in vulnerability to capture.

Baited videos record species attracted to the bait plume or camera station, species attracted to the commotion caused by feeding and aggregation at the station, and species indifferent to the station but present in or passing through the field of view. The dynamics of visitation, attraction (or repulsion) and species replacements are species-specific and largely unknown (see Chapter 2.1.2). Strongly site-attached and territorial species might have been unavailable for survey by BRUVS settling outside their territory. Agonistic behaviour may have repelled, or caused competition for, visitation opportunity by other species and conspecifics. However, there were no clear indications of these factors in the BRUVS footage.

Whilst BRUVS may have better described the spatial patterns of relative abundance for fish biodiversity assessments, their results could not be simply expressed in terms of absolute

density or biomass. The 'biomass per swept area' of each species can be readily calculated from timed trawls, but this statistic can be severely biased by the behaviour, size, body shape and position in the water column of different fish species (Ramm *et al.* 1993; Adams *et al.* 1995; Ramm & Xiao 1995). The 'area fished' by BRUVS was unknown, and the depth and width of the field of view was not fixed. The use of stereo-video camera systems can overcome some of these deficiencies by providing range, aspect, bearing and size of subjects. Fields of view can therefore be readily fixed, and fish within them can be precisely and accurately measured for length (and weight) estimates.

Robust models of bait plume dynamics and fish visitation rates will be needed to estimate the sampling areas of BRUVS and convert the counts of fish sightings to density estimates. Models using fish swimming speed, current velocity, *TFAP* and *MaxN* at given time periods have been developed to estimate density of abyssal scavengers but they require accurate knowledge of many parameters. The BRUVS used in this chapter had the bait canister resting flat on the seabed where frictional forces enforced a 'boundary layer' not simply represented in bait plume models by prevailing current speed in the upper water column.

The spacing of the BRUVS 450 metres apart along transects was designed to minimise the possibility of large-scale interference of the replicates in our study. It is possible that some large, mobile species (such as cobia *Rachycentron canadum* and hammerhead sharks *Sphyrna* spp) may have visited more than one BRUVS replicate within a transect, but confusion of catch amongst trawling locations was also observed when there was inadequate removal of meshed fish from the net wings between trawls.

4.4.4 The role of BRUVS in assessments of seafloor biodiversity

There may be a particular role for baited video techniques in studies of large elasmobranchs and teleosts (e.g. serranids) of special conservation interest. These groups have undergone global decline (Myers & Worm 2003) and non-extractive, fishery-independent sampling techniques are desirable to assess their population status (Robbins *et al.* 2006). Stobutzki *et al.* (2002) proposed that the elasmobranchs least likely to sustain populations in one prawn fishery were demersal batoids that feed on benthic organisms and are highly susceptible to capture in trawls. Some of these more vulnerable species have been recorded by BRUVS, but the rarer ones will always remain difficult to assess because the sampling unit cannot match their distribution and low abundance. The use of stereo-video pairs would improve the information gained from such rare

sightings by providing morphometric measurements and recognition of individuals (Shortis *et al.* 2009).

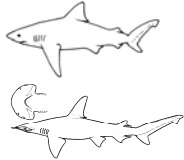
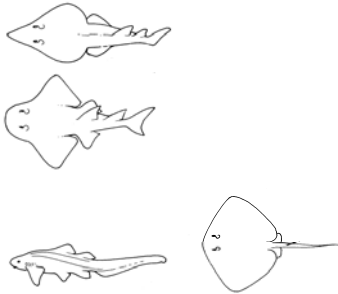
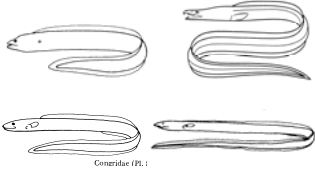

There is unlikely to be much potential for the use of BRUVS in assessing status and trends in the individual populations of teleost ‘bycatch species’ most vulnerable to prawn trawling in this region. Using meta-analysis of life history traits and susceptibility to capture, Stobutzki *et al.* (2001a) concluded that these teleosts came from the families Apogonidae, Ariidae, Bathysauridae, Callionymidae, Congridae, Diodontidae, Labridae, Opisthognathidae, Plotosidae, Synodontidae and Tetraodontidae. Our comparison showed that BRUVS were not as useful as prawn trawls in recording many species from these families. A Frank and Bryce fish trawl might offer a better sampling technique than a combination of BRUVS and prawn trawls to accumulate species inventories, but catch rates are so high ($395 \pm 141.3 \text{ kg hr}^{-1}$ in Wassenberg *et al.* 1997) that their routine scientific use in the GBRMP would be undesirable.

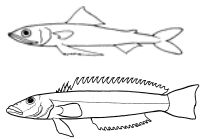

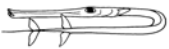
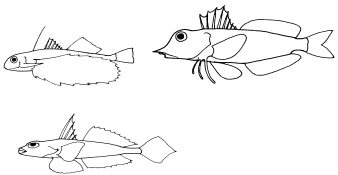




Trawls can be used in most currents, sea states and any time of day and levels of turbidity. The performance of BRUVS was limited most by prevailing clarity of the water column and light levels. The ability to more accurately identify retained trawl specimens enabled a refinement of species identifications made from the BRUVS imagery. Logistically, trawls are attractive to survey fish biodiversity on suitable seabeds because they can be deployed and the catch partially processed whilst the research vessel is continually steaming toward new stations. BRUVS can be deployed from smaller, less costly platforms by unskilled operators, but the easy completion of many transects produces a much larger workload for skilled observers in tape interrogation than that needed to process trawl samples. Greater gains in efficiency of the BRUVS technique can be made by assessing the accumulation of new species sightings with a reduced number of BRUVS replicates and with reduced set times. These relationships are likely to be habitat-specific.






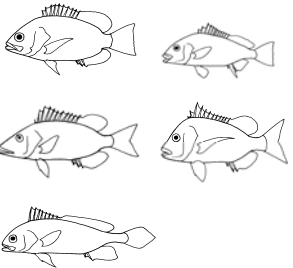


The ability to rapidly, precisely and non-extractively sample reef edges and bases, hard outcrops and shoals is a major advantage offered by BRUVS for comprehensive surveys of seafloor biodiversity. Research trawls are not accomplished easily on such seabed topographies, nor are they permitted in many zones of the GBRMP. Trawls cannot detect small-scale variation in species composition and abundance along transects, nor do they provide any information about the immediate habitat that fish are taken from. For example, Watson and Goeden (1989) concluded that the soft-sediment fish fauna in the GBRMP is abruptly distinct from the fauna inhabiting complex topography such as reef bases. The use of BRUVS provides imagery of the benthos and sediments inhabited by the fish targets, allowing detection of such small-scale (metres to hundreds of metres) differences in species composition and behaviour, and providing


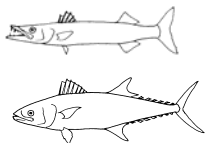

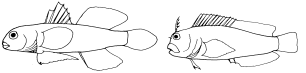

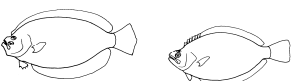
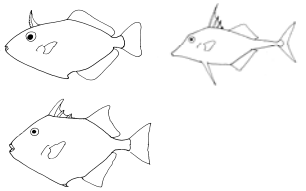
a basis for explanation of the existence of distinct fish assemblages in terms of directly measured environmental covariates.

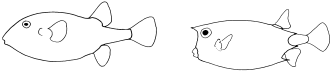
Table 4.8. The functional morphology, habits and approximate, reported size range of adults (or juveniles, as indicated with an asterisk) (after Gloerfelt-Tarp and Kailola 1984; Sainsbury *et al.* 1985) of the genera and families mentioned in the text and tables, grouped by their form and trophic level.

Genera	Form	Family and Common Names	Total length (cm)	Habit and morphology
<i>Carcharhinus, Sphyrna</i>		Carcharhinidae, Sphyrnidae: whaler and hammerhead sharks	200-350	pelagic, fusiform macro-carnivores
<i>Rhynchobatus, Rhina, Stegastoma, Dasyatis</i>		Rhynchobatidae, Stegastomatidae, Dasyatidae: shovelnose and shark rays, stingrays	200-350	demersal, dorso-laterally flattened benthic carnivores of macro-invertebrates
<i>Gymnothorax, Muraenesox, Conger</i>		Muraenidae, Congridae, Muraenesocidae, Ophichthidae: moray, conger, snake eels	150	demersal, burrowing, elongate carnivores
<i>Euristhmus</i>		Plotosidae: eel-tail catfish	75	demersal, elongate, heavy venomous spines

Genera	Form	Family and Common Names	Total length (cm)	Habit and morphology
<i>Saurida</i> , <i>Trachinocephalus</i> , <i>Parapercis</i>		Synodontidae, Pinguipedidae: lizardfish, grubfish	20-60	demersal, cryptic, carnivorous ambush predators, somewhat dorso-laterally flattened
<i>Antennarius</i>		Antennariidae: anglerfish	5	sedentary, demersal, ball-shaped ambush predators
<i>Fistularia</i>		Fistularidae: cornetfish	50	extremely elongate, hovering ambush predators
<i>Dactyloptena</i> , <i>Lepidotrigla</i> , <i>Dactylopus</i>		Dactylopteridae, Triglidae, Callionymidae: flying gurnards, gurnards, dragonets	10-30	demersal, casque-like or flattened shape, bony or spiny heads; some venomous or toxic; broad or wing-like pectoral or dorsal fins used to perch or glide
<i>Centriscus</i>		Centriscidae: razorfish	10	armoured, extremely laterally compressed, elongate
<i>Elates</i> , <i>Suggrundus</i> , <i>Apistus</i>		Platycephalidae, Scorpaenidae: flathead, scorpionfish	10-40	demersal, sedentary and cryptic, dorso-ventrally flattened, heavy heady spination (sometimes venomous)
<i>Pseudochromis</i> , <i>Epinephelus</i>		Pseudochromidae, Serranidae*: dottybacks, groupers	10-30*	demersal, carnivorous, sedentary
<i>Terapon</i>		Teraponidae: grunters	25	mobile, schooling, demersal omnivores and scavengers

Genera	Form	Family and Common Names	Total length (cm)	Habit and morphology
<i>Priacanthus</i>		Priacanthidae: bigeyes	25	nocturnal planktivore; thick rough skin , heavy spines
<i>Apogon</i>		Apogonidae: cardinalfish	5-10	nocturnal, schooling; hovering planktivore
<i>Carangoides, Selaroides, Alepes, Rachycentron</i>		Carangidae, Rachycentridae: jacks, trevallies, cobia	20-150	gregarious, pelagic, laterally compressed or fusiform, fast-moving carnivores and planktivores
<i>Echeneis</i>		Echeneidae: remoras	70	pelagic scavenger
<i>Leiognathus, Pentaprion</i>		Leiognathidae, Gerreidae: ponyfish, mojarras	10-15	schooling, deep-bodied, laterally compressed benthic carnivores of invertebrate infauna and epifauna
<i>Lutjanus, Pomadasys, Lethrinus, Argyrops, Nibea</i>		Lutjanidae*, Haemulidae, Lethrinidae, Sparidae, Sciaenidae: snappers, grunts, emperors, porgies, croakers	15-40*	laterally compressed, heavily scaled, mobile, demersal carnivores of epibenthic invertebrates and fishes
<i>Nemipterus, Pentapodus, Scolopsis</i>		Nemipteridae: threadfin breams	20-35	mobile, schooling benthic predators of invertebrates
<i>Upeneus</i>		Mullidae: goatfish	15-30	mobile, predators of benthic invertebrate infauna

Genera	Form	Family and Common Names	Total length (cm)	Habit and morphology
<i>Pristotis</i>		Pomacentridae, Caesionidae: damselfish, fusiliers	5-30	schooling planktivores
<i>Sphyraena, Scomberomorus</i>		Sphyraenidae, Scombridae: barracuda, spanish mackerels	38-70	pelagic, fusiform piscivores
<i>Choerodon, Xiphocheilus</i>		Labridae: wrasse	10-15	demersal, benthic carnivores of invertebrates
<i>Yongeichthys</i>		Gobiidae, Blenniidae: gobies, blennies	5-10	demersal, sedentary carnivore; in holes and burrows
<i>Siganus</i>		Siganidae: rabbitfish	20	schooling, demersal herbivores with venomous spination
<i>Engyprosopon, Pseudorhombus, Grammatobothus</i>		Bothidae, Psettodidae: flounders, soles	20-40	demersal, sedentary, cryptic ambush predators and carnivores of benthic invertebrates
<i>Paramonacanthus, Anacanthus, Pseudotriacanthus</i>		Monacanthidae, Triacanthidae, Balistidae: filefishes, triplespines, triggerfishes	10-50	demersal, omnivorous, heavy barbed spines, thick rough skin or heavy armoured scales, laterally compressed

Genera	Form	Family and Common Names	Total length (cm)	Habit and morphology
<i>Lagocephalus</i> , <i>Torquigener</i>		Tetraodontidae, Ostracidae: puffers, boxfishes	15-30	demersal, ball-shaped, slow-moving, omnivorous with thick or armoured skin; some with toxic flesh

5. ENVIRONMENTAL GRADIENTS AND SHELF-SCALE PATTERNS OF SPECIES RICHNESS IN INTER-REEFAL WATERS

5.1 INTRODUCTION

In a definitive partitioning of global marine biomes and provinces, Longhurst (2007) introduced the ideal components of marine biogeography as the study of how and why species are distributed globally, how these species form ecosystems sustaining maximum biomass under characteristic regional conditions, and in what areas these ecosystems may be expected to occur. Much progress has been made in the explanation of variation in species richness along gradients in terms of evolutionary and palaeogeographic history, extrinsic, environmental factors and intrinsic, biological factors (Hawkins *et al.* 2003; Bellwood *et al.* 2005; Hawkins & Agrawal 2005; Diez & Pulliam 2007; Field *et al.* 2009). Macroecological studies have outlined the patterns and processes sustaining some marine ecosystems and predicting their response and resilience to perturbations through ‘phase shifts’ (Hughes *et al.* 2003; Bellwood *et al.* 2004; Hughes *et al.* 2005). On the whole, however, Longhurst (2007) concluded that oceanographers and marine ecologists have not been as interested as they should be in how ecosystems are constrained spatially.

In Longhurst’s regionalisation, each biogeochemical province has a characteristic suite of atmospheric, oceanographic, and topographic forcing factors to which there is a characteristic response of the pelagic ecosystem. These responses determine delivery of nutrients to the euphotic zone and demersal communities (Longhurst 2007). The boundaries of the provinces and their partitions are deterministic, even though the forcing factors are known to vary temporally. There are numerous types of faunal and floral assemblages whose locations do not vary, though their habitat is part of, or affected by, a surrounding or overlying pelagic ecosystem. The boundaries of these communities are considered to reflect the long-term average of the boundaries of the overlying pelagic system rather than tracking their location through time (Watson *et al.* 2003). The reef fishes of the Galapagos, for example, do not shift their location when El Niño conditions drastically alter the water column and its productivity (Robinson 1987), although their abundance and growth rates change (Meekan *et al.* 1999).

In Longhurst’s regionalisation, the GBRMP lies in the northern partition of the East Australian Coastal Province (AUSE) from the Papuan Barrier Reef down to Sandy Cape (25°S) where the wide shelf quickly constricts. It is considered with the lagoon system of New Caledonia’s reefs for some purposes. Longhurst (2007) makes no mention of general patterns in the demersal fish

fauna and its association with benthic habitats in this province, in contrast with his bold generalisations about the zonation of ‘brown’ (ariid catfish, sciaenid croakers), ‘red’ (lutjanid snappers) and ‘silver’ (sparid sea breams) assemblages predominating on Atlantic tropical shelves. Although the GBR is classified in its own ‘Large Marine Ecosystem’ (Sherman *et al.* 2003) in the East Australian Shelf Province (Brodie 2003), there has been no detailed description of the spatial organisation of demersal fishes at the provincial scale in relation to sedimentary facies, depth and epibenthic communities – in contrast to the Gulf of Carpentaria (Blaber *et al.* 1994), Gulf of Thailand (Pauly & Chuenpagdee 2003) and Guinea shelf (Bianchi 1992b; 1992a; Koranteng 2001).

In this thesis, I focus on relating patterns of species richness, assemblage structure and species occurrence, at the provincial scale of the entire GBR shelf, with some of the key environmental covariates characterising the seafloor and water column. To set the background for the remaining analyses, I describe in this chapter latitudinal and longitudinal environmental gradients in the entire GBRMP, from Cape York to the Capricorn Bunker Group, and correlate them with the spatial patterns in vertebrate species richness determined with BRUVS. At this scale, the influences on species richness of habitat type and properties of the water column can be interpreted with geographic ranges of the fauna to detect the presence of any random, ‘mid-domain’ effects (Colwell & Hurtt 1994).

I use covariates from two major approaches currently employed in macroecological studies. The first is a suite of “mechanistic” (or causative) variables relating to temperature, salinity, sediment composition, epibenthic ‘cover’ and depth. These were derived from the largest exploration of seafloor biodiversity ever undertaken in a tropical shelf ecosystem (Pitcher *et al.* 2007), and follow the approach of Longhurst (2007) of measuring (often by remote sensing) and interpolating key environmental variables to define ecosystems. Studies of fish-habitat associations on tropical shelves are not common in the literature, but they generally correlate spatial patterns of fish abundance with depth, sediment type, salinity and temperature (Al-Ghais 1993; Bouchon-Navaro *et al.* 1997; Letourneur *et al.* 1998; Peterson *et al.* 2000; Garces *et al.* 2006b).

The second approach uses ‘heuristic’ spatial predictors representing the position ‘across’ and ‘along’, and the depth, on the GBR shelf of the sampling sites. Introduced by Fabricius & De’ath (2001b), the theory behind this philosophy was that any sampling region encompassing environmental gradients can be spatially divided in three dimensions in a manner that represents those gradients. Furthermore, it acknowledges that many mechanistic environmental factors can vary along the same gradient, and it is probable that some of these may be important but not

measured (or measurable) in a given sampling program. This can lead to spurious inferences about the variables that have been measured.

In theory, the difference in variation of a response along a gradient explained by models based on purely spatial predictors, and those based on the suite of explanatory covariates, represents the contribution of unknown environmental variables not measured in the study. However, this argument can become somewhat circular if the environmental covariates themselves have been derived by spatial interpolation in the study region.

In this chapter I have three major aims. Firstly, I describe the spatial and environmental gradients in the GBRMP, examine correlations amongst the explanatory variables, and test the degree of interpolation by latitude of some variables representing properties of the water column and sediments. Secondly, I use boosted regression trees to select models that best explain and predict the richness of the suite of vertebrates found at each of 366 BRUVS sites covering the breadth and width of the GBR shelf. Heuristic (spatial) and mechanistic (environmental) covariates, either measured at, or interpolated for, each site are allowed to compete in the models to identify the spatial gradients in species richness and interpret the environmental influences underlying them. Finally, I present measures of the location and range of each species, in comparison with random models, to detect the presence of any geographical mid-domain effect causing ‘hotspots’ of species richness across and along the GBR shelf. These results will guide my interpretation of patterns in species assembly and abundance in the final chapters of the thesis.

5.2 METHODS

5.2.1 Sampling area and species identifications

The GBRMP is the largest coral reef ecosystem on earth, with an area of 210,000km², excluding reefs and islands, extending over two thousand kilometres of coastline and fifteen degrees of latitude in an approximately northwest-southeast direction (Figure 5.1). The lip of the GBR shelf occurs at the relatively shallow depth of eighty metres, and the shelf plain is very flat, with a seaward gradient of less than 1:1,000 (Larcombe & Carter 2004). The deployment of BRUVS was part of a multidisciplinary exploration of seafloor biodiversity in the GBRMP involving a suite of sampling devices (Pitcher *et al.* 2002; Pitcher *et al.* 2007). The sampling strategy was based on biologically informed stratification of major physical variables to achieve representative sampling of the ‘environment space’ in the GBRMP. This stratification was

rationalised further, in order to sample as many different habitats types as possible, given the vessel time and resources available.

Six cruises of approximately one month duration were made between September 2003 and December 2005. A fleet of BRUVS were deployed during daylight hours about 350-400 metres apart with the prevailing wind to bracket the coordinate of each sampling site. Each replicate was considered to be sampling independently from the others at this separation (see Chapter 2.1.2). At each site, a stereo-video BRUVS was deployed first, followed by three (or occasionally four) BRUVS with single cameras. Adverse conditions at a small number of sites caused loss of some replicates, so footage from the stereo-video was included to make up a minimum number of three replicates at 366 sites in the BRUVS data analysed here (Figure 5.1).

The design and deployment of the BRUVS has been described in Chapter 2.2. They were set to provide at least 45 minutes worth of filming at the seabed (mean \pm s.d. = 53.3 \pm 11.3 minutes). Interrogation of each tape to record *MaxN* was conducted using the protocols described in Chapter 2.3. Species identifications were confirmed by checking the collection of reference images with museum taxonomists. Some distinct taxa within genera were labeled as ‘sp’. Other genera, families or orders contained several species that could not be reliably separated from each other in video records. These records were pooled at the level of species groups (*_grp*) at the level of genus, family or order. For example, flatfishes on the seabed were so indistinct that they could be identified only as far as family (e.g. *Platycephalidae_grp*) or order (*Pleuronectiformes_grp*), or (at worst) “*Flatfish_grp*”. The Australian blacktip sharks *Carcharhinus tilstoni*, *C. limbatus* and *C. amblyrhynchoides* resembled each other very closely and were pooled as *C. tilstoni_grp*. *Upeneus tragula_grp* covered *U. tragula* and some other mullids with barred tails (such as *U. sundaicus* and *U. sulphureus*). The small and comparatively elongate *Nemipterus balinensoides_grp* were distinct from other nemipterids, but may have included *N. celebicus* as well as *N. balinensoides*. However, the footage was too poor to separate them. Lizardfishes in the genus *Saurida* were all grouped as *Saurida_grp*. All these ‘taxa’ are hitherto referred to as species, and they are defined in Appendix 5.1 at the end of the chapter.

The species lists were pooled over all single BRUVS replicates at a site, and analysed at the level of individual sites. The positions of the sites were defined by mean depth derived from echosounder, relative distance across and along the GBRMP (Fabricius & De’ath 2001a) and distance to the nearest reef (centroid) in the GBRMPA reef inventory.

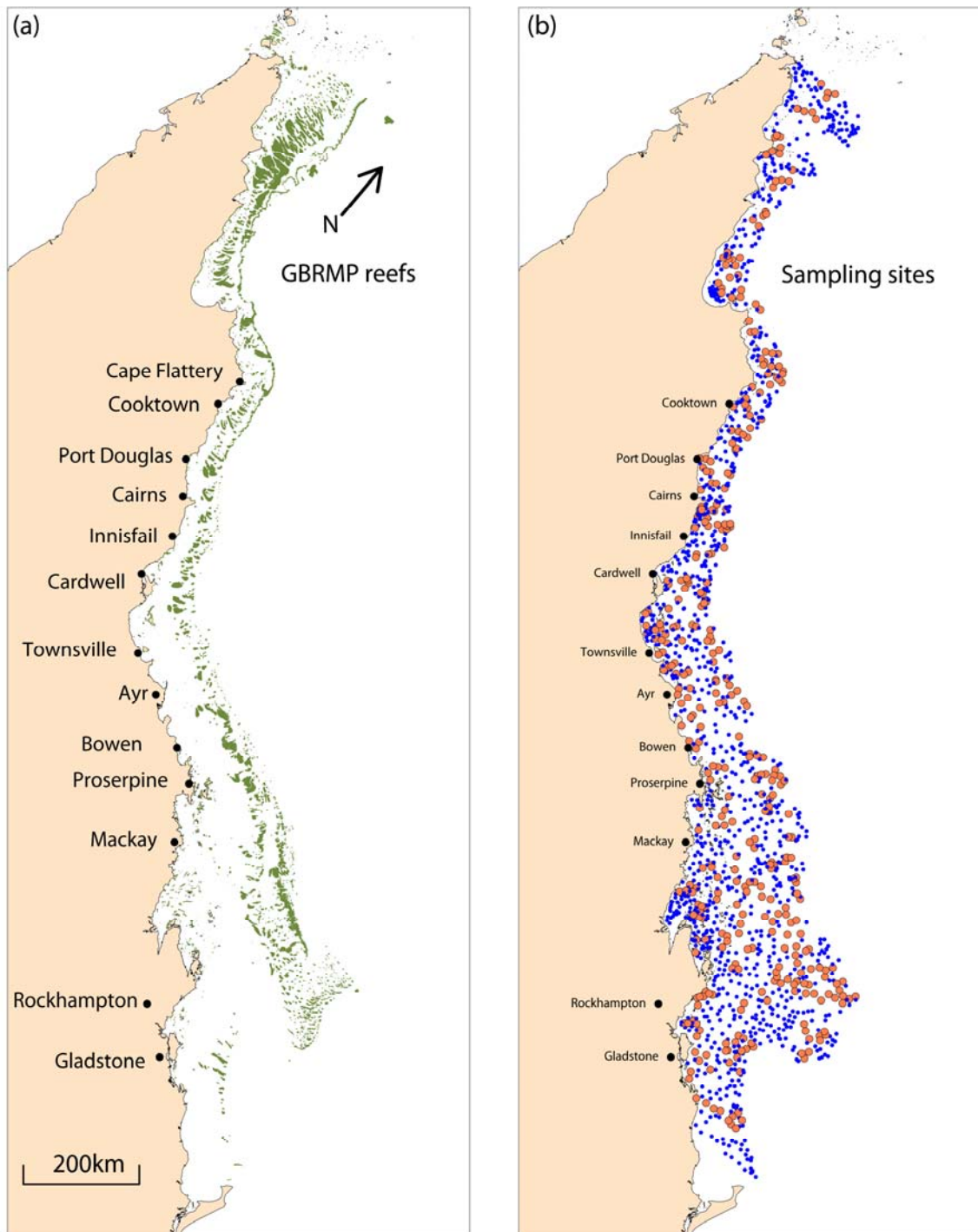


Figure 5.1. Rotated maps of the Great Barrier Reef Marine Park (GBRMP) showing (a) locations of the reef matrix (olive). All 1,531 sampling sites (blue), including the 381 BRUVS sampling sites (orange), are shown without the reef matrix (b).

5.2.2 Environmental covariates

At each of the 366 BRUVS sites, a wide variety of biotic and abiotic explanatory variables were measured directly, or interpolated from models based on information obtained by sediment sampling on site, remote sensing, or ‘ships of opportunity’ (Condie & Dunn 2006). Categorical variables concerning the nature of the substratum and coverage by epibenthos at each BRUVS site were derived from a towed television camera (CSIRO) with a digital stills camera attached (see Pitcher *et al.* 2007). The camera array was towed along and above the seabed at each site wherever possible, for a distance of ~500m, to characterise habitats and visible biota. The footage was analysed by CSIRO in real-time classifications at sea, and in more detail in the laboratory. The still images were subject to detailed examination to derive estimates of ‘cover’ of different categories of substratum, epibenthos and bioturbation. I mounted this raw data in a relational database (SBP_rawdata.mdb) for data aggregation and synthesis at various levels suitable for my analyses.

The variables interpolated for each BRUVS site at the seafloor comprised: the coarse fractions, mud, sand and gravel content, and carbonate composition of each fraction of sediment (GeoSciences Australia, see Mathews *et al.* 2007); means and standard deviations of water salinity and temperature (‘CSIRO Atlas of Regional Seas’; Condie & Dunn 2006); and the ‘seabed current shear stress’ (root-mean-square Newtons per metre²) (James Cook University; Bode & Mason, unpub.). High shear stress was known to be associated with large tidal ranges and narrow passages, and scours the seafloor. An index to the explanatory variables is provided in Table 5.1.

Most of the raw variables from the CSIRO analysis of video footage and still images of the seafloor were in categorical form, with percentage ‘cover’ in each category. These proved to be unwieldy in pilot analyses, because they were based on numerous, complementary categories on an increasing scale. For example, there were nine categories of substratum from mud to coral reef, with an increasing rugosity of the seafloor at each step in the data supplied.

The function `MatFunWgt` was devised for my use by Dr G. De’ath to provide measures of ‘location and spread’ of the percentage values within these categorical variables. For example, the variable ‘*rugosity.vid.av*’ represented a measure of location (the arithmetic mean) of the scores of substratum coarseness from mud to rocky-reef categories on the towed video footage. The lowest value implied prevalence of fine mud, and higher values implied coarser topography and substratum. A complete coverage (100%) of any one category on a given video tow would have been represented by ‘mud’ (*rugosity.vid.av* = 0), ‘silt’ (0.125), ‘sand’ (0.25), ‘coarse sand’

(0.375), 'gravel' (0.5), 'rubble' (0.625), 'stones' (0.75), 'rocks' (0.875) or 'rocky-reef' (1). A measure of the spread of particular parts of the spectrum (standard deviation), of the scores of substratum coarseness from these mud-to-reef categories was represented by '*rugosity.vid.sprd*'. Smaller values implied lower patchiness of the substratum along five-hundred metre video transects. For example, a high value of '*rugosity.vid.av*' and low value of '*rugosity.vid.sprd*' indicated a consistently rugose seabed. Low values indicated flat, mud seafloors.

Table 5.1. Definition of 28 explanatory variables supplied, or derived, for use in multivariate analyses.

Variable name	Definition of explanatory variable
BRUVS site information	
across, along	Cross-shelf position where zero was on the coast and along-shelf position where zero was the south-west corner of the GBRMP. The corners of the polygon formed in this way were 142.530° E, -10.690° S; 144.060° E, -10.680° S at the northern end, and 152.490° E, -25.000° S; 152.900° E, -24.220° S at the southern end.
depth	Depth in metres, recorded at each BRUVS site by echo-sounder
Current	CSIRO seabed current shear stress (Pascals; Newtons per metre ²) [Bode-Mason models, JCU]
Salin.av, Salin.sd	CSIRO CARS2000 average Salinity, standard deviation Salinity
Temp.av, Temp.sd	CSIRO CARS2000 average Temperature, standard deviation Temperature
dist.reef	The linear distance (km) from the BRUVS site to the nearest emergent reef (from GBRMPA reef centroids)
Towed video classification of substratum and biota along the five-hundred metre video transect through BRUVS sites	
rugosity.vid.av	A measure of location (mean) of the scores of substratum coarseness from towed video footage (nine classes) from mud to rocky-reef categories; the lowest value implied prevalence of fine mud along five-hundred metre video transect; higher values implied coarser topography and substratum. A complete coverage (100%) of any one category on a given video tow would have been ‘mud’ (rugosity.vid.av = 0), ‘silt’ (0.125), ‘sand’ (0.25), ‘coarse sand’ (0.375), ‘gravel’ (0.5), ‘rubble’ (0.625), ‘stones’ (0.75), ‘rocks’ (0.875), or ‘rocky-reef’ (1).
rugosity.vid.sprd	A measure of spread, or prevalence of particular parts of the spectrum (standard deviation), of the scores of substratum coarseness (nine classes) from mud to reef categories. Smaller values implied lower patchiness of the substratum.
bare.pc.vid, biotrb.pc.vid	Percentage of transect where epibenthos was absent (no fauna/flora visible), or where seafloor was bioturbated by animal burrows
plant.pc.vid	Percentage of transect where epibenthos was plants. The ‘algae’ + ‘unidentified flora’ + ‘seagrass’ covers were combined into one summed percentage
mgbnth.pc.vid	Percentage of transect where the epibenthos was ‘megabenthos’. This statistic pooled (summed) the percentage covers (in all densities) of ‘alcyonarians’, ‘sea whips’, ‘gorgonians’, ‘sponges’ and ‘corals’

Variable name	Definition of explanatory variable
Classification of biota and substratum characteristics from still images (<i>nframes</i>) along the five – hundred metre video transect	
rugosity.pho.av	A measure of location (mean) of the average covers of substratum coarseness in stills frames (eight classes from mud to boulder categories: mud; sand; coarse sand; small pebbles; large pebbles; cobbles; boulders; large boulders). The lowest value implied prevalence of fine mud amongst all frames. Higher values implied coarser substrata.
rugosity.pho.sprd	A measure of spread (standard deviation) of the average covers of substratum coarseness in stills frames (eight classes) from mud to boulder categories. The lowest value implied prevalence of particular parts of the spectrum.
bioturb.pc.pho	Average percentage cover of ‘bioturbated seabed’ amongst <i>nframes</i> within site.
seagr.pc.pho	Average percentage cover of ‘seagrass’ amongst <i>nframes</i> within site.
algae.pc.pho	Average percentage cover of ‘algae’ amongst <i>nframes</i> within site.
mgbnth.pc.pho	Average percentage cover of ‘megabenthos’ amongst <i>nframes</i> within site (sum of ‘alcyonarian-other’ + ‘alcyonarian-scleraxonian’ + ‘black coral’ + ‘hard coral’ + ‘pennatulacea’ + ‘sponges’).
othranim.pc.pho	Average percentage cover of other animals amongst <i>nframes</i> within site (sum of ‘anemone’ + ‘bivalve shell beds’ + ‘tube anemone’ + ‘zoantharian’ + ‘bryozoan’ + ‘hydroid’ + ‘ascidian’).
nobiota.pc.pho	Average percentage cover of ‘bare seabed’ amongst <i>nframes</i> within site.
GeoSciences Australia: interpolations from sediment analysis	
coarsns.pc	Coarse fraction of sieved sediment: ratio of sieve contents [1 or 2 mm sieve], divided by total sediment sample weight
carbnte.pc	Percentage carbonate content of sediments
gravl.pc	Percentage of gravel [= particles >2000 microns]
sand.pc	Percentage of sand [= particles 64-2000 microns]
mud.pc	Percentage of mud [= particles <63 microns]

5.2.3 Data analysis

5.2.3.1 Correlations amongst explanatory variables

Spearman-rank correlations were tabulated for all 28 variables in Table 5.1 to allow for coarse comparison of covariates. The information supplied by the CSIRO on depth, seabed current shear stress, salinity, temperature, carbonate content and composition of sediments for 1,531 sites were interpolated by general additive models with smoothed spline terms (see Chapter 2.4.5), and three hundred degrees of freedom, as a function of latitude and longitude. This was done to determine to what degree these variables were correlated with position (latitude and longitude) on the GBRMP shelf, and to visualize their distributions on colour-coded maps.

5.2.3.2 Mapping of dependencies of environmental variables and species richness

The dependence of key explanatory variables, and site richness, on spatial location and depth was assessed using boosted trees and partial dependence plots. The spatial location of BRUVS sites ‘across’ and ‘along’ the GBR shelf (Table 5.1, Figure 5.2) followed Fabricius & De’ath (2001a), setting distance along to range from 0 at the southern end to 1 at the far northern end. Distance across was 0 on the coast and 1 on the eighty-metre isobath. The coordinates of this system are locally orthogonal and run at right angles and parallel to the coast. They have repeatedly proven more efficient and interpretable than the grid of latitude and longitude because the GBR does not lie in a strictly north-south orientation, and the shelf width varies from about fifty kilometres in the north to over two hundred kilometres in the south (Fabricius & De’ath 2008).

Aggregated boosted trees (De’ath 2007) were used to quantify the influence on site richness of each one of the full set of 28 environmental covariates, and permutation tests ($n=5,000$ permutations) were used to test the significance of omission of each predictor in changing prediction error of the models. Five-fold cross-validation of the ABTs based on individual BRUVS sites as the sampling unit was made to select the best ABT models, including up to 5th order interactions and monotonic constraints applied to the functional form of selected predictors (see Chapter 2.4.2). Four statistics and methods, developed by De’ath (2007) and Fabricius & De’ath (2008), were used to interpret and compare models:

- The mean square prediction error for each model, expressed as a percentage of the variance of the response variable (%PE);
- The ‘importance’ of each predictor variable, represented as the percentage of variation in the response attributed to it;

- The significance of each predictor based on randomised permutation tests; and
- Partial dependency plots illustrating the relationship between richness and the environmental covariates.

All analyses used the ‘R’ statistical package (‘R’ Development Core Team 2006) including packages `gbmplus` and `vegan`.

5.2.3.3 Testing for a ‘mid-domain effect’ along environmental gradients

The mid-domain effect occurs when the overlap of species ranges in a particular region causes ‘hot spots’ of diversity. It can occur with an assembly of random location of species’ ranges along a spatial gradient, independent of any major environmental forcing at that particular region. Despite the theoretical interest in this phenomenon, there is a dearth of empirical techniques available in the literature to test for it. The technique chosen here uses the ‘R’ code of Fabricius & De’ath (2008).

This method assessed the spatial distribution of each taxon by calculating its location and range size along the two spatial gradients (‘across’ and ‘along’ the shelf). The location of a taxon along each gradient was defined as the median spatial coordinate of the BRUVS sites where that taxa occurred, and the range size (henceforth range) was the difference between the minimum and maximum coordinates of those occupied sites. To test for a mid-domain effect, these locations and ranges were compared against boot-strapped distributions (n=5,000 boot-strap samples) based on taxa occurring randomly at any BRUVS sites with a probability equal to their observed probability of occurrence over all the sites sampled. The observed locations and ranges were plotted with their boot-strapped counterparts and the 2.5th and 97.5th percentiles were used to label taxa with values within and outside the bounds expected under a hypothesis of random geographic distributions.

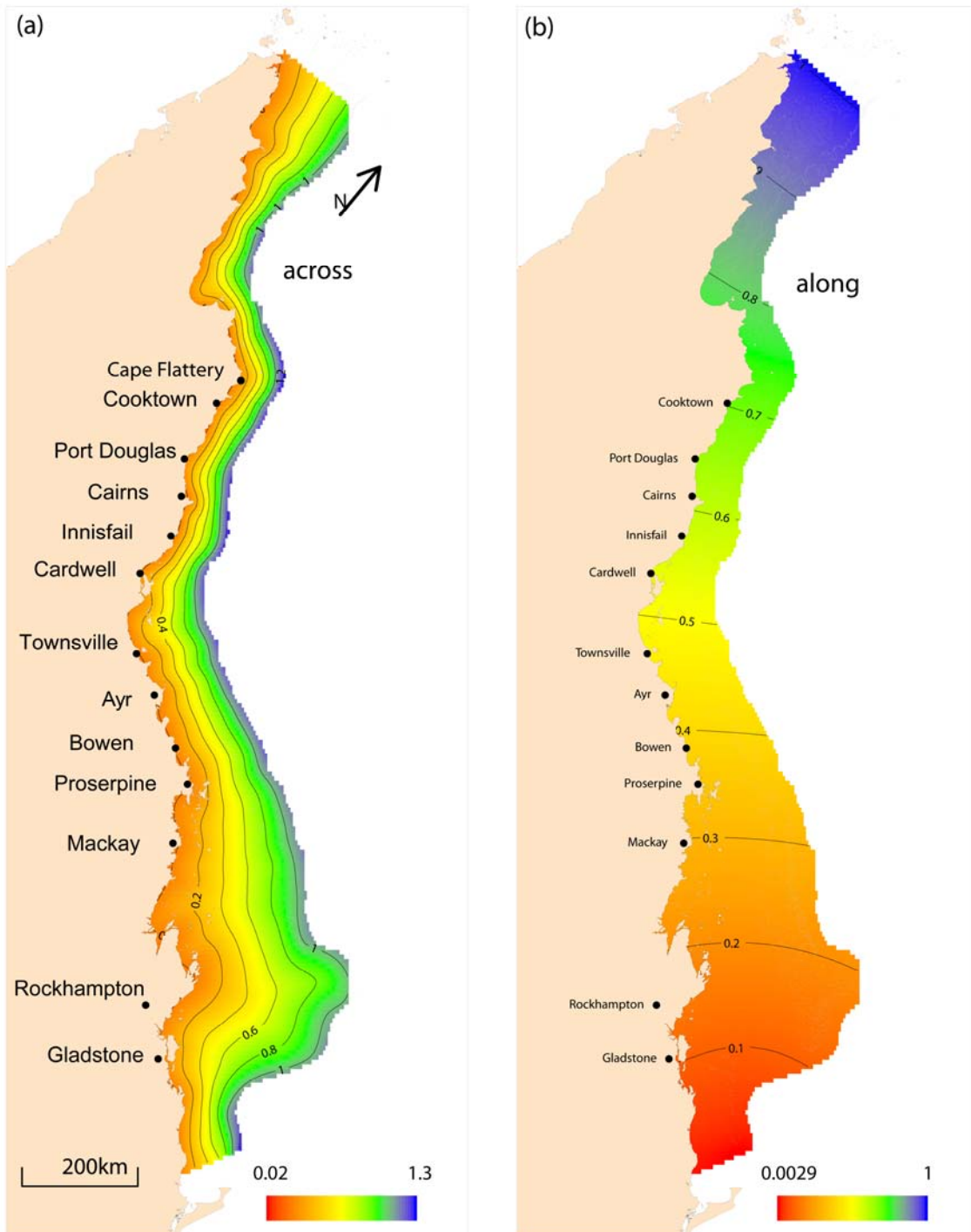


Figure 5.2. Patterns of variation of location (a) “across” and (b) “along” the shelf for the study area (rotated) smoothed using thin plate splines with three hundred degrees of freedom (see Chapter 2.4.5). Distance along was set to range from 0 at the southern end to 1 at the far northern end. Distance across was 0 on the coast and 1 on the 80m isobath.

5.3 RESULTS

5.3.1 Environmental covariates

A small subset of the 28 predictor variables had relatively high correlations, and is shown in Table 5.2. These correlations showed that ‘across’ and ‘along’ the shelf were likely to be surrogates for a variety of important predictors. Average salinity declined (and average temperature increased) with increasing distance northwards along the shelf. Depth and the percentage of carbonate in sediments increased with increasing values of ‘across’. Positive correlations between the records of epibenthos and seafloor topography on the real-time video classification running aboard ship (‘vid’ suffixes) and the detailed laboratory post-processing of still imagery (‘pho’ suffixes) were strong indications that the video tools and synthetic measures of location and spread were representing habitat types and data accurately.

A variety of predictors were negatively correlated with the percentage of mud in sediment samples, including the presence on video footage of plants, megabenthos and mobile animals. The presence of bioturbation visible as burrows in the seabed, and the variability in salinity (represented by the standard deviation), were positively correlated with the levels of mud in the sediments. This might represent the inflow of rivers to sites close to shore where the mud was of terrigenous origin and dominated the sediments. However, fine mud was also found offshore in carbonate facies. The other sediment fractions were complementary, so they were all negatively correlated with the mud fraction.

These correlations among explanatory covariates made interpretation of analyses difficult. If significant relationships were found between responses (such as species richness) and any covariate(s), the correlation did not imply the causal mechanism, nor did it mean that other correlated covariates were unimportant. These other variables may or may not have been measured in the study.

The summary of the smoothed GAM fits in Table 5.3 showed that the site data supplied by the CSIRO on sediments ($r^2 = 68\%-88\%$) and hydrology ($r^2 = 94\%-98\%$) for use as environmental predictors were spatially interpolated by latitude and longitude to a high degree. This implied their use would compete with cross-shelf and long-shore position in multivariate analyses of species-site dissimilarity matrices. Put simply, ‘across’ and ‘along’ would always represent some environmental covariates better than the interpolated values supplied for each BRUVS site. Partial regression plots can distinguish the influences of these covariates, and maps of the sedimentary and hydrological regime presented in the figures below will aid interpretation of the biological patterns documented in the thesis.

Table 5.2. Spearman rank correlation matrix for the entire set ($n=28$) of explanatory variables where the modulus of correlations >0.29 . Field names are defined in Table 5.1. The largest correlations (>0.69) are highlighted in bold. In this case, average water temperature (Temp.av) was positively correlated, and salinity (Salin.av) was negatively correlated, with increasing position northward along the shelf ('along').

var	coarsns.pc	carbnte.pc	gravl.pc	sand.pc	mud.pc	across	along	depth	Current	Salin.av	Salin.sd	Temp.av	Temp.sd	rugosity.vid.av	rugosity.vid.sprd	bare.pc.vid	biotrb.pc.vid	plant.pc.vid	mgbnths.pc.vid	bioturb.pc.pho	seagr.pc.pho	algae.pc.pho	mgbnths.pc.pho	othr.anim.pc.pho	nobiota.pc.pho	rugosity.pho.av	rugosity.pho.sprd	dist.reef		
coarsns.pc	1																													
carbnte.pc	0.3	1																												
gravl.pc	0.8	0.4	1																											
sand.pc	-	-	-	1																										
mud.pc	-0.4	-0.3	-0.4	-0.7	1																									
across	-	0.8	-	-	-0.3	1																								
along	-	-	-	-0.4	0.5	-	1																							
depth	-	0.6	-	-	-	0.7	-0.4	1																						
Current	0.4	0.3	0.4	-	-0.5	-	-0.5	0.3	1																					
Salin.av	-	-	-	0.5	-0.4	-	-0.9	0.5	0.4	1																				
Salin.sd	-	-0.4	-	-0.4	0.4	-0.6	0.4	-0.6	-	-0.5	1																			
Temp.av	-	-	-	-0.4	0.4	-	0.6	-0.4	-	-0.7	0.6	1																		
Temp.sd	-	-0.4	-	-	-	-0.5	-0.6	-0.3	-	0.5	0.4	-0.3	1																	
rugosity.vid.av	0.4	0.5	0.5	0.3	-0.6	0.5	-	-	0.3	-	-0.4	-0.3	-	1																

var	coarsns.pc	carbnte.pc	gravl.pc	sand.pc	mud.pc	across	along	depth	Current	Salin.av	Salin.sd	Temp.av	Temp.sd	rugosity.vid.av	rugosity.vid.sprd	bare.pc.vid	biotrb.pc.vid	plant.pc.vid	mgbnth.pc.vid	bioturb.pc.pho	seagr.pc.pho	algae.pc.pho	mgbnth.pc.pho	othranim.pc.pho	nobiota.pc.pho	rugosity.pho.av	rugosity.pho.sprd	dist.refef
rugosity.vid.sprd	0.3	0.3	0.4	-	-0.4	0.3	-	-	-	-	-0.3	-	-	0.7	1													
bare.pc.vid	-	-	-	-	-	-	-	-	0.3	-	-	-	-	-	-	1												
biotrb.pc.vid	-0.5	-0.3	-0.4	-0.3	0.6	-	0.3	-	-0.5	-0.3	0.3	0.3	-	-0.5	-0.4	-0.5	1											
plant.pc.vid	-	-	0.3	-	-0.4	-	-	-	-	-	-	-	-	0.4	0.3	-0.3	-0.3	1										
mgbnth.pc.vid	0.5	0.3	0.5	-	-0.3	-	-	-	0.4	-	-	-	-	0.5	0.5	-	-0.4	-	1									
bioturb.pc.pho	-0.4	-0.3	-0.5	-	0.5	-	0.3	-	-0.5	-0.3	-	-	-	-0.5	-0.4	-	0.6	-	-0.4	1								
seagr.pc.pho	-	-	-	-	-	-	-	-	-	-	-	-	-	-	-	-	0.5	-	-	1								
algae.pc.pho	-	0.3	0.3	-	-	0.4	-	-	-	-	-	-	-0.3	0.4	0.3	-	-	0.5	-	-	-	1						
mgbnth.pc.pho	0.5	0.4	0.5	-	-0.4	0.3	0	-	0.3	-	-	-	-	0.6	0.5	-	-0.4	0.3	0.6	-0.4	-	0.3	1					
othranim.pc.pho	0.4	0.4	0.5	-	-0.3	0.3	-	-	0.3	-	-	-	-	0.5	0.4	-	-0.4	-	0.5	-0.4	-	-	0.6	1				
nobiota.pc.pho	-	-	-	-	-	-	-0.3	-	-	0.3	-	-	0.4	-	-	0.3	-	-0.4	-	-0.4	-	-0.6	-	-	1			
rugosity.pho.av	0.3	0.4	0.4	0.3	-0.6	0.5	-0.3	-	0.3	-	-0.4	-	-	0.7	0.5	-	-0.4	0.3	0.4	-0.5	-	0.4	0.5	0.5	-	1		
rugosity.pho.sprd	0.4	0.3	0.4	-	-0.4	0.3	-	-	-	-	-	-	-	0.6	0.5	-	-0.4	-	0.4	-0.4	-	-	0.6	0.5	-	0.7	1	
dist.refef	-	-0.3	-	-	-	-0.3	-	-	-	0.3	-	-0.3	-	-0.3	-0.3	-	-	-	-	-	-	-0.3	-0.3	-	-	-	-	1

Table 5.3. Variation in predictor variables explained by general additive models with smoothed spline terms, and three hundred degrees of freedom. The models were based on information supplied by the CSIRO for 1,531 sites. The high values of the adjusted r^2 show that these environmental variables, supplied by the CSIRO, were spatially interpolated by latitude and longitude to a high degree.

Variable	Adjusted r^2
depth	89.4%
Current	86.04%
Salin.av	97.97%
Salin.sd	97.02%
Temp.av	93.85%
Temp.sd	98.52%
carbnte.pc	88.75%
mud.pc	82.68%
sand.pc	74.33%
gravl.pc	68.32%

5.3.2 Broad-scale spatial patterns in hydrological and sedimentary explanatory variables

Plots of the distribution and magnitude of the environmental predictors were the best way to comprehend the broad-scale patterns in the inter-reef habitats of the GBRMP. Whilst depth generally increased from north to south, and with across-shelf position (Figure 5.3), the ‘lagoonal’ waters south of Mackay (~50-80m) were much deeper than similar positions in the far north (~35m). Most of the GBRMP had low levels of seabed current shear stress when compared to the macrotidal region (Porter-Smith *et al.* 2004) in the southern section near Mackay (especially Broad Sound and Shoalwater Bay), and the major (Hydrographers Passage) and minor passages in the offshore ‘hard line’ of the Pompey and Swain groups of barrier reefs (Figure 5.3). Elsewhere in the GBRMP, high levels of seabed current shear stress were localised to narrow reef passages.

Long-term annual averages in salinity showed that the cooler, southern section of the GBR had higher salinity across the lagoon. Interaction of the shelf with oceanic water also induced higher salinities on the outermost margins of much of the GBR reef matrix (Figure 5.4). The variability in salinity was highest in the shallow, northern region of the GBRMP (Figure 5.4) under the influence of riverine inputs trapped in the narrow lagoon north of Cape Flattery where flushing rates are low (Hancock *et al.* 2006). Average temperatures at the seabed were about 2°C cooler in the south than in the north (Figure 5.5), and the higher variability in the south indicated higher seasonal, tidal and episodic fluctuations in this parameter.

A cold wedge in the Capricorn Channel and high variability in the far southern region may be caused by vertical mixing, due to the southward passage of the East Australian Current past the open end of the GBRMP (Middleton *et al.* 1994). The Coriolis force and south-easterly trade winds may combine to form internal waves that bring cool water upward and northward inshore, as well as moving sand in the same direction. The higher salinities and slightly slower temperatures in the region between Cardwell and Bowen (Figure 5.5) might be interpreted as representing the cross-shelf upwelling (Furnas & Mitchell 1996) and impingement of cool oceanic currents (Brinkman *et al.* 2002) known to occur there. These shoreward, cross-shelf flows of cooler water are permitted by the relatively wide and deep passages (e.g. Palm, Flora and Geranium Passages) between a looser matrix of widely spread emergent reefs (Figure 5.1).

The percentage of carbonate in sediments increased abruptly and strongly across the shelf (Figure 5.6), but there was no clear demarcation based on depth, as might be expected if wave energy alone shaped the transport of terrigenous sediments. Sediments high in carbonate were closest to emergent reefs (including the Capricorn-Bunker Group off Gladstone), but also

occurred around sunken shoals, or relict Pleistocene reefs, in the far northern section. The accumulation of fine mud was most evident north of Innisfail and inshore in northward-facing bays such as those around Bowen, Cairns and Cape Flattery. However, the deep water far offshore in the Capricorn Channel was also a vast zone of deposition of fine mud, scoured from the macro-tidal coastal region south of Mackay and sifted and moved inshore from the carbonate facies of the Swain Reefs (Figure 5.6).

The coarse fraction of sediment samples was highest in the outer barrier reef in general but especially off the macro-tidal coast of Mackay-Yeppoon in the Pompey and northern Swain groups of reefs. Seabed rugosity and the presence of rocks and large boulders were highest in the outer reef matrix, around the Capricorn-Bunker Group, and in the highly-scoured region between Yeppoon and the Whitsunday islands (Figures 5.7 and 5.8). The sediments were very coarse in Broad Sound and Shoalwater Bay around this node of high tidal energy. The percentages of sand and gravel in sediment facies also reflected the major physical factors at work in the water column (Figure 5.9).

Outer reef sediments were generally high in gravel, as were the Broad Sound and Shoalwater Bay regions close inshore (Figure 5.9). A northward-moving tongue of sand extended from Fraser Island along the shore through the Great Sandy Straits formed a sandy shelf around the Capricorn-Bunker Group as far north as Yeppoon. Elsewhere the sandy sediments were generally further offshore and amongst the reef matrix, but there were major mid-shelf sandy regions associated with the outflows of the Burdekin River (between Townsville and Ayr) and the Fitzroy River offshore from Rockhampton. These formed vast dunes and ripples in the vicinity of Old and Stanley Reefs off Cape Upstart. Such dunes are known to shift northward in cyclonic events (Larcombe & Carter 2004). There were also notable accumulations of coastal silica sands in the far north around Cape Bedford and Cape Flattery.

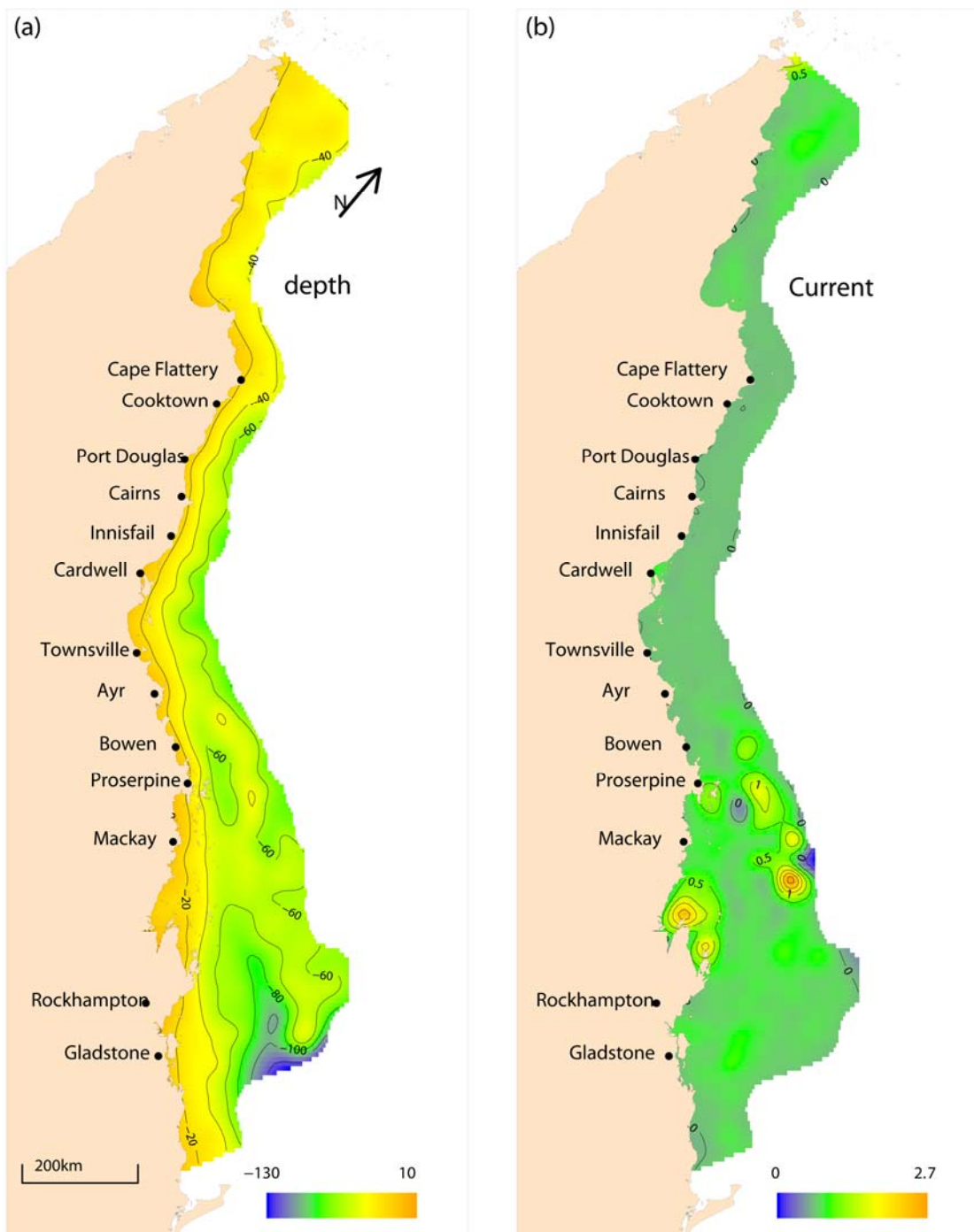


Figure 5.3. Plots of (a) depth and (b) the seabed current shear stress (Current; Newtons per square metre) interpolated for the entire GBRMP by general additive models with smoothed spline terms. The models were based on information supplied by the CSIRO for 1,531 sites.

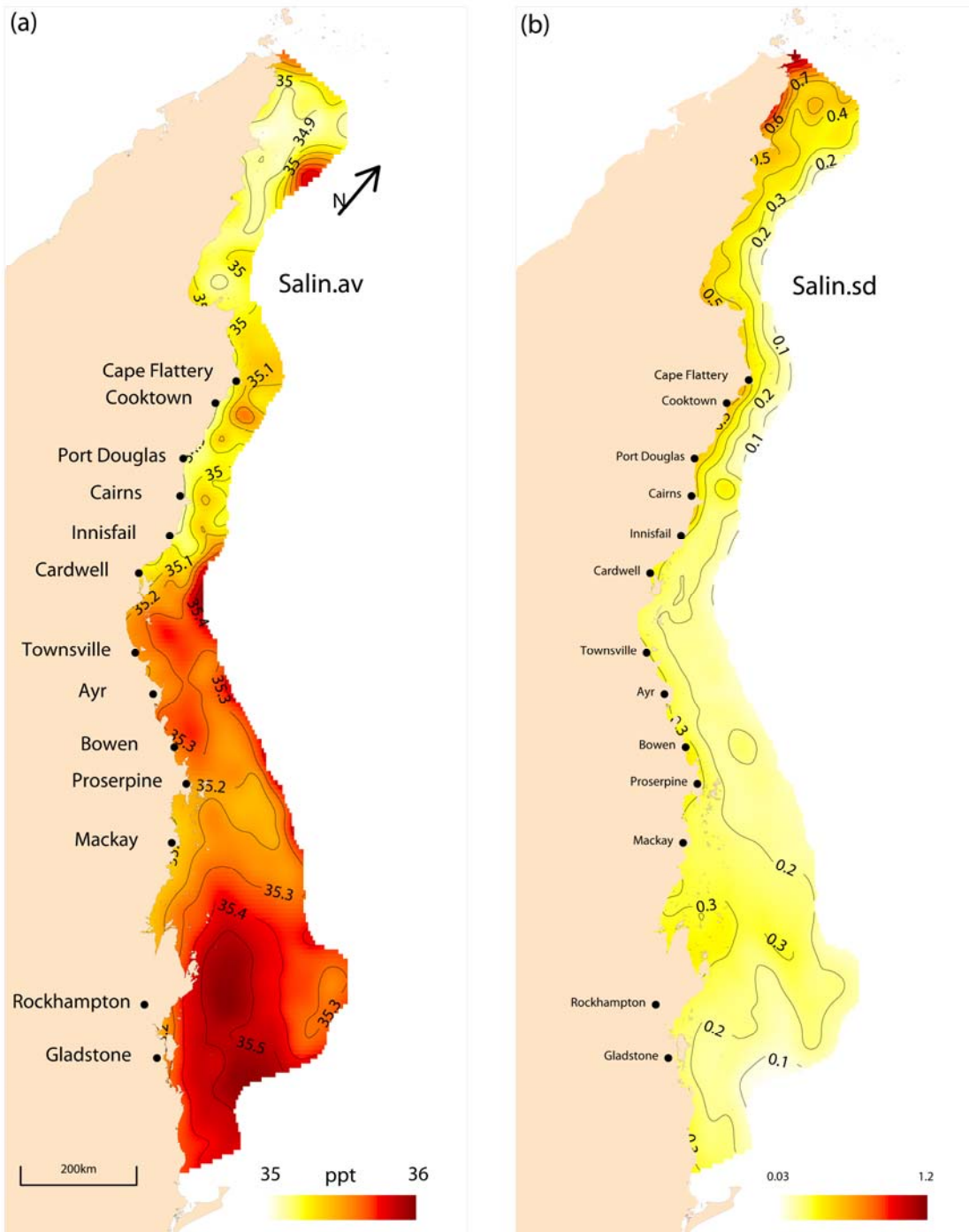


Figure 5.4. Plots of (a) the average (*Salin.av*) and (b) standard deviation (*Salin.sd*) in salinity at the seabed. Heat colour contours represent the relationship between each covariate and the position of 1,531 locations, interpolated to the entire GBRMP by general additive models with smoothed spline terms.

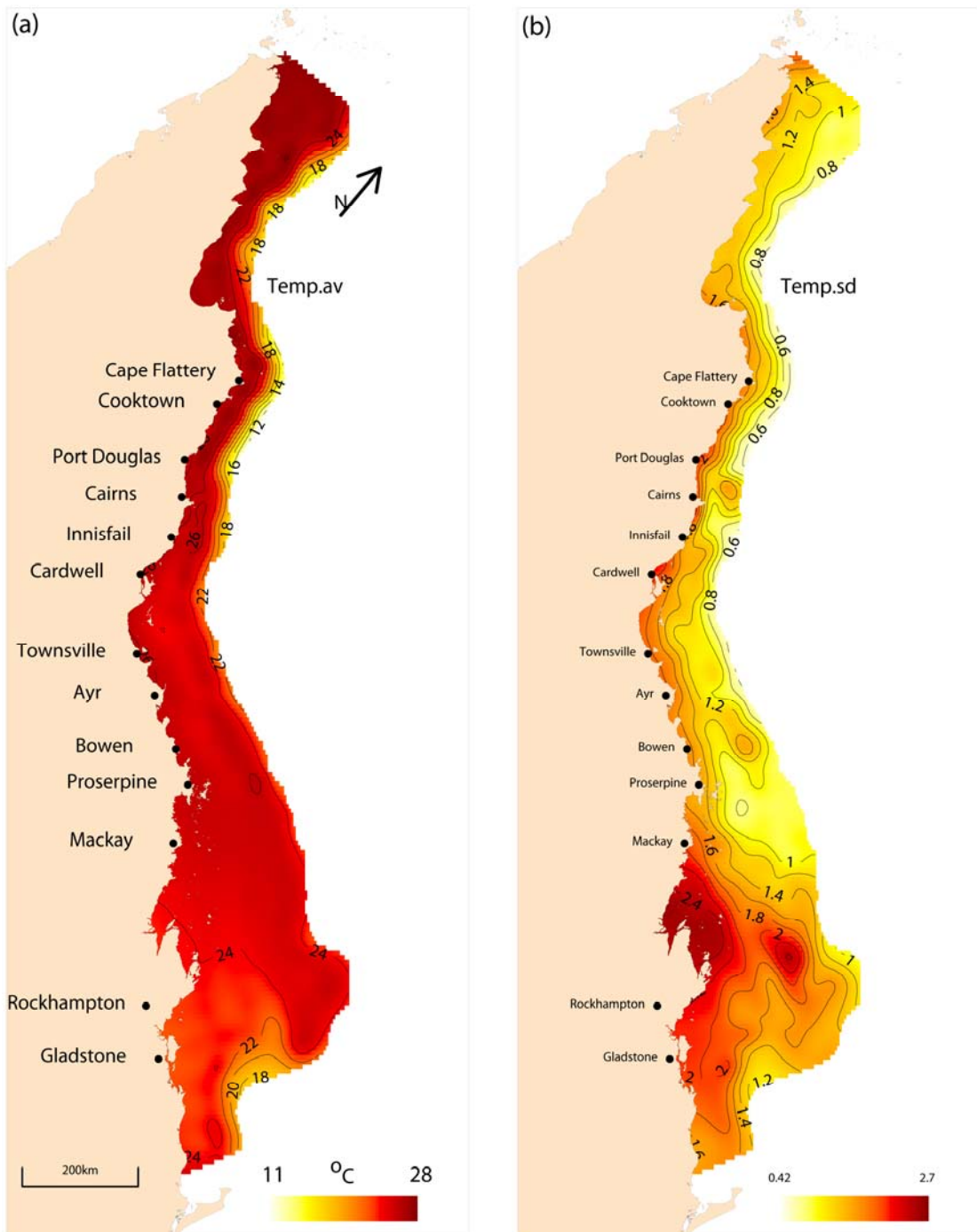


Figure 5.5. Plots of (a) the average ($Temp.av$) and (b) standard deviation ($Temp.sd$) in water temperature at the seabed interpolated by CSIRO in the GBRMP. All other conventions as per Figure 5.4.

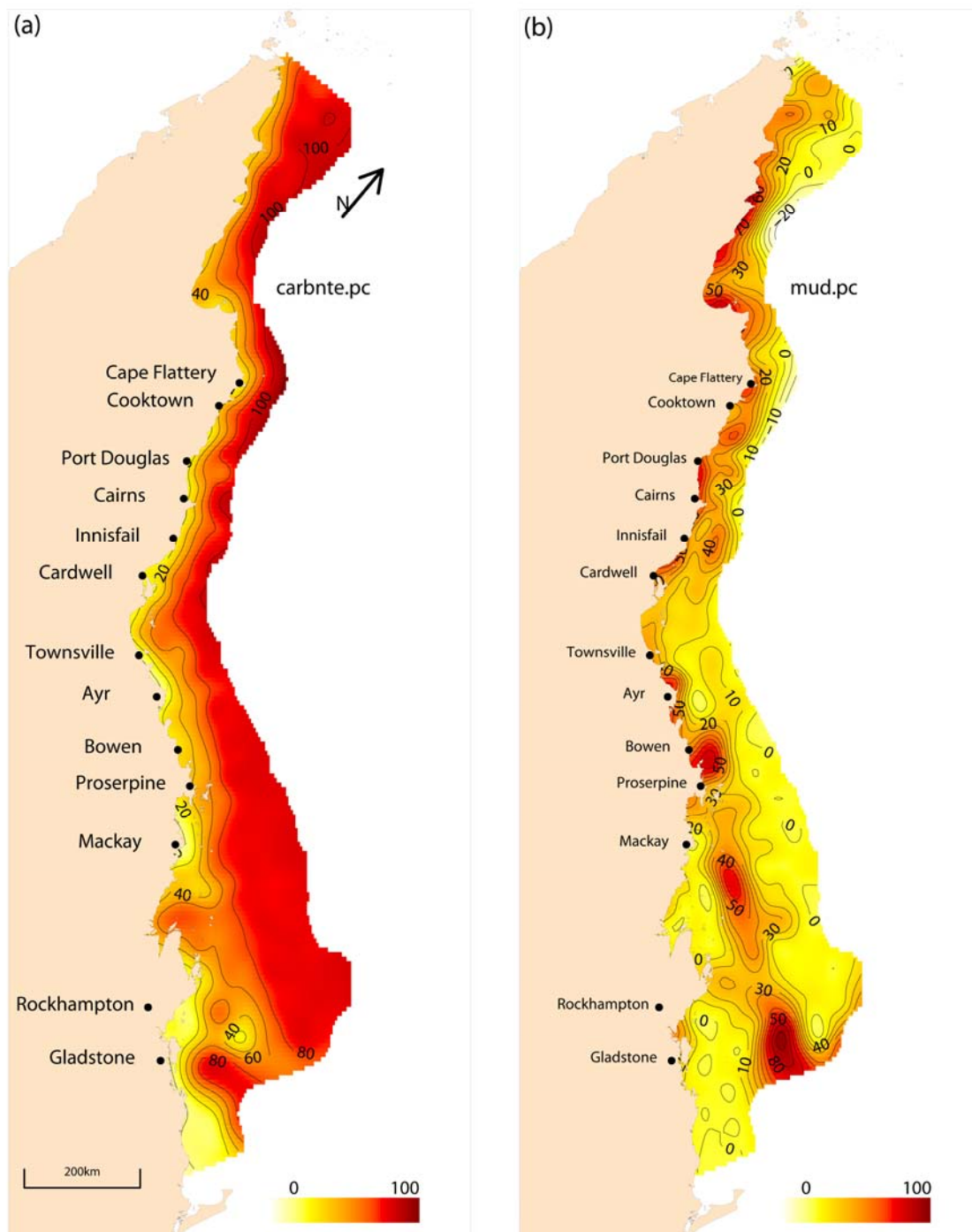


Figure 5.6. Plots of the percentage composition of (a) ‘carbonate’ (*carbnte.pc*) and (b) ‘mud’ (*mud.pc*) in sediment fractions interpolated by the CSIRO in the GBRMP. All other conventions as per Figure 5.4.

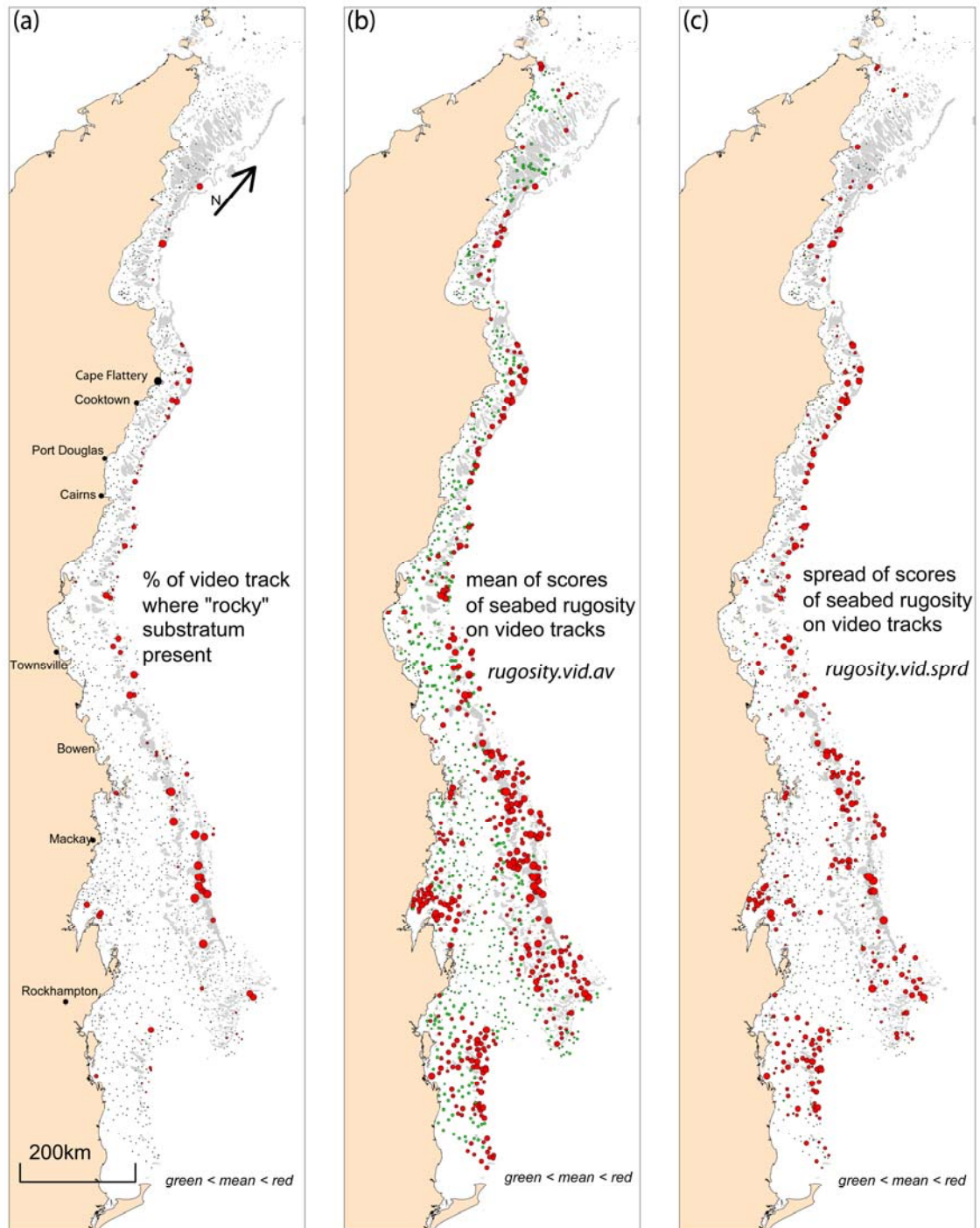


Figure 5.7. Plots of (a) the percentage of the towed video track on each site where ‘rocky’ substratum was present, and (b) measures of ‘location’ (mean: ‘*rugosity.vid.av*’) and (c) ‘spread’ of seabed rugosity (standard deviation: ‘*rugosity.vid.sd*’) on tracks. Symbols portray site measurements scaled to the maximum value at all sites for that covariate. Coloured symbols show sites with values less than (green) or greater than (red) the overall mean.

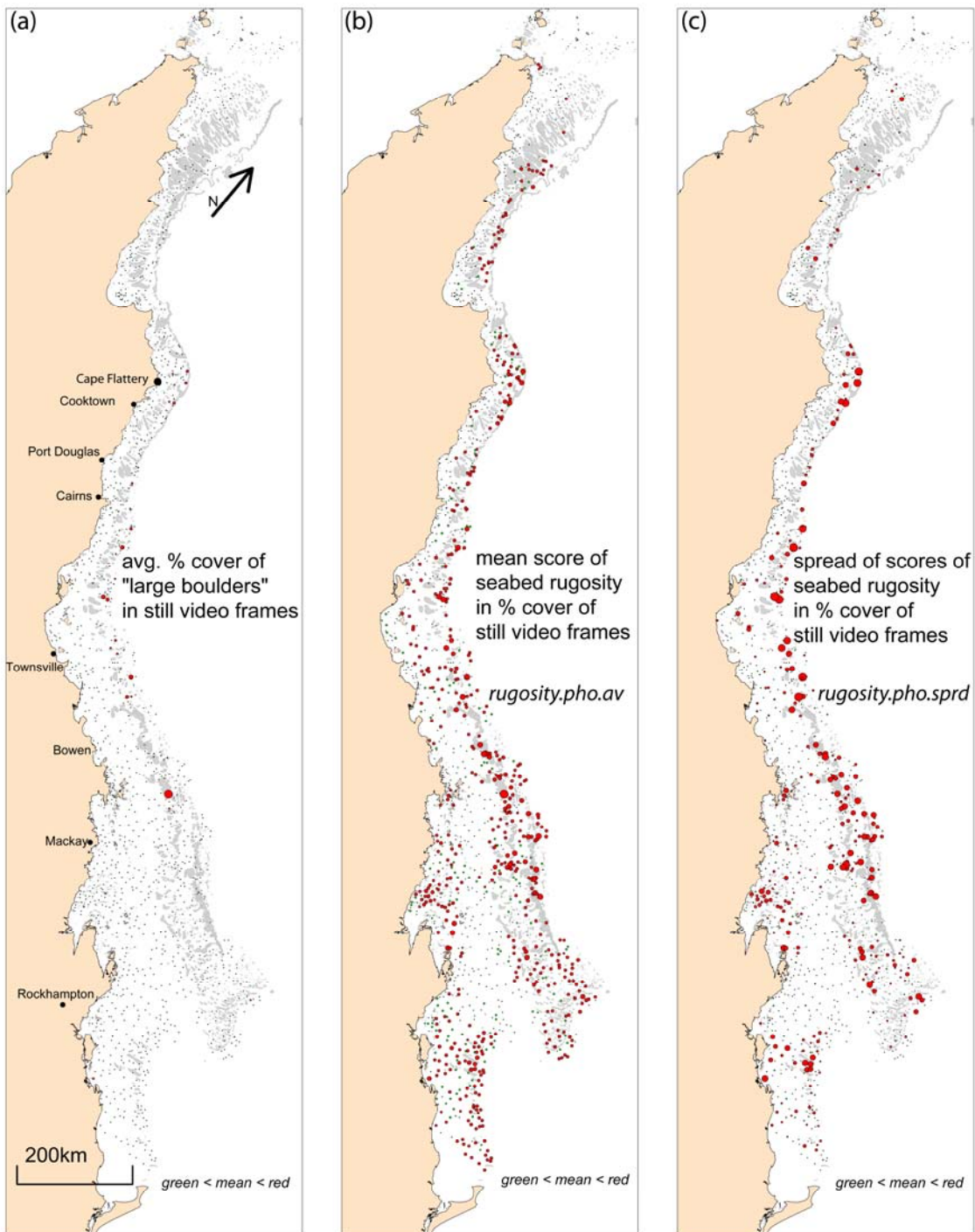


Figure 5.8. Plots of (a) the average percent cover within still video frames of ‘large boulders’ at sites, and measures of (b) ‘location’ (mean: ‘*rugosity.pho.av*’) and (c) ‘spread’ (standard deviation: ‘*rugosity.pho.sprd*’) of an index of seabed rugosity in still video frames. All other conventions as per Figure 5.7.

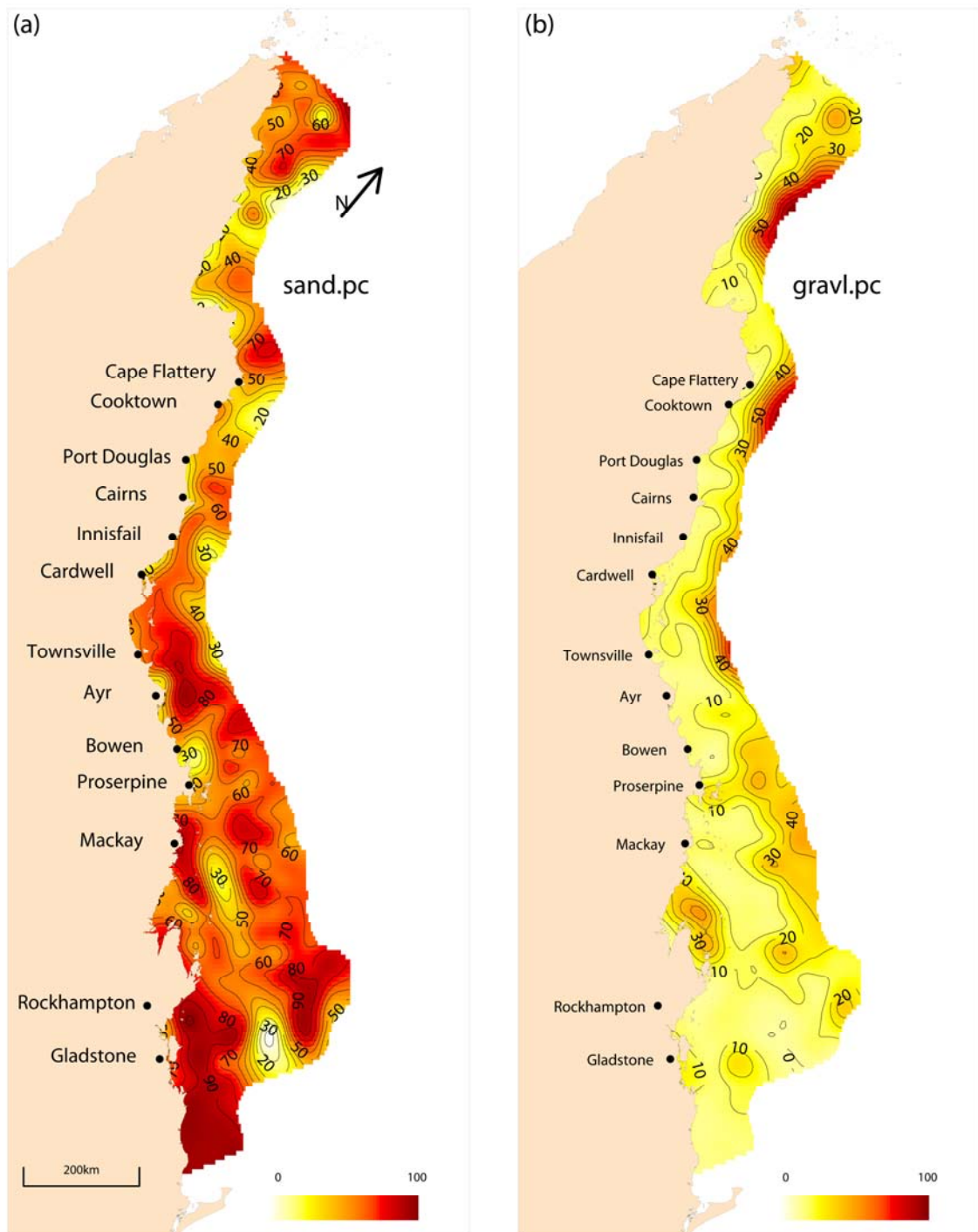


Figure 5.9. Plots of the percentage composition of (a) ‘sand’ (*sand.pc*) and (b) ‘gravel’ (*gravl.pc*) in sediment fractions interpolated by the CSIRO in the GBRMP. All other conventions as per Figure 5.4.

5.3.3 Broad-scale patterns of epibenthic habitats

Video tows indicated very significant banks of marine plants on the sandy Capricorn-Bunker shelf, in the central section off Townsville, and near the major passages off Cape Flattery (Figure 5.10). The presence of deepwater seagrasses on video tows (Figure 5.10) coincided with the occurrence of cooler seawater temperatures and sandy sediments in the central section off Townsville, on the southern shelf around the Capricorn-Bunker group of reefs, and on the northern reef rim. However, there were also significant beds offshore from Cape Flattery around the Turtle group of islands. A 'mid-shelf band' of marine plants was clearly evident in the central section where oceanic waters intrude across the shelf. Marine plants of all types were largely absent from the deeper, mid-shelf, lagoonal waters south of Bowen. The carbonate sediments in the cooler waters of the reef rim were inhabited in some regions by beds of *Halimeda* spp. and fleshy green, brown and red algae. These banks were developed into thick 'bioherms' in the northern GBR where tidal jetting of nutrient-rich water was trapped in the calm lee of the Ribbon Reefs (see Drew 2001). These general patterns probably reflect the level of irradiance at the seabed as well as the nutrient inputs and sedimentary regimes measured here.

The presence of filter-feeding and autotrophic 'megabenthos' (ascidians, sponges, gorgonians, alcyonarians) was more widespread (Figure 5.11), and less interpretable in simple terms of broad patterns in properties of the water column and sediments. There may have been wider occurrence of these organisms in the southern half of the GBRMP where higher seabed current shear stress prevailed.

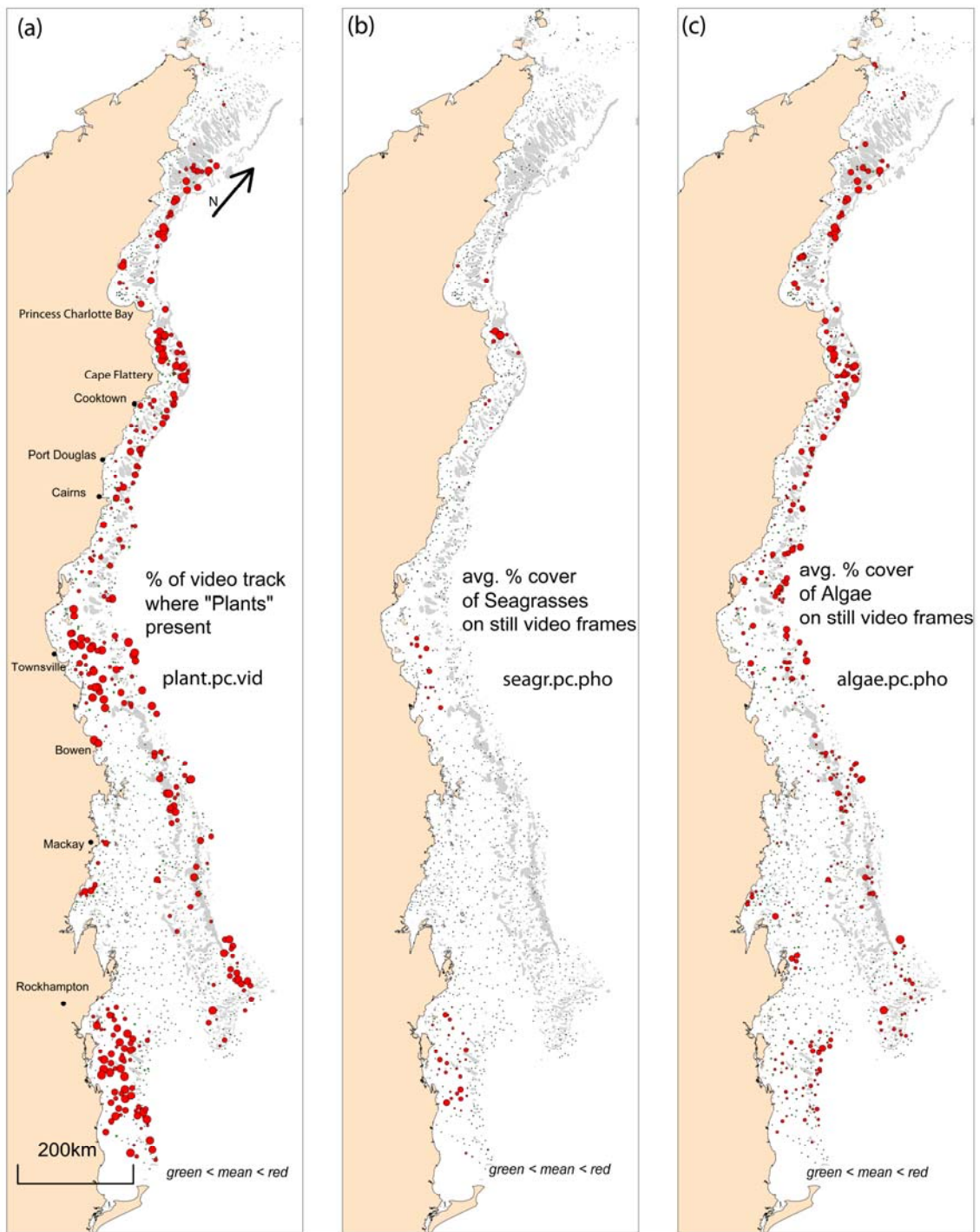


Figure 5.10. Plots of (a) the average percent of video tracks where marine ‘plants’ were recorded (*plant.pc.vid*), and average percentage cover of still video frames occupied by (b) ‘seagrasses’ (*seagr.pc.pho*) and (c) ‘algae’ (including *Halimeda* spp; *algae.pc.pho*). Symbols portray site measurements scaled to the maximum value at all sites for that covariate. Symbol colours show sites with values less than (green) or greater than (red) the overall mean.

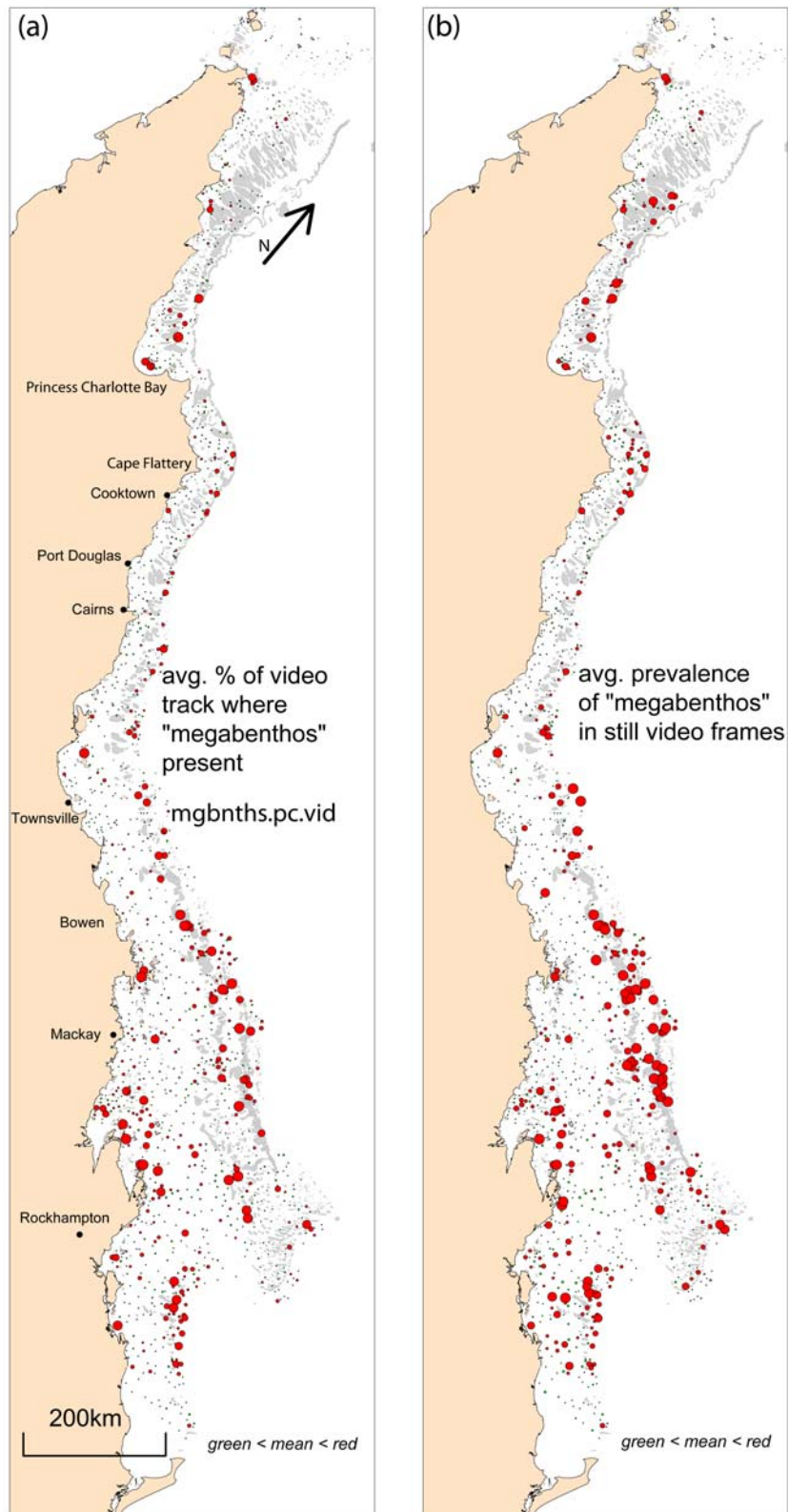


Figure 5.11. Plots of (a) the average percentage of video tracks where ‘megabenthos’ was present (*mgbnth.pc.vid*), and (b) the average number of still video frames on which ‘megabenthos’ occurred. All other conventions follow Figure 5.10.

5.3.4 Species occurrence and site richness

The final dataset consisted of 366 sites and 39,989 individuals from 347 species of fishes, sharks, rays and seasnakes. The bony fishes were from ten orders, dominated by Perciformes (267 species), Tetraodontiformes (27), Anguilliformes (6), Aulopiformes (3), Scorpaeniformes, Clupeiformes, Beryciformes with two species, and Siluriformes, Pleuronectiformes and Gasterosteiformes each with a single species. The chondrichthyans were well represented by the Carcharhiniformes (15 species), Rajiformes (13) and Orectolobiformes (3). There were five species of seasnakes from the family Hydrophiidae.

Most of the 347 species recorded were rare or uncommon, occurring in only a very small percentage of the sites surveyed. There was an average of 13.8 ± 6 (s.d.) species per site, ranging from 2 to 43. Ordering of the most diverse sites produced a sigmoidal curve (Figure 5.12A). Only ~14% of sites had comparatively high species richness (≥ 20 species per site), ~41% had moderate richness (≥ 13 species), and 18% had relatively low richness (≤ 8 species). Just over ninety percent of the species were recorded in less than ten percent of the sites and ~43% were recorded only between one and three times (Figure 5.12B). Only ~5% of the species were moderately prevalent, occurring in $\geq 20\%$ of the sites and, of these, only *Nemipterus furcosus* had a prevalence $>50\%$.

General patterns in species richness interpolated by latitude and longitude showed that cross-shelf and long-shore gradients were not simple (Figure 5.13). Higher richness occurred at sites in the outer reef matrix, particularly north of Proserpine (20.4°S), with a 'hotspot' off Cape Flattery (15°S) in the far north. Richness in the southern half of the GBRMP was higher around the Capricorn-Bunker (23.5°S) island group, and consistently lower for the coastal bays, the deep mid-shelf waters of the Capricorn trough ($\geq 22.5^\circ\text{S}$), and the inter-reef waters of the outer barrier reefs (Figure 5.13).

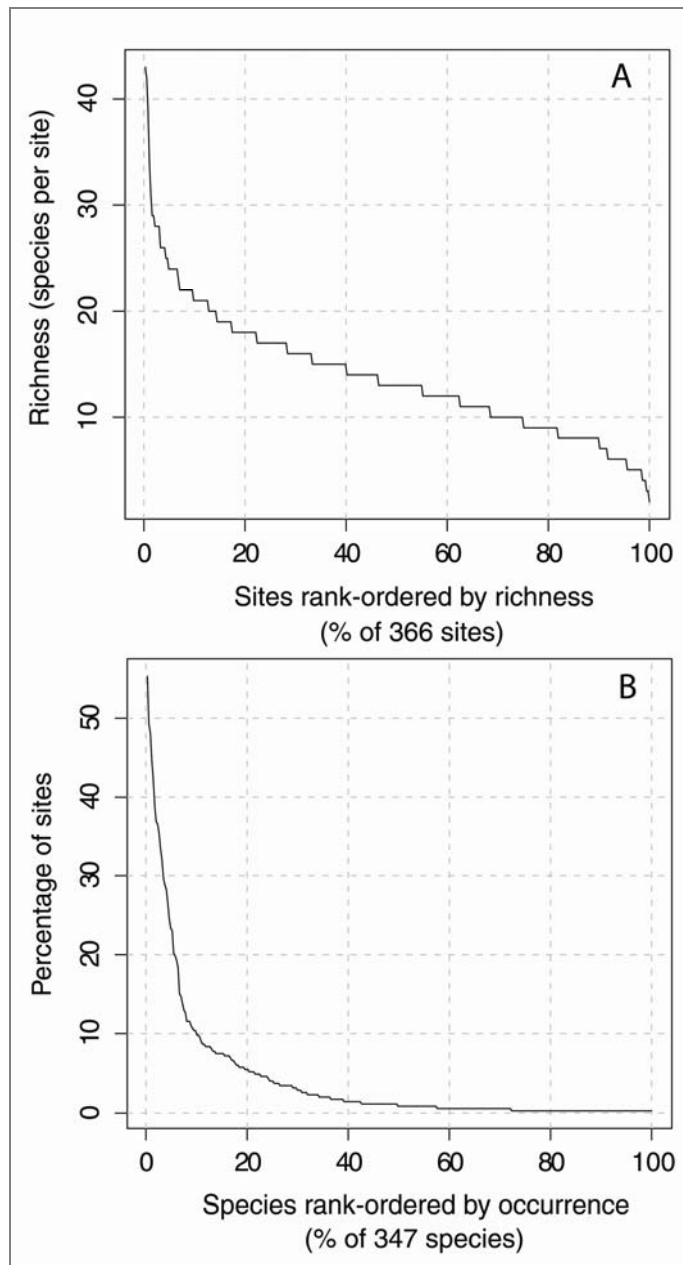


Figure 5.12. Summaries of (A) species richness by cumulative number of sites, and (B) prevalence of 347 species at 366 BRUVS sites ranked in descending order of occurrence.

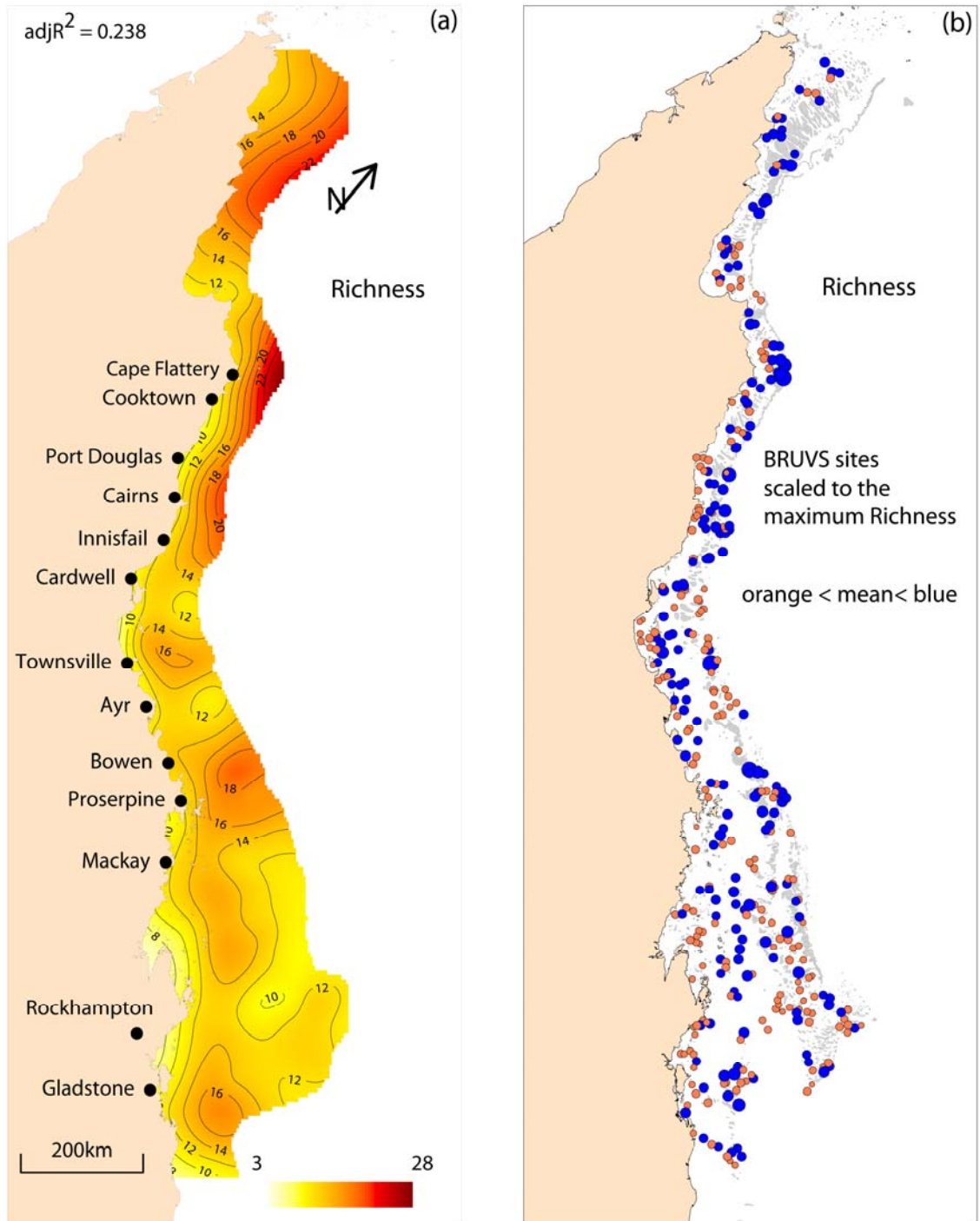


Figure 5.13. A smoothed spline fit of species richness ($k=150$ degrees of freedom) by latitude and longitude (a). The observed richness on which the fit was based (b), is shown scaled to the maximum value and colour-coded according to the mean value amongst all sites.

5.3.5 The influence of shelf position and depth on species richness

The correlations amongst explanatory variables outlined in Table 5.2 and the high spatial interpolation of hydrological and sedimentary covariates evident in Table 5.3 required an assessment of how well species richness was explained and predicted by position and depth on the shelf. The first approach, using only shelf position and depth, would represent the relevant gradients in the ecosystem in a manner that was both useful and easy to interpret. The best BRT model explained about 71% of the variation in species richness, with a relative prediction error of PE = 83%. In order of importance in the model were, (a) position across the shelf (45%); (b) site depth (39%); and (c) position along the shelf (16%). This model had richness increasing monotonically in response to relative distance along the shelf from the southern boundary (Figure 5.14), and incorporated an interaction depth of three.

Richness increased with relative distance across the shelf, and a sharp peak occurred at about 'across' ~0.8. Sites at this distance had approximately three or more species on average than elsewhere. This isopleth coincides with the mid-shelf reef matrix south of Cardwell (18.25°S) and the outer barrier reef north of Cardwell (Figure 5.2). There was a modal relationship between richness and depth, with peak richness predicted for depths in the 30-35m range. This isobath occurred in the lagoon and on the banks and shoals amongst the reef matrix (Figure 5.2). The average decline in richness beyond depths of ~35m was about 0.1 species per metre.

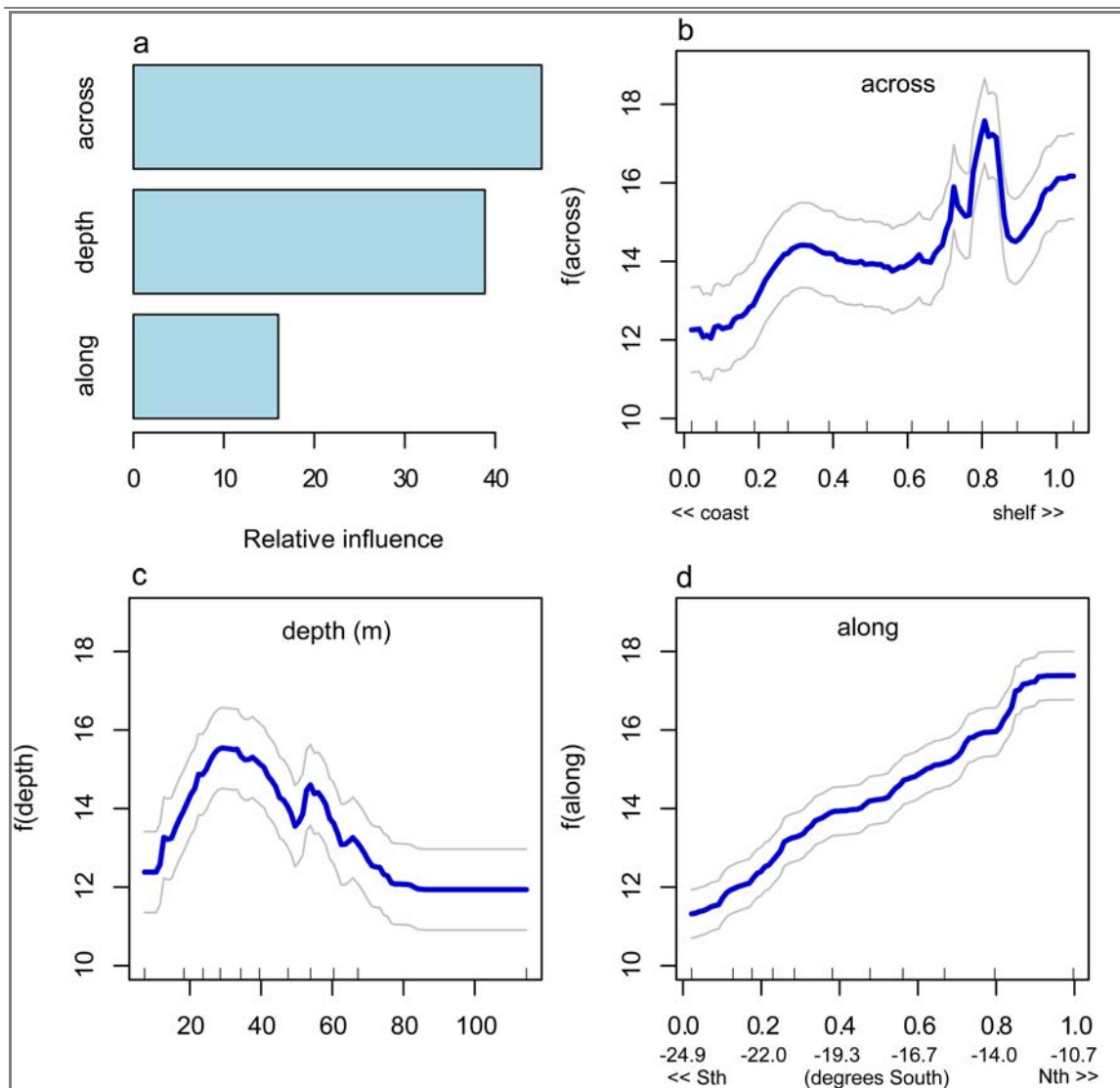


Figure 5.14. Relative influence of location and depth as predictors of species richness in a gradient boosting model (a), and dependency of site species richness on location (b, d) and depth (c). Richness was constrained to increase monotonically in response to distance along the shelf. Distance along the shelf ranges from 0 at the southern end of the GBRMP to 1 at the far northern end (corresponding degrees in latitude are given in brackets). Distance across takes the value 0 on the coast and 1 on the 80m isobath. The short dashed lines (rugs) along the x-axes indicate the ten percentiles in location of the BRUVS sites. Values were predicted for each variable, holding values for both other variables at their mean for the BRUVS dataset. Grey lines indicate two standard errors for the predicted values, estimated from predictions made from five hundred trees fitted in five-fold cross validation of the BRUVS dataset.

The first order interactions showed that cross-shelf increase in richness was most pronounced for shallower sites ~35m, but the peak in richness at ~0.8 occurred for all depths. There was a slight decline in richness with increasing distance across the shelf for sites deeper than 50m (Figure 5.15). The decline in richness for depths >35m was most pronounced for sites at cross-shelf positions offshore from ~0.6, coinciding with the inner edge of the reef matrix south of Cardwell, and the offshore reef matrix north of Cardwell (Figure 5.2). There was also a considerably higher rate of northward increase in species richness at sites within the inter-reef waters ~0.8 across the shelf (Figure 5.15).

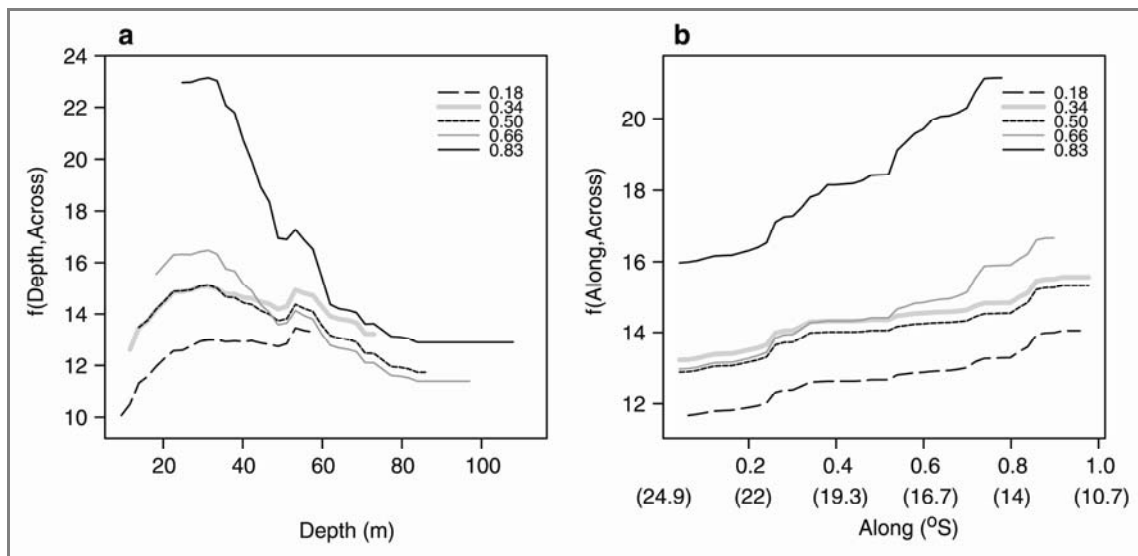


Figure 5.15. Partial dependency of site species richness at five distances across the shelf on depth (a), and the distance along the shelf (b). Other conventions described in Figure 5.14.

5.3.6 The comparative influence of spatial and environmental covariates on species richness

The second approach used ABT models including the entire 28 predictors detailed in Table 5.1. The best ABT model incorporated only main effects, and explained a relatively high level (~76%) of the variation in species richness amongst the 366 BRUVS sites. The relative prediction error (PE%) was relatively low (~65%); an improvement of about 18% upon the purely spatial model presented above. The influence of each predictor in this ABT model is shown in Table 5.4. The most important variables related to information collected by video and photography on the abundance of marine epibenthos and measures of the spread and location in the seafloor rugosity at the BRUVS sites. However, some interpolated variables relating to seabed current shear stress and sediment coarseness appeared in the top six influences that produced significant changes in PE% when omitted from the model.

It was notable that position across the shelf, but not along, had similar influence to some of these environmental variables and also produced highly significant increases in PE when omitted. This implied two things. Firstly and as expected, some of the interpolated environmental covariates (such as temperature and salinity) were redundant in the full model in the presence of the spatial predictors. Secondly, the suite of environmental covariates was missing some important factors characterising the cross-shelf gradient in species richness.

Table 5.4. The diagnostics for the predictors of species richness, showing the relative importance of each predictor (% var. rel. influence), the percentage change in prediction error (% change) after its omission from the model, and the significance of the omission of predictors based on permutation tests ($\text{Pr}>|z|$; $n = 5000$ permutations). A decline is denoted by the – symbol. The full model, with monotonic main effects, had a relative prediction error (%PE) ~65.2%.

Variable (predictor)	%var. rel. influence	% change	$\text{Pr}> z $
plant.pc.vid	12.15	13.62	<0.0001
rugosity.vid.sprd	11.83	11.26	<0.0001
mgbnth.pc.pho	7.81	2.92	0.014
coarsns.pc	7.79	4.15	<0.0001
rugosity.vid.av	6.92	2.20	0.028
Current	4.45	6.16	<0.0001
Temp.av	3.92	0.44	0.306
rugosity.pho.sprd	3.62	0.42	0.311
depth	3.53	2.19	0.001
rugosity.pho.av	3.42	<-0.1	0.526
across	3.42	2.53	<0.0001
along	3.08	1.23	0.045
mgbnth.pc.vid	3.05	<-0.3	0.663
carbnte.pc	2.98	1.16	0.027
gravl.pc	2.68	0.76	0.084
Temp.sd	2.59	0.58	0.169
algae.pc.pho	2.36	0.48	0.199
Salin.av	2.27	0.40	0.230
bare.pc.vid	2.18	0.80	0.079
othranim.pc.pho	1.88	0.35	0.211
dist.reef	1.80	0.80	0.078
sand.pc	1.73	0.58	0.113

Variable (predictor)	%var. rel. influence	% change	Pr> z
nobiota.pc.pho	1.66	0.14	0.337
bioturb.pc.pho	1.22	-0.68	0.741
Salin.sd	0.76	-0.05	0.604
mud.pc	0.75	0.05	0.420
biotrb.pc.vid	0.08	-0.02	0.260
seagr.pc.pho	0.02	0	0.481

A third application of the ABT approach showed that, on average, about 35% of the variation in each of the 25 environmental covariates was predicted by across, along and depth (Table 5.5). The average relative influence of these variables was along (43.5%), across (30.3%), and depth (26.1%). However, the spatially interpolated variables (such as temperature and salinity) were predicted very well, with 74% to 93% of their variation explained by position and depth.

Table 5.5. Percentage of the variation in interpolated (bold) covariates and other environmental variables, at the 366 BRUVS sites, predicted by spatial position and depth on the shelf of the GBR.

Variable (predictor)	Var%	Variable (predictor)	Var%	Variable (predictor)	Var%
Salin.av	92.9	Current	44.7	gravl.pc	19.8
Temp.sd	88.9	rugosity.pho.av	37.1	algae.pc.pho	19.2
Salin.sd	87.4	rugosity.vid.av	36.9	rugosity.vid.sprd	17.5
carbnte.pc	77.9	sand.pc	35.5	biotrb.pc.vid	13.8
Temp.av	74.5	plant.pc.vid	31.7	rugosity.pho.sprd	11.3
mud.pc	51.7	nobiota.pc.pho	24.2	bioturb.pc.pho	11.3
dist.reef	45.5	coarsns.pc	23.0		

Partial dependency plots of the response of the 6 most influential environmental predictors to the purely spatial predictors from this third ABT analysis (Figure 5.16) were an ideal way to visualize and interpret why there were 'hotspots' in species richness at cross-shelf positions ~ 0.8 and water depths of 30-35m (Figure 5.14, Figure 5.16). The seabed current shear stress was predicted to be lowest at across ~ 0.8 , but the predicted abundance of marine plants and megabenthos showed strong modes there with a marked peak in predicted coarseness of the sediments. The measure of the mean rugosity of the seabed was predicted to be at the higher end of the scale from fine mud to boulders at this cross-shelf position, and the measure of spread in this scale also approached a peak there – indicating a strong patchiness in the seabed topography and complexity. The northward increase in species richness was not matched by the same habitat factors coinciding with the cross-shelf mode in richness. In fact, seafloor complexity was predicted to decline with position northward along the shelf, and there were strong modes in the coarseness of sediments, seafloor current shear stress and abundance of megabenthos around along $\sim 0.3-0.4$. This position lay offshore in the macrotidal Whitsunday Islands region between Mackay and Bowen (Figure 5.2). There were two longitudinal modes in the abundance of marine plants, off shore from the central Ayr-Cardwell region (along $\sim 0.4-0.5$) and the far northern Cooktown-Cape Flattery region (along ~ 0.7). All six environmental covariates declined with increasing depth, although modes in the seabed current shear stress and sediment coarseness around forty to seventy metres probably coincided with the narrow inter-reef passages beyond the open lagoon.

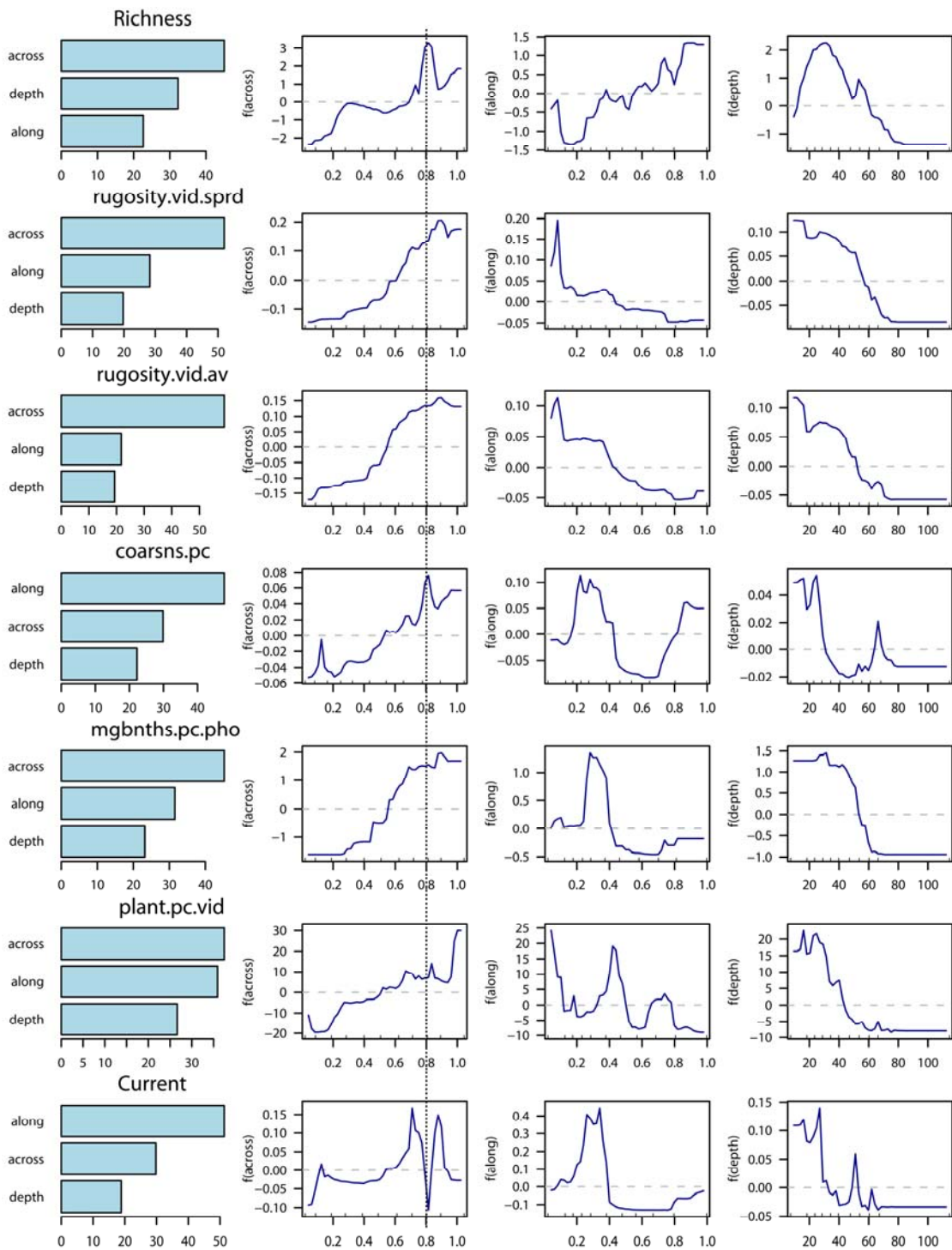


Figure 5.16. Partial dependency plots of richness and six environmental predictors (untransformed) as a function of spatial location and depth. The responses are centered on their mean values at $y=0$. The dotted line indicates values of ‘Across’ ~ 0.8 . All other conventions and definitions as per Figure 5.15 and Table 5.1.

5.3.7 Did a random ‘mid-domain effect’ account for the ‘hotspots’ in species richness?

Modal peaks in species richness along spatial gradients are known to occur wholly or partly due to overlaps in random species distributions (Colwell *et al.* 2009). Without the knowledge presented in Figure 5.16 it could be argued, for example, that the peak in diversity at ‘across’ ~ 0.8 was due solely to a zone of overlap of the ranges of inshore, lagoonal species and offshore, inter-reef species at the inner rim of the mid-shelf reef matrix. Plots of the mean ranges of all species in the study area showed that there was indeed a hotspot of species diversity of both common and rare species at ‘across’ ~ 0.8 , and this was not due to simple overlap of species ranges (Figure 5.17). There was also evidence of a northern peak in smaller ranges of less common and rarely recorded species about ‘along’ $\sim 0.6-0.8$ (Figure 5.18).

Boot-strapped random distributions of species locations and ranges in the study area were estimated on their probability of occurrence in the dataset (Figure 5.19). For example, a species that occurred at only one site (a singleton) might randomly occur anywhere along and across the shelf. The mean location of such a species from a probability distribution would occur in very wide spatial bounds, but the range size could not be simulated from a single occurrence. The 2.5th and 97.5th percentiles of the probability distribution for a singleton approach the spatial boundaries of the study region (Figure 5.19). In contrast, boot-strapped locations for the most commonly occurring species had narrow bounds tending to converge to the mean positions of the 366 BRUVS sets across (~ 0.49) and along (~ 0.42) the shelf. These values should not be confused with the means plotted on Figure 5.19, which were derived in units of across and along from the values observed for each site where a particular species occurred. The boot-strapped ranges declined in width, toward unitary values representing the entire width and length of the GBR, for the most commonly occurring species (Figure 5.19).

The mean observed values were location across ~ 0.62 and location along ~ 0.47 , with mean species ranges of 0.35 units of ‘across’ and 0.37 units of ‘along’.

Counts of species whose location and range were within, or significantly outside, the bounds expected under a random distribution are presented in Table 5.6. Somewhat more of the species locations outside these bounds, for both across and along the GBR shelf, were above the 97.5th percentile, implying locations offshore and to the north. The magnitude of species ranges, but not their ‘randomness’, increased in line with the prevalence of the species in the dataset (Figure 5.19). About 27% (range across) and 12% (range along) of all species had smaller ranges than expected under an hypothesis of random distributions. The prevalence of rare species in the dataset, shown in Figure 5.12 must be kept in mind when interpreting these summaries.

Table 5.6. The numbers of 347 species with locations and ranges across and along the GBR shelf between (within), and outside (below and above) the bounds of boot-strapped random distributions based on their probability of occurrence in the dataset.

	Location:across	Range:across	Location:along	Range:along
below	30 (8.6)	93 (26.8)	25 (7.2)	43 (12.4)
above	54 (15.6)	2 (0.6)	37 (10.7)	1 (0.3)
within	263 (75.8)	252 (72.6)	285 (82.1)	303 (87.3)

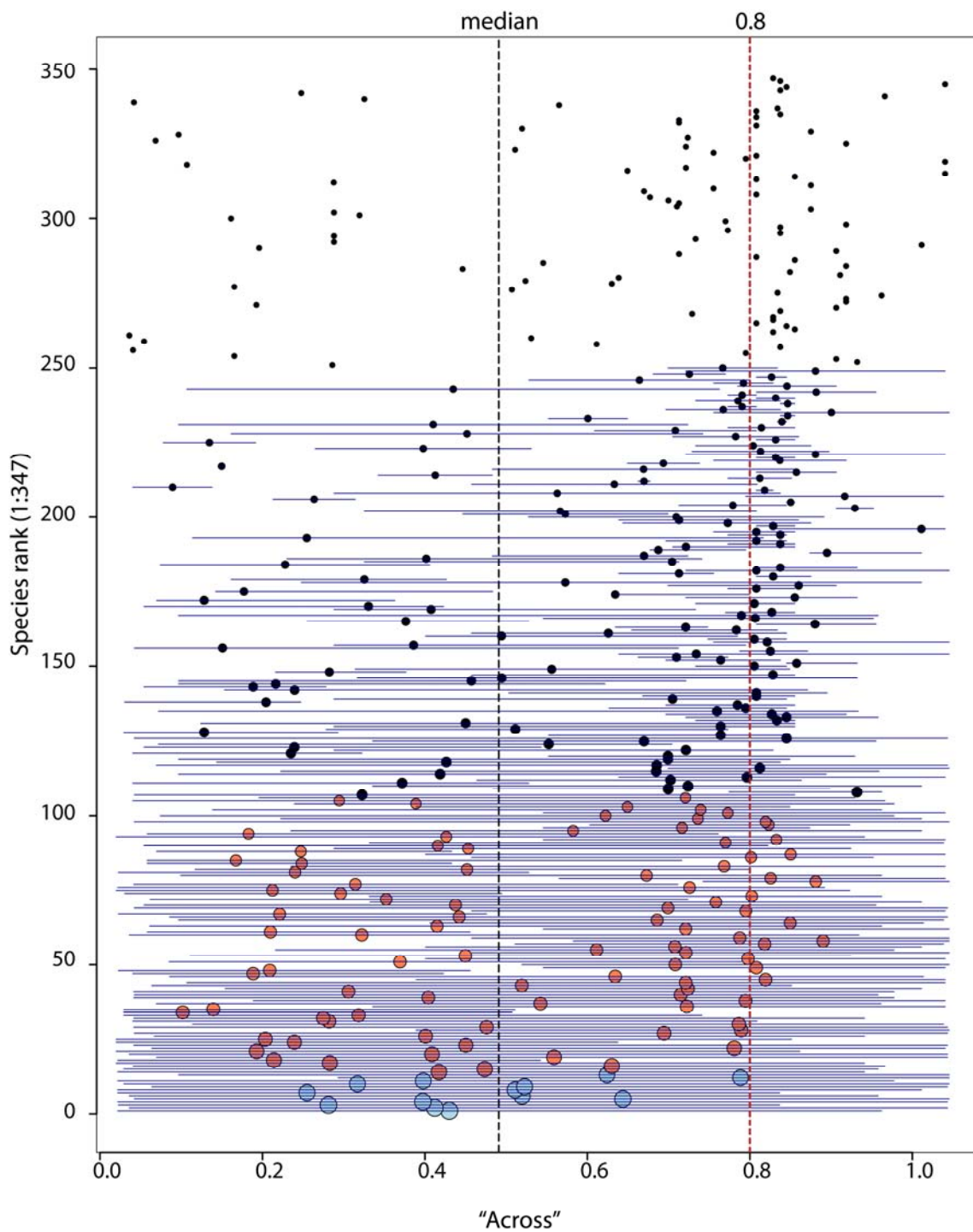


Figure 5.17. Species ranges across the GBRMP. The 347 species were ranked by prevalence from $y=1$ (*Nemipterus furcosus* at 192 sites) to the numerous singletons at $y = 250:347$. Symbols representing the median value of ‘across’ for each species were scaled and coloured by Log_{10} of the number of BRUVS sites on which the species was found. Species found on more than 100, 40-100, and less than 40 sites were represented by light blue, orange and black symbols respectively. Horizontal lines show species ranges. Vertical lines show the median value of all the 366 sites, and across = 0.8.

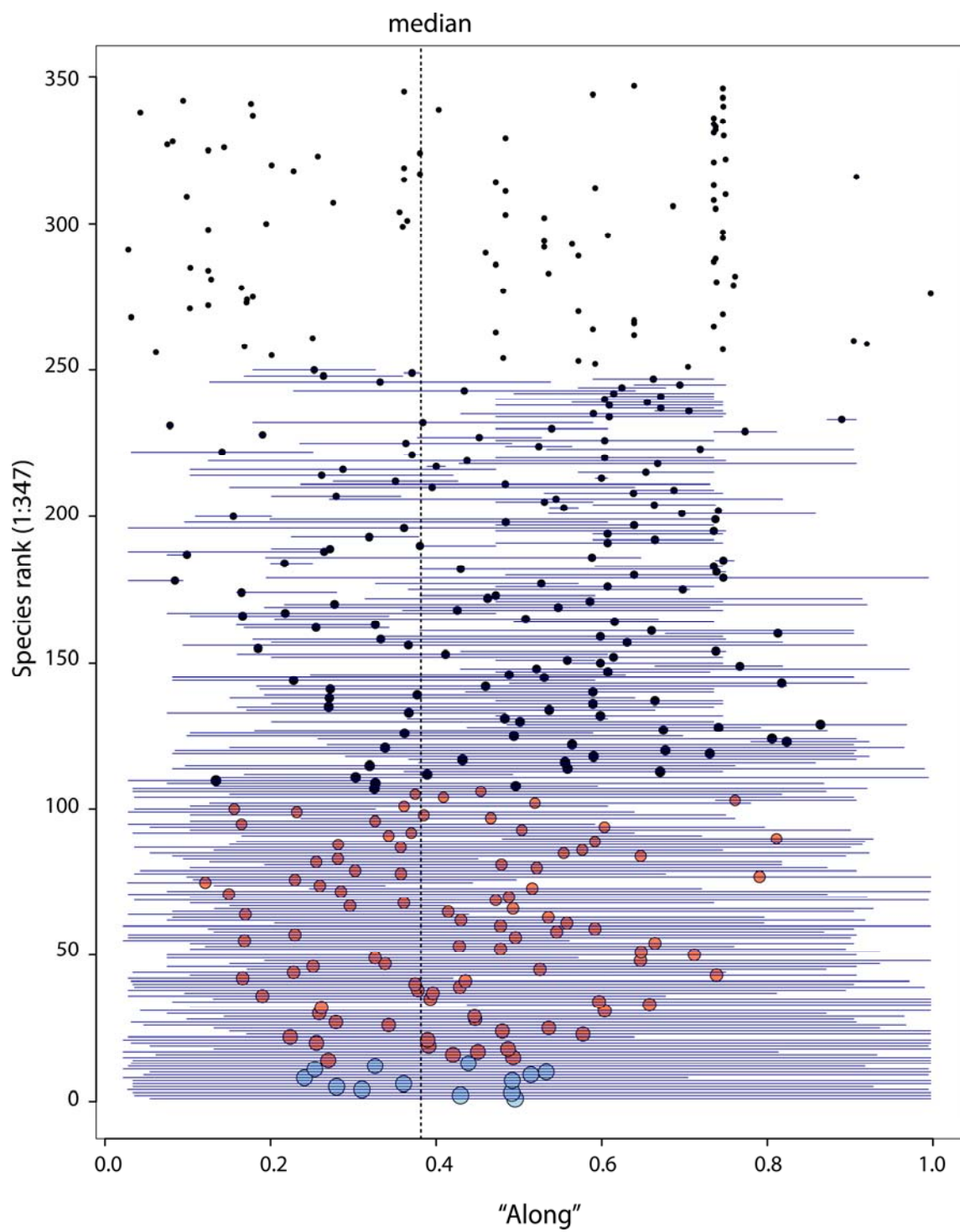


Figure 5.18. Spatial ranges of 347 species along the GBRMP. All conventions follow Figure 5.17.

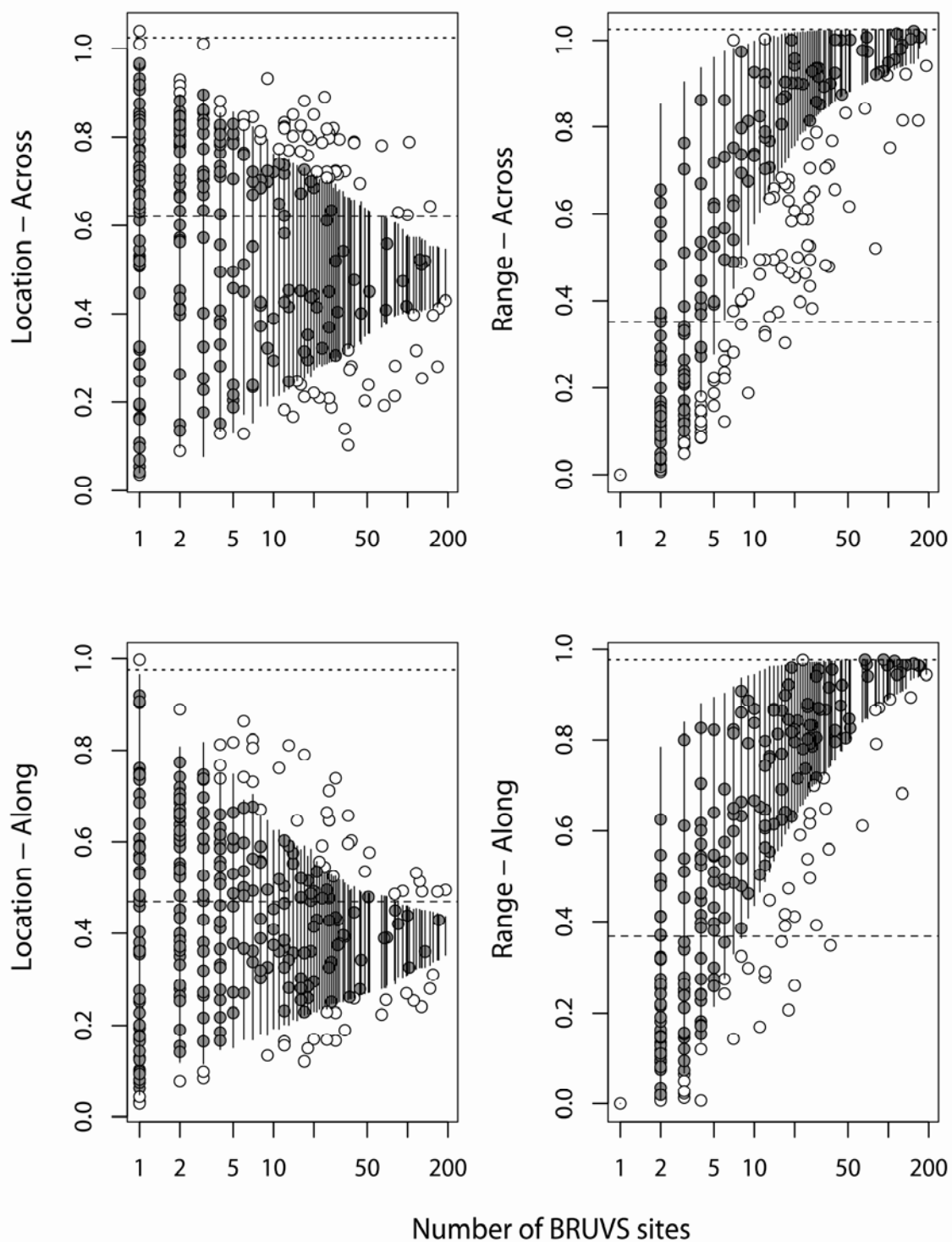


Figure 5.19. Plots of locations and ranges of all 347 species across and along the GBRMP shelf. The vertical bars indicate 95% confidence intervals under the assumption that the taxa are randomly distributed conditional on their observed probability of occurrence. Species beyond the bounds expected under this assumption (open circles), and species within these bounds (grey circles) are shown with mean observed values (dashed) and maximum values expected under random distributions (dotted).

5.4 DISCUSSION

The description of strong cross-shelf gradients in the fauna and flora of the GBRMP has been a major research theme since the inception of the park in the 1970s. In close proximity to major research centres, and safely accessible amongst the well-charted reefs of the central section of the GBRMP, the ‘Townsville transect’ has been the subject of a variety of intensive geomorphological, oceanographic, biological and geochemical studies. Those studies proposed three sedimentary belts in seabed composition and topography parallel to shore in the GBRMP (Larcombe & Carter 2004) that defined changes in community structure of algae, seagrass, echinoderms, hard and soft corals, crustaceans and fish (Cappo & Kelly 2001). These changes were associated with a transition from fine, terrigenous sediments above the 22-25 metre isobath, to biogenic carbonate sediments overlying Pleistocene clays in the deeper, less turbid, offshore waters of this region. Sediment resuspension and seafloor disturbance by wave action above the 22-25 metre isobath have been invoked as a mechanism controlling the enucleation of sessile megabenthos and the offshore extent of seagrass beds (Birtles & Arnold 1988; Carruthers *et al.* 2002), and a ‘coastal boundary layer’ in the same vicinity has been described as a feature that may concentrate secondary production (Brinkman *et al.* 2002).

Few studies of species richness have incorporated the latitudinal gradient along the shelf and these have been restricted to the depth limits of SCUBA diving observations on shallow reefs (Williams 1991; DeVantier *et al.* 2006; Fabricius & De’ath 2008). The results reported here are the first attempt at describing the patterns in vertebrate richness in terms of both the horizontal cross-shelf and along-shelf environmental gradients, seafloor epibenthos and topography, and the vertical dimension of the full range of shelf depths.

5.4.1 Broad regional differences in the three sections of the GBR

This chapter has shown that the far northern and southern regions of the GBRMP are indeed as different from the central section as they are from each other, in terms of shelf width, tidal regime, riverine inputs, sediment composition, epibenthic cover and ‘permeability’ of the outer barrier reefs to oceanic inflows. Mud, for example, is not distributed in these same cross-shelf facies elsewhere on the GBR shelf. Fine terrestrial muds are trapped in northward-facing bays and inshore above 20-25 metres in the mesotidal region, but they are lifted from the coarse gravels of the macrotidal bays in the southern region and deposited well offshore in deep (~50-80m) waters in a mix with carbonate fines driven inshore from the Swain and Pompey groups of reefs. This poses a number of questions regarding the utility of patterns observed off Townsville in understanding and predicting the nature of faunal assemblages elsewhere in the park.

The macrotidal southern section is wider, deeper, cooler and more saline than the rest of the shelf, with a variety of sediment types ranging from the sand shelf around the Capricorn-Bunker Group to the coarse gravels of the Shoalwater Bay-Broad Sound region and the fine muds in the zone of deposition in the deep Capricorn Channel. Seafloor current shear stress is higher in this section than any other, and high turbidity prevails inshore in the Whitsunday region. This led Birtles & Arnold (1988) and Pitcher *et al.* (2002) to predict that epibenthic communities of large filter-feeding gorgonians, sponges and soft corals would most likely be found there, as they are in similar conditions on the northwest shelf of Australia (Sainsbury *et al.* 1997; Pitcher *et al.* 2000) and Torres Strait. Significant beds of seagrass were not expected to occur in those macrotidal conditions (Carruthers *et al.* 2002). However, Pitcher's group (2007) found that widespread beds of marine plants, including seagrass, were present in relatively deep water on the Capricorn-Bunker sand shelf, and that large 'gardens' of megabenthos were not as widespread as predicted.

The central section off Townsville is unique in the cross-shelf intrusion of upwelled, or surface, oceanic waters through the more permeable matrix of isolated reefs and major passages (Furnas & Mitchell 1996). The clearer waters and associated nutrient inputs may act together to drive the development of a long mid-shelf band of marine plants (including seagrasses) growing in relatively deep (30-40m) waters of the lagoon proper. This band may also be associated with the offshore and northward movement of sand (and nutrients) outwelled from the Burdekin River. This sand is visible in the vast Cape Bowling Green Spit, but also offshore around Old and Stanley Reefs in vast underwater dunes.

The far northern section is narrow, with low flushing rates through the minor passages of the Ribbon reefs and waters of higher temperature. The waters have lower salinity and higher turbidity, induced by the outflow of numerous small coastal rivers, of which the Normanby River has the largest catchment west of the coastal ranges. Fine sediments extend far offshore amongst numerous submerged shoals and extinct Pleistocene reefs. In the clearer, sheltered waters in the lee of the Ribbon reefs, and enriched by tidal jets of upwelled water through narrow passages, there are vast bioherms of marine algae, dominated by *Halimeda* spp. These are major features of the northern section (Drew 2001). Seagrasses were found by Coles *et al.* (2009) to be uncommon north of Princess Charlotte Bay (along ~0.76, near Cape Flattery). The East Australian Current diverges offshore in this vicinity with deep oceanic water flowing shorewards and splitting north and south (Brinkman *et al.* 2002), and it is possible there is both recruitment limitation of seagrasses and less nutrients for seagrass growth in the coastal silica sands found there where stream outflows are low (Coles *et al.* 2009).

This chapter has demonstrated that the variables supplied to represent major gradients in sediments ($r^2 = 68\%-88\%$) and hydrology ($r^2 = 94\%-98\%$) at any particular BRUVS site had been interpolated by latitude and longitude to a high degree. The GBR does not follow a strictly north-south alignment, and the shelf varies in width by about four-fold from one extremity to the other. Therefore the use of measures of 'across' and 'along' developed by Fabricius & De'ath (2001a) provided a much better spatial grid on which to base statistical analyses. On average, about 35% of the variation in each of the 25 environmental covariates was predicted by across, along and depth. However, the spatially interpolated variables (such as temperature and salinity) were predicted very well, with 74% to 93% of their variation explained by position and depth. These two covariates were out-competed by spatial variables in any model attempting to explain and predict the richness of vertebrates recorded by BRUVS. This prevented any simulations of unknown sources of variance by simple subtraction of fits of models dropping or including those spatial predictors.

Correlations among explanatory covariates can make interpretation of some analyses difficult. If significant relationships were found between species richness and any covariate(s), the correlation did not necessarily imply the causal mechanism, nor did it mean that other correlated covariates were unimportant. For example, a variety of covariates were negatively correlated with the percentage of mud in sediments (e.g. measures of marine plants, megabenthos, and mobile animals), whilst others were positively correlated (e.g. indices of bioturbation and variability in salinity).

5.4.2 The nature of species records in BRUVS data

The great majority of species recorded by the BRUVS occurred rarely. This pattern seems characteristic of tropical fish faunas sampled over soft seabeds. The widespread sampling with BRUVS recorded a similar number of species (347) to those recorded by trawling (300-350) in similar latitudes by the studies reviewed in Chapter 4.4. Those trawl inventories were also dominated by species that occurred rarely and in low abundance. Like estuarine fish faunas (Magurran & Henderson 2003), the vertebrates in the 'inter-reef' waters of the GBRMP probably comprise 'core species', which are persistent, abundant and biologically associated with particular habitats, and 'occasional species' which occur infrequently in surveys, are typically low in abundance and have different habitat requirements.

5.4.3 Spatial and environmental influences on species richness

Position and depth alone explained about 71% of the variation in species richness, with a relative prediction error of PE = 83%. Richness increased from south to north and with relative distance across the shelf. Sharply modal peaks in richness occurred for depths in the 30-35 metre range and at about 'across' ~ 0.8 , coinciding with the mid-shelf reef matrix south of Cardwell and the outer barrier reef north of Cardwell. This isobath occurred in the lagoon and on the banks and shoals amongst the reefs. The first order interactions showed that cross-shelf increase in richness was most pronounced for shallower sites $\sim 35\text{m}$, but the peak in richness at ~ 0.8 occurred for all depths. There was also a considerably higher rate of northward increase in species richness at sites within the inter-reef waters ~ 0.8 across the shelf.

The full model including the entire 28 predictors improved the level of explanation of species richness only by about five percent but improved the relative prediction error by nearly 18%. The most important influences were the abundance of marine plants and filter-feeding epibenthos and measures of the seafloor rugosity and composition along a scale from fine mud to rocks and boulders. These variables were measured at each BRUVS site by video and stills photography. However, some interpolated variables relating to seabed current shear stress and sediment coarseness appeared in the top six influences that produced significant changes in prediction error when omitted from the model, as did the position 'across' the shelf. This implied redundancy in temperature and salinity in the full model and also that the suite of environmental covariates was missing some important factors characterising the cross-shelf gradient in species richness. This was expected given the primacy of chlorophyll-a, irradiance at the seabed, wave energy or measures of benthic primary production in other studies of species richness along gradients in the GBRMP (see Fabricius & De'ath 2001a; 2001b; Gust *et al.* 2001; Fabricius *et al.* 2005; Furnas *et al.* 2005; Fabricius *et al.* 2008).

Partial dependency plots were an ideal way to visualise and interpret why there were 'hotspots' in species richness at cross-shelf positions ~ 0.8 and water depths of 30-35 metres. At this position, seabed current shear stress was predicted to be lowest, and abundance of marine plants and megabenthos highest, with a marked peak in predicted coarseness of the sediments. The measure of the mean roughness and patchiness in the seabed rugosity was predicted to be at the higher end of the scale at this cross-shelf position. The northward increase in species richness was not matched by the same habitat factors coinciding with the cross-shelf mode in richness.

In summary, the modal peak in species richness ~ 0.8 across the GBR shelf was influenced most by the presence there of beds of seagrasses and/or algae in conditions of low current, patches of

sessile megabenthos, or complex seafloor topography. These features and this position were associated often, but not always, with the shallow (30-35 metres) offshore ‘shoals’ between emergent coral reefs. These features are known in some places to comprise extinct reef edges and exposed clay banks of the Pleistocene era that emerge through the sediments (Beaman & Harris 2007). Elsewhere, the shoals are accumulations of carbonate produced by coralline algae and *Halimeda* spp. (Pitcher *et al.* 2007). The patchiness of complex seafloor topography, such as rocks and boulders, and ‘edge effects’ in complex habitats (such as vegetated or coral reefs and seagrass beds) are known to enhance species diversity of fishes by moderating competition and predation (Jones & Syms 1998; Syms & Jones 2000; Jones *et al.* 2004; Syms & Kingsford 2009).

5.4.4 Relevance to biogeographic models

The northward increase in species richness over about fourteen degrees of latitude was expected, given general latitudinal gradients predicted for diversity of shallow marine species (Crame & Clarke 1997; Gray 1997; Ormond & Roberts 1997; Taylor 1997; Gray 2001) and previous studies of other groups in the GBRMP. The northward increase of about one species for every three degrees of latitude was a relatively weak influence. In this regard, Williams (1991) reported that variation in reef fish assemblages over nine degrees of latitude was outweighed by the influence of position of reefs across the shelf. Reef fish richness was greatest on the mid-shelf reefs, intermediate on the outer shelf, and lowest near shore – a trend with some similarities to the influences demonstrated here. The alpha (within habitat) diversity of eastern Australian coral reefs was reported by Ormond & Roberts (1997) to decline from more than 2,000 species in the far north to about 1,000 in the Capricorn-Bunker Group, with 314 at Elizabeth and Middleton Reefs and 447 at Lord Howe Island.

In the case of tropical marine fishes, sharks and rays, the development of biogeographic models has been hampered by both lags in taxonomic description of a vast fauna (the ‘Linnaean shortfall’) and an inadequate knowledge of global, regional, and sometimes local distributions. This latter problem has been termed by Bini *et al.* (2006) as the ‘Wallacean shortfall’. Despite these shortcomings, the general pattern that species richness declines with increasing latitude has been accepted for tropical fishes (Ormond & Roberts 1997), and a number of theoretical meta-analyses have been undertaken to explain why (Hillebrand 2004a; 2004b; Bellwood *et al.* 2005; Field *et al.* 2009).

Mid-domain models propose random placement of species ranges in any domain to predict a peak in diversity in the geometric middle of this domain, without invoking any ecological or

evolutionary processes (Colwell & Lees 2000; Colwell *et al.* 2004; Carranza *et al.* 2008; Colwell *et al.* 2009). All other models use latitude as a surrogate variable for factors co-varying with latitude. Gradients of decreasing energy supply (light, heat, primary production, nutrient inputs) (Fraser & Currie 1996; Taylor 1997; Roy *et al.* 1998) and decreasing areas of suitable habitat (Rohde 1998) toward the poles have been proposed as ultimate causes for the latitudinal diversity decline. Finally, ‘the effective evolutionary time hypothesis’ (Rohde 1999) assumes higher speciation in the tropics because the higher energy inputs, higher metabolic rates (Da Silva Cassemiro *et al.* 2007) and larger areas of habitat there support increased mutation rates and decreasing generation times. Other studies have attributed combinations of a mid-domain effect with temperature for plankton (Brayard *et al.* 2005), with habitat area for coral reefs and their fish fauna (Bellwood *et al.* 2005), and with illumination at the seabed for soft corals (Fabricius & De’ath 2008).

The measures of location and range in the distribution presented here showed no evidence of a role for the mid-domain effect in producing the modal ‘hotspot’ of alpha diversity at a position about ~0.8 across the GBR shelf. There was no evidence of overlap in ranges of ‘inshore’ and ‘offshore’ species at this position. Instead, the modal peak was produced by the occurrence there of numerous different species – some ubiquitous ones, others with restricted ranges and many (singletons) that occurred nowhere else. The magnitude of species ranges increased in line with the prevalence of the species in the dataset. About 27% (range across) and 12% (range along) of all species had smaller ranges than expected under a hypothesis of random distributions.

The important influence of benthic marine plants on vertebrate species richness may indicate the role of a gradient in energy supply through irradiance at the seabed and nutrient inputs from oceanic waters. Marine plants elsewhere are known to provide shelter for juveniles and support food chains directly for herbivores and benthic microcarnivores (Edgar & Shaw 1995), and indirectly through detrital subsidies to local microbial loops (Alongi 1990). In this regard, the role of deep water seagrass and *Halimeda/Caulerpa* algal beds is unknown for the GBR (Carruthers *et al.* 2002). Further interpretation of the processes shaping species richness require the analysis of beta (between habitat) diversity on the GBR shelf, which forms the next chapter of this thesis.

Appendix 5.1. Definition of species groups identified with the suffix ‘_grp’ in this thesis. The use of ‘_grp’ indicated that there was uncertainty in identification, due to the limitations of video footage, but also that the name preceding the suffix was the most plausible level of identification.

Order	Family	Nomenclature	species group
Carcharhiniformes	Carcharhinidae	<i>Carcharhinus amboinensis</i> _grp	<i>C. amboinensis</i> , <i>C. leucas</i>
		<i>Carcharhinus tilstoni</i> _grp	<i>C. tilstoni</i> , <i>C. limbatus</i> , <i>C. amblyrhynchoides</i>
		<i>Rhizoprionodon taylori</i> _grp	<i>R. taylori</i> , <i>R. acutus</i>
Rajiformes	Dasyatidae	<i>Himantura fai</i> _grp	<i>H. fai</i> , <i>H. toshi</i> , <i>H. jenkinsii</i>
Siluriformes	Ariidae	<i>Arius thalassinus</i> _grp	<i>A. thalassinus</i> , <i>A. graefi</i>
Aulopiformes	Synodontidae	<i>Saurida</i> _grp	<i>S. undosquamis</i> , <i>S. nebulosus</i> , <i>S. micropectoralis</i>
		<i>Synodus</i> _grp	All <i>Synodus</i> spp
Perciformes	Apogonidae	<i>Apogon</i> _grp	All unknown apogonids
Perciformes	Blenniidae	<i>Meiacanthus</i> _grp	All unknown <i>Meiacanthus</i>
		<i>Plagiotremus</i> _grp	All unknown <i>Plagiotremus</i>
Perciformes	Carangidae	<i>Carangoides dinema</i> _grp	<i>C. dinema</i> , <i>C. humerosus</i>
		<i>Carangoides malabaricus</i> _grp	<i>C. malabaricus</i> , <i>C. equula</i>
		<i>Carangoides talamparoides</i> _grp	<i>C. talamparoides</i> , <i>C. bajad</i>
Perciformes	Labridae	<i>Choerodon</i> _grp	Unknown <i>Choerodon</i> spp
		<i>Coris</i> _grp	Small unknown <i>Coris</i> spp
		<i>Suezichthys devisi</i> _grp	<i>S. devisi</i> , <i>S. gracilis</i>
		<i>Xyrichtys</i> _grp	All <i>Xyrichtys</i> spp
Perciformes	Mullidae	<i>Upeneus</i> _grp	All unknown mullids
		<i>Upeneus tragula</i> _grp	<i>U. tragula</i> , <i>U. sulphureus</i> , <i>U. sundaicus</i>
Perciformes	Nemipteridae	<i>Nemipterus balinensoides</i> _grp	<i>N. balinensoides</i> , <i>N. celebicus</i>
Perciformes	Pinguipedidae	<i>Parapercis nebulosa</i> _grp	<i>P. nebulosa</i> and sub-species
		<i>Parapercis xanthozona</i> _grp	<i>P. xanthozona</i> and sub-species
Perciformes	Serranidae	<i>Anthias</i> _grp	All unknown <i>Anthias</i>

Order	Family	Nomenclature	species group
Perciformes	Siganidae	<i>Siganus fuscescens</i> _grp	<i>S. fuscescens</i> , <i>S. canaliculatus</i>
Perciformes	Sillaginidae	<i>Sillago</i> _grp	All <i>Sillago</i> spp
Scorpaeniformes	Platycephalidae	<i>Flathead</i> _grp	All unknown flatheads
Pleuronectiformes	unknown	<i>Flatfish</i> _grp	All unknown flatfish
Tetraodontiformes	Ostraciidae	<i>Ostracion</i> _grp	All unknown boxfish
Tetraodontiformes	Tetraodontidae	<i>Arothron</i> _grp	Unknown <i>Arothron</i> spp
		<i>Lagocephalus</i> _grp	Unknown <i>Lagocephalus</i> spp
		<i>Torquigener</i> _grp	<i>T. whitleyi</i> , <i>T. pallimaculatus</i>